NUREG/CR-1807
ANL-81-10

(Distribution
Code: R7)

ARGONNE NATIONAL LABORATORY
9700 South Cass Avenue
Argonne, Illinois 60439

COMMIX-2:
A STEADY/UNSTEADY SINGLE-PHASE/TWO-PHASE THREE-DIMENSIONAL COMPUTER PROGRAM FOR THERMAL-HYDRAULIC ANALYSIS OF REACTOR COMPONENTS

by

H. M. Domanus,* W. T. Sha,* V. L. Shah,*
J. G. Bartzis, J. L. Krazinski,
C. C. Miao, and R. C. Schmitt

Components Technology Division

October 1980

Prepared for the
U. S. NUCLEAR REGULATORY COMMISSION
Office of Nuclear Regulatory Research
Washington, D.C. 20555
under Interagency Agreement DOE 40-550-75
NRC FIN No. A2045

*Principal Investigators

8104230433

COMMIX-2:
A STEADY/UNSTEADY SINGLE-PHASE/TWO-PHASE
THREE-DIMENSIONAL COMPUTER PROGRAM
FOR THERMAL HYDRAULIC ANALYSIS
OF REACTOR COMPONENTS

by

H. M. Domanus, W. T. Sha, V. L. Shah,
J. C. Bartzis, J. L. Krazinski,
C. C. Miao, and R. C. Schmitt

ABSTRACT

This report describes the numerical procedure of COMMIX-2 for the calculation of steady/unsteady, single-phase/two-phase, three-dimensional fluid flow and heat transfer. The procedure is based on the control-volume approach, which enables the derivation of physically meaningful finite-difference equations. The conservation equations employed are based on a two-fluid model, and this permits the analyses of nonhomogeneous and nonequilibrium flow conditions. The conservation equations of mass, momentum, and energy of each phase are solved as an elliptic system. In addition, the porous-medium formulation with concept of volume porosity, surface permeability, distributed resistance, and distributed heat source is employed and provides a greater range of applicability. The concept of surface permeability is new and greatly facilitates modeling of anisotropic flow and temperature fields.

NRC FIN No.	Title
A2045	3-D Time-dependent Code Development

TABLE OF CONTENTS

TABLE OF CONTENTS

TABLE OF CONTENTS

LIST OF FIGURES

LIST OF TABLES

NOMENCLATURE

A	Area
a	Finite-difference coefficients
a^0	Finite-difference coefficients arising from the unsteady term
B	Defined in Eq. 6.3
b_0	"Constant" term in the finite-difference method
c_p	Specific heat at constant pressure
D	Diffusion strength, Eq. 5.9; diameter
d	Pressure coefficient, Eq. 7.4
F	Flow rate, Eq. 6.4
g_j	Gravitational acceleration in the jth direction
h	Heat-transfer coefficient; enthalpy
h_{fg}	Latent heat
H	Enthalpy
J	Total (convection + diffusion) flux
k	Thermal conductivity
K	Interfacial drag coefficient
Nu	Nusselt number
p	Pressure
p'	Pressure correction
Pr	Prandtl number
Q	Heat generation per unit volume, Eq. 2.5
R	Interfacial heat transfer coefficient, Eq. 2.5; the distributed frictional resistance per unit fluid volume
S	Source term, Eq. 2.6
S_C, S_P	Parts of the linearized source term, Eq. 5.14
S_1, S_2	Positive and negative parts of S, Eq. 12.7
T	Temperature
t	Time
u, v, w	Velocity components
$\hat{u}$, $\hat{v}$, $\hat{w}$	Pseudo-velocities, Eq. 7.3
V	Viscous source term; volume
α	Thermal diffusivity; defined in Eq. 9.10

NOMENCLATURE

NOMENCLATURE

Γ	Diffusion coefficient, Eq. 2.6
Δt	Time step
Δx, Δy, Δz	Control-volume dimensions
λ	Thermal conductivity; coefficient in Eqs. 4.2 and 4.3
μ	Viscosity
ρ	Density
β	Defined in Eq. 9.10; coefficient of thermal expansion
ϕ	General dependent variable, Eq. 2.6
θ	Fluid volume fraction; angle between fuel-pin centerline and helical wire wrap centerline
γ_v	Volume porosity
γ_x, γ_y, γ_z	Surface permeability in x, y, and z directions
Ω, Ω_m, Ω_h	Source due to phase change (evaporation or condensation) in the continuity, momentum, and energy equations
Φ	Viscous dissipation, Eq. 2.5
ν	Kinematic viscosity
σ	Surface tension

Superscripts

*	Last iteration value; guessed value
0	Old values
w	Wire wrap
'	Correction to last iterated value

Subscripts

0	Grid location under consideration; center of the control volume
1.	(i-1, j,k) location
2.	(i+1, j,k) location
3.	(i, j-1, k) location
4.	(i, j+1, k) location
5.	(i, j, k-1) location
6.	(i, j, k+1) location
m	Momentum
h	Energy

EXECUTIVE SUMMARY

This report describes the COMMIX-2 computer program. The program is designed to analyze steady/unsteady, single-phase/two-phase, three-dimensional fluid flow with heat transfer in reactor components. It uses a two-fluid model to describe the conservation equations for two-phase flow. Consequently, one can analyze a wide spectrum: from homogeneous and equilibrium to non-homogeneous and nonequilibrium flow conditions. The volume porosity, surface permeability, distributed resistance, and distributed heat source are included in the conservation equations to permit analyses of flow domain with solid objects. The discretization equations are obtained by integrating the conservation equations over a control volume. The convective, diffusion, interfacial friction and interfacial heat-transfer terms are made implicit for more stable formulation. The final form of all discretization equations is such as to permit various solution schemes, e.g., cell by cell, line by line, etc.

At present, COMMIX-2 has two alternative forms of the pressure-correction equation. One form is derived from the combined continuity equation, and in the second procedure we make use of the condition.

Sum of fluid volume fraction = 1.

At present, both forms are retained in the code, as not enough experimentation has been performed to determine the computational efficiency and suitability of these two forms of pressure-correction equation.

The COMMIX-2 code has a modular structure. It permits analysis of single-phase (gas or liquid) or two-phase flow problems. The code has also an option permitting use of either a sodium-property package or a water-property package.

The report describes in detail the formulation, solution procedures, iteration sequence, flow chart, and input instructions. It also includes the description of models used in COMMIX-2 for the following phenomena:

1. Interfacial mass, momentum, and energy exchange.
2. Wall-heat transfer and their regimes.
3. Distributed resistance due to internal structures.
4. Thermal interaction between structures and fluid.
5. Interaction due to the presence of wire wrap.

Even though the interfacial and wall heat transfer models for other flow regimes have been incorporated into the code, the current version of COMMIX-2 is geared specifically for dispersed flow analyses.

As two-phase flow is a very active and developing field, new and better physical models and constitutive relations are expected to emerge. COMMIX-2 will therefore remain a dynamic code. We will make all efforts to retain the same structure of the code while incorporating new developments in physical models and solution procedures. As we make modifications in the code, some changes are expected to occur in the input structure. Users of the code are therefore requested to follow the latest version of the input description.

1. INTRODUCTION

The present-generation computer speed and storage capacity, coupled with recent advances in numerical-solution techniques for systems of quasilinear partial differential equations, have made possible detailed numerical simulation of many engineering problems. With the anticipated improved performance of the next generation of computers and further advances in numerical-solution techniques, use of numerical simulation for solving engineering problems is expected to increase for many years to come.

Basically, numerical simulation in engineering applications can be classified into two categories: the system computer program and the component computer program. Generally, the system computer program consists of a number of components; therefore, it cannot afford to give a detailed numerical modeling of each component. In contrast, the component computer program deals with one component of interest; therefore, it can afford to provide a detailed numerical simulation. The work presented in this report is focused on the component computer program.

During loss of coolant or transient overpower accident situations, boiling of liquid coolant in a reactor core is expected due to high temperatures of fuel pins. The fluid mixture of liquid and vapor, in such circumstances, is nonhomogeneous with both phases being in nonequilibrium thermodynamic states. It is, therefore, desirable to develop a computer code for obtaining numerical solutions of three-dimensional, transient, two-phase (gas-liquid) flow system with nonequilibrium and nonhomogeneous conditions.

The COMMIX-2 code is a steady/unsteady, three-dimensional two-phase computer code for thermal hydraulic analysis of reactor components under normal and off-normal operating conditions. It uses the two-fluid model of Harlow and Amsden[1] to describe the conservation equations of mass, momentum and energy. Consequently, we can analyze a wide spectrum of flow conditions; i.e., from homogeneous and equilibrium to nonhomogeneous and nonequilibrium conditions. The interactions between two fluids are accounted for by incorporating the corresponding terms in all of the conservation equations. The staggered grid system is used to describe the field variables at the center of a cell and flow variables at the surface of a cell.

The structure of the code is similar to that of COMMIX-1A.[2] The calculation procedure employed is an extension of the single-phase numerical procedure,[3] known as SIMPLER (Semi-Implicit Method for Pressure Linked Equation-Revised). In this procedure, we use the liquid phase continuity equation to obtain the void fractions, and use the combined continuity equation to derive the pressure and pressure correction equations.

The specific features of COMMIX-2 are the following:

1. To permit an analysis of a flow domain with solid objects, the volume porosity, surface permeability, distributed resistance and distributed heat source are incorporated in the conservation equations.

2. An approximate form of Spalding's equation[4] is used to derive the finite difference formulation of the convective and diffusion terms. This equation is a function of the Peclet number and it combines the best features of both, the central difference and upwind difference schemes.

3. The discretization equations are obtained by integrating the conservation equations over a control volume surrounding a grid point. Thus, the derivation process and the resulting equations have direct physical meaning, and the consequent solution satisfies the conservation principles.

4. The convective, diffusion, interfacial friction and interfacial heat transfer terms are made implicit for more stable formulation and to permit larger time steps.

5. The discretization equations are formulated with time step size appearing only in the denominator of all transient terms. With this arrangement, for a steady state calculation, all of the transient terms can be eliminated from computation by specifying a very large value of time step size.

6. The general form of all discretization equations is

$$a_0\phi_0 + \sum_{nb} a_{nb}\phi_{nb} = b_0,$$

where, ϕ is a dependent variable and subscript nb stands for neighboring points. This general form of the discretization equation permits various solution schemes, e.g., cell by cell, line by line, plane by plane, block iterative, direct inversion etc.

7. The COMMIX-2 code is structured such as to permit solution of single phase (gas or liquid) as well as two-phase (gas and liquid) flow problems. In addition, it permits 1D, 2D, or 3D calculation.

8. The COMMIX-2 code has modular structure. This permits rapid implementation of the latest available drag models, heat transfer models, boiling models etc.

9. The code has also an option permitting use of either sodium property package or water property package.

10. The program also contains

(i) A generalized resistance model to permit determination of resistance due to internal structures (fuel rods, wire wrap, baffles, grid spacers, etc.)

(ii) A generalized thermal structure formulation to model thermal interaction between structures (fuel rods, wire wraps, duct wall, baffles, etc.) and surrounding fluid, and

(iii) A local regional mass rebalancing scheme, such as plane by plane, for improving the convergence rate.

This report describes the COMMIX-2 program for the solution of the governing equations for three-dimensional, single-phase/two-phase, steady/unsteady flow with heat transfer. The description here starts with the differential equations and deals with numerical method incorporated into a computer program. Section 2 is devoted to the set of governing equations for the situation considered. In Subsection 2.4, the general form of all the governing equations is recognized; this generalization facilitates a unified development of the numerical method and the construction of the computer program.

The conservation equations for quasi-continuum regime are presented in Section 3. We define the quasi-continuum regime as a medium which contains finite, dispersed, stationary heat generating (or absorbing) solid objects. The effects of solid objects in a medium are accounted for by introducing volume porosity surface permeabilities, distributed resistance, and distributed heat sources. The physical models and constitutive equations used in COMMIX-2 for describing the mass, momentum and energy exchange phenomena are presented in Section 4.

In Section 5 we present some preliminary considerations before we start assembling the finite difference equations. The finite difference formulation of the general equation is presented in Section 6. As we use a staggered grid system, the control volumes for momentum equations are different and require special considerations. The special features of the finite-difference equations for momentum are discussed in Section 7. In Section 8 we have presented the finite difference forms of the continuity equations.

Section 9 contains the derivation of pressure and pressure correction equations. In the present program we have two alternative forms of pressure correction equation leading to two alternative solution procedures. The first procedure is an extension of the single-phase numerical procedure,[3] known as SIMPLER (Semi-Implicit Method for Pressure Linked Equation-Revised). In this procedure we use one of the two phase continuity equations to determine the liquid volume fractions, and use the combined continuity equation to derive the pressure correction equation. In the second procedure we use both of the phase continuity equations to determine the liquid volume fractions; the difference lies in the derivation of the pressure correction equation. In this procedure we differentiate the phase continuity equations and momentum equations and then combine them to obtain the pressure correction equation. This is analogous to the numerical procedure[5] known as Inter Phase Slip Analyzer [IPSA].

Section 10 deals with the boundary conditions for the different dependent variables. A discussion of the ways of handling irregular geometries is included in Subsection 10.4. A line-by-line procedure for solving the finite-difference equations is presented in Section 11. For most of the problems analyzed, this procedure has been found to be superior to the usual point-by-point procedure without rebalance technique. In Section 12, we take an overall view of the entire calculation sequence. The various steps in the iteration scheme are listed in Section 12.1, while the remainder of Section 12 is devoted to matters that enhance the chances of obtaining a converged solution. Section 13 describes the flow chart.

The thermodynamic and transport properties of sodium and water are given in Appendix A. The thermal structure module is described in Appendix B. Appendix C contains the descriptions of the resistance and wire wrap models. The code input description and sample problems are given in Appendices D and E, respectively.

2. DIFFERENTIAL EQUATIONS: CONTINUUM

The governing equations for a single-phase/two-phase, three-dimensional, unsteady flow with heat transfer are given here in Cartesian tensor notation. For two-phase flow, we use the two-fluid model of Harlow and Amsden[1] to describe the conservation equations of mass, momentum and energy. The three coordinate directions, x, y, z, are denoted by x_i, and the three velocity components, u, v, and w are denoted by u_i. A repeated index implies the sum of three terms; that is:

$$\frac{\partial u_i}{\partial x_i} = \frac{\partial u}{\partial x} + \frac{\partial v}{\partial y} + \frac{\partial w}{\partial z}. \tag{2.1}$$

The subscripts ℓ and g are used to denote liquid-phase and gas-phase respectively. However, when the formulation is applicable to both phases or when the formulation is for a specific phase, we have avoided the subscript ℓ or g.

2.1 Continuity Equations

The phase continuity equation:

$$\frac{\partial[\rho\theta]}{\partial t} + \frac{\partial}{\partial x_i}[\rho\theta u_i] = \Omega. \tag{2.2a}$$

Here, Ω is the source term due to phase change [evaporation or condensation] and θ is the void fraction. By combining the two continuity equations, we eliminate the source terms, because $\Omega_\ell = -\Omega_g$, and obtain

$$\frac{\partial}{\partial t}[\rho_\ell\theta_\ell + \rho_g\theta_g] + \frac{\partial}{\partial x_i}[\rho_\ell\theta_\ell u_{\ell i} + \rho_g\theta_g u_{gi}] = 0. \tag{2.2b}$$

2.2 Momentum Equations

For liquid-phase and for the j direction:

$$\frac{\partial}{\partial t}[\rho\theta u_j] + \frac{\partial}{\partial x_i}[\rho\theta u_i u_j] = -\theta\frac{\partial p}{\partial x_j} + \frac{\partial}{\partial x_i}\left(\mu\theta\frac{\partial u_j}{\partial x_i}\right) + \rho\theta g_j + V_j$$

$$+ K[u_{gj} - u_{\ell j}] + S_{m\Omega} \tag{2.3}$$

The subscript j can take the value 1, 2, or 3 depending on the momentum direction chosen. The subscript i is a repeated index and implies the summation convention outlined in Eq. 2.1. The term $S_{m\Omega}$ is a source to the momentum field due to phase change and K is the interfacial drag coefficient. The viscous contribution to the momentum equation is expressed by two terms:

$$\frac{\partial}{\partial x_i}\left[\mu\theta \frac{\partial u_j}{\partial x_i}\right],$$

and V_j, which is given by

$$V_j = \frac{\partial}{\partial x_i}\left[\mu\theta\left(\frac{\partial u_i}{\partial x_j}\right)\right]. \tag{2.4}$$

For turbulent flow, all quantities in Eqs. 2.3 and 2.4 are considered time averaged values and the viscosity μ is interpreted as the effective viscosity.

2.3 Energy Equations

For liquid-phase:

$$\frac{\partial}{\partial t}[\rho\theta h] + \frac{\partial}{\partial x_i}[\rho\theta u_i h] = \frac{\partial}{\partial x_i}\left(\Gamma_h \theta \frac{\partial h}{\partial x_i}\right) + \theta\left(\frac{\partial p}{\partial t}\right) + R[T_g - T_\ell] + \Phi + Q + S_{h\Omega} \tag{2.5}$$

Here, Γ_h stands for λ/c_p, where λ is the thermal conductivity, and c_p is the specific heat at constant pressure. The heat generation rate per unit volume, the source due to phase change, the interfacial heat transfer coefficient, and viscous dissipation are denoted by Q, $S_{h\Omega}$, R, and Φ, respectively. The term $\partial p/\partial t$ accounts for the fact that the internal energy [rather than enthalpy] is stored in a fluid.

For turbulent flow, Γ_h is interpreted as the effective transport coefficient for enthalpy. Calculation of the effective viscosity and the effective transport coefficient for the enthalpy often requires additional differential equations. One such proposal is the K-ε-g model described in Ref. 6.

2.4 General Form

Equations 2.2, 2.3, and 2.5 can be seen to possess a common form. If the general dependent variable is denoted by ϕ, the corresponding differential equation has the form:

$$\frac{\partial}{\partial t}[\rho\theta\phi] + \frac{\partial}{\partial x_i}[\rho\theta u_i \phi] = \frac{\partial}{\partial x_i}\left(\Gamma_\phi \theta \frac{\partial \phi}{\partial x_i}\right) + S_\phi + S_{\phi\Omega}, \tag{2.6}$$

where the five terms can be referred to as: the unsteady term, the convection term, the diffusion term, the source term and the source term due to phase change. The density ρ and the velocity components u_i satisfy the continuity equation 2.2. The diffusion coefficient Γ_ϕ and the source term S_ϕ are specific to each meaning of ϕ. Source terms for all conservation equations are given in Table 2.1. The recognition of this general form of the governing differential equations is important as much of the formulation described in the following sections is referenced to Eq. 2.6 alone.

TABLE 2.1. Source Terms for Continuity, Momentum, and Energy Equations

Equation	Variable	ϕ	Source Term S_ϕ	Source Term $S_{\Omega\phi}$
Continuity	Volume fraction (Liquid phase)	1	-	Ω_ℓ
Momentum	Velocity Liquid phase; i-direction	U_ℓ	$\rho\theta g_{x_i} + V_{x_i} + K(U_g - U_\ell) - \theta\frac{\partial p}{\partial x_i}$	$-\Omega_g U_\ell$
Momentum	Velocity Gas phase; i-direction	U_g	$\rho\theta g_{x_i} + V_{x_i} + K(U_\ell - U_g) - \theta\frac{\partial p}{\partial x_i}$	$\Omega_g U_\ell$
Energy	Enthalpy Liquid phase	h_ℓ	$\theta\frac{\partial p}{\partial t} + \Phi + Q + R(T_g - T_\ell)$	$-\Omega_g h_g$
Energy	Enthalpy Gas phase	h_g	$\theta\frac{\partial p}{\partial t} + \Phi + Q + R(T_\ell - T_g)$	$\Omega_g h_g$

3. CONSERVATION EQUATIONS: QUASI-CONTINUUM

3.1 Flow Domain with Solid Objects

The presence of solid objects in a flow domain has two effects on fluid flow. One is the geometrical effect; here the presence of solid objects influences the flow by reducing the available space. This effect is taken into account by including volume porosity and surface permeabilities in the governing equations. The second is the physical effect; here, the solid objects influence the momentum and heat transfer to fluid flow. This effect is taken into account by considering solid objects within a control volume as distributed resistances to momentum transfer and distributed heat sources (or sinks) for heat transfer.

In applying the concept of volume porosity and surface permeability, we are assuming that a real system containing numerous solid objects can be replaced by an idealized system having distributed solid objects such that both systems have the same volumetric porosities, same surface permeabilities, and same interactions [momentum and heat transfer] between fluid and solid surfaces.

3.2 Volume Porosity and Surface Permeability

We consider a fixed finite region of volume V in space with enveloping surface A. There are finite numbers of dispersed, fixed heat generating solids inside V; some may be cut through by A as illustrated in Fig. 3.1. Clearly, $V = V_f + V_s$, where V_f is the total fluid volume and V_s is the total solid volume. Only a fraction of the enveloping surface A is unobstructed to fluid flow.

We define γ_v as the volume porosity, i.e., the fraction of the local volume inside V that is occupied by the fluid. It may take on a value equal to or between

0 and 1. If the volume under consideration is completely inside a dispersed solid, $\gamma_v = 0$; if it is completely in the fluid, $\gamma_v = 1$. If the volume is partly in a dispersed solid and partly in fluid, then $0 < \gamma_v < 1$. Hence, in general, $0 \leq \gamma_v \leq 1$.

The surface permeability γ_a is defined as the fraction of the local surface in A that is unobstructed to fluid flow. It is easy to see that, in general, $0 \leq \gamma_a \leq 1$. We define the average volume porosity as:

$$\gamma_v = \frac{1}{V} \int_v \bar{\gamma}_v \, dv, \tag{3.1}$$

and the average surface permeability as

$$\gamma_{x_i} = \frac{1}{A_{x_i}} \int_{A_{x_i}} \bar{\gamma}_{x_i} \, da_{x_i}. \tag{3.2}$$

Here, $\bar{\gamma}_v$ and $\bar{\gamma}_{x_i}$ are the local volume porosity and local surface permeability respectively, with their values equal to unity while in fluid and equal to zero while in solid, and the subscript x_i refers to the direction normal to the surface area under consideration. Since the unobstructed area $(A_f)_{x_i}$ that is available for free fluid flow is

$$(A_f)_{x_i} = \int_{A_{xi}} \gamma_{x_i} \, da, \tag{3.3}$$

it follows immediately that

$$(A_f)_{x_i} = \gamma_{x_i} A_{x_i}. \tag{3.4}$$

Similarly,

$$V_f = \gamma_v V. \tag{3.5}$$

3.3 Continuity Equations

The formulations of the conservation equations for quasi-continuum flow domain are given in Ref. 7. We are presenting here only the final equations.

We consider a stationary volume element

$$\Delta V = \Delta x \Delta y \Delta z, \tag{3.6}$$

through which fluid is flowing (see Fig. 3.2). Its enveloping surface in Cartesian coordinates is

$$\Delta A = 2(\Delta y \Delta z + \Delta z \Delta x + \Delta x \Delta y).$$

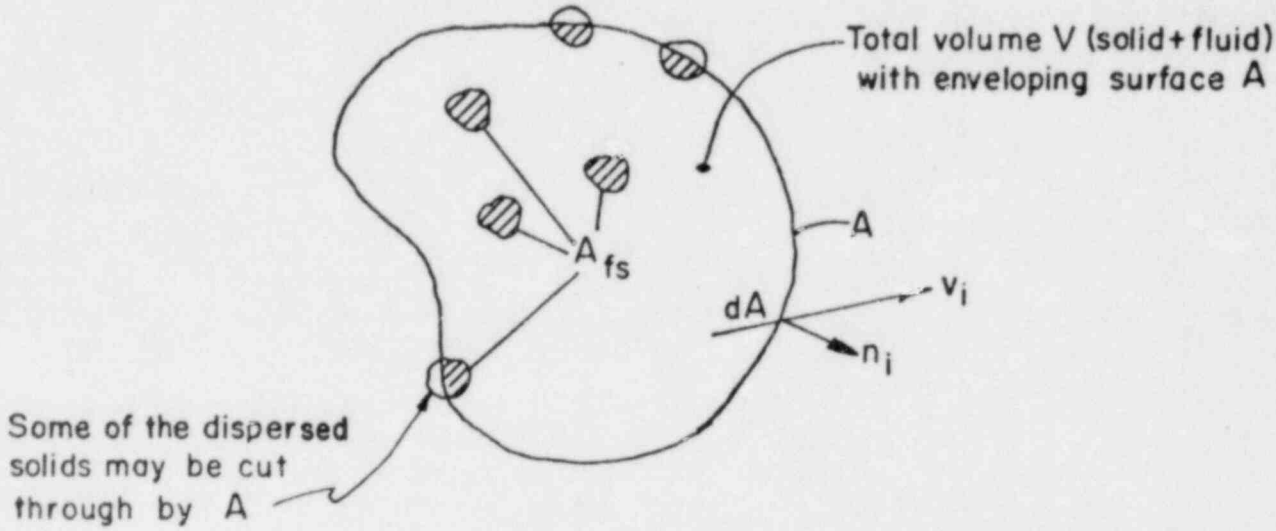

Fig. 3.1. Domain containing dispersed solid objects

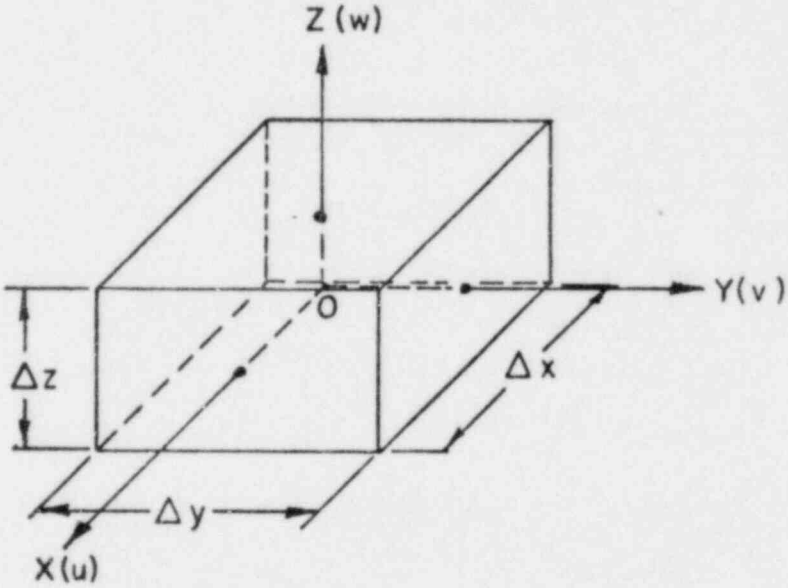

Fig. 3.2. Finite control volume in Cartesian coordinates

The centroid of V is located at 0 (x,y,z). The velocity components in the x, y and z directions are u, v, and w respectively. The phase continuity equation is:

$$\gamma_v \frac{\partial(\rho\theta)}{\partial t} + \frac{\Delta(\rho\theta u\gamma_x)}{\Delta x} + \frac{\Delta(\rho\theta v\gamma_y)}{\Delta y} + \frac{\Delta(\rho\theta w\gamma_z)}{\Delta z} = \Omega\gamma_v. \tag{3.7}$$

Here, Ω is the source per unit fluid volume and we define,

$$\frac{\Delta()}{\Delta x_j} = \frac{()_{x_j + \Delta x_j/2} - ()_{x_j - \Delta x_j/2}}{\Delta x_j}. \tag{3.8}$$

3.4 Momentum Equations

The momentum equation for liquid phase in the x direction is

$$\frac{\partial}{\partial t}[\rho\theta u\gamma_v] + \frac{\Delta[\rho\theta u^2\gamma_x]}{\Delta x} + \frac{\Delta[\rho\theta uv\gamma_y]}{\Delta y} + \frac{\Delta(\rho\theta uw\gamma_z)}{\Delta z} = (\rho\theta g_x\gamma_v) - \theta\gamma_x\frac{\Delta p}{\Delta x}$$

$$+ \frac{\Delta(\theta\tau_{xx}\gamma_x)}{\Delta x} + \frac{\Delta(\theta\tau_{xy}\gamma_y)}{\Delta y} + \frac{\Delta(\theta\tau_{xz}\gamma_z)}{\Delta z} + \gamma_v K(u_g - u_\ell) - \gamma_v R_x + \gamma_v S_{m\Omega}. \tag{3.9}$$

Here, R_x is the distributed frictional resistance per unit fluid volume in the x direction. Equations for gas-phase and for other directions are similar.

3.5 Energy Equations

The energy equation for the liquid phase is

$$\frac{\partial}{\partial t}[\rho\theta h\gamma_v] + \frac{\Delta(\rho\theta uh\gamma_x)}{\Delta x} + \frac{\Delta(\rho\theta vh\gamma_y)}{\Delta y} + \frac{\Delta(\rho\theta wh\gamma_z)}{\Delta z} = \gamma_v\frac{d(p\theta)}{dt}$$

$$+ \gamma_v[\dot{Q}_s + \dot{Q} + \Phi + R(T_g - T_\ell) + S_{h\Omega}] + \left[\frac{\Delta\left(\theta\gamma_x\lambda\frac{\partial T}{\partial x}\right)}{\Delta x} + \frac{\Delta\left(\theta\gamma_y\lambda\frac{\partial T}{\partial y}\right)}{\Delta y}\right.$$

$$\left. + \frac{\Delta\left(\theta\gamma_z\lambda\frac{\partial T}{\partial z}\right)}{\Delta z}\right]. \tag{3.10}$$

Here, $\dot{Q}$ is the distributed heat source per unit fluid volume and $\dot{Q}_s$ is the rate of heat transfer between fluid and dispersed solid objects per unit fluid volume. The energy equation for the gas phase is similar.

4. CONSTITUTIVE EQUATIONS

The constitutive equations that are currently incorporated in COMMIX-2, are described here. Most of these constitutive equations are suitable only for dispersed flow analysis. However, the subroutines are designed such that one can modify any correlation or incorporate a new correlation with minimal changes.

4.1 Phase Change Rates

The mass exchange rates between the phases, evaporation and condensation rates, are determined in the subroutine BOIL using the following expressions.

$$\Omega_g = -\Omega_\ell = J_{evap} - J_{cond} \tag{4.1}$$

$$J_{evap} = \lambda A \rho_\ell \bar{\theta}_g (T_\ell - T_{sat})(R/T_{sat\ abs})^{1/2}, \quad T_\ell > T_{sat}$$

$$= 0, \text{ for } T_\ell < T_{sat} \tag{4.2}$$

$$J_{cond} = \lambda A \rho_g \bar{\theta}_\ell (T_{sat} - T_g)(R/T_{sat\ abs})^{1/2}, \quad T_{sat} > T_g$$

$$= 0, \text{ for } T_{sat} < T_g. \tag{4.3}$$

Here,

$$A = (4\pi N/3)^{1/3}\, \bar{\theta}_g^{\,2/3}, \quad \bar{\theta}_g < 0.5$$

$$= (4\pi N/3)^{1/3}(1 - \bar{\theta}_g)^{2/3}, \quad \bar{\theta}_g > 0.5 \tag{4.4}$$

$$\bar{\theta}_g = \min\left\{0.9999,\ \max(0.0001, \theta_g)\right\}, \tag{4.5}$$

N is the number of bubbles, R is the gas constant (J/kg•K) and λ is the constant coefficient.

4.2 Interfacial Friction

In the subroutine KCOEF four different correlations are included for computing the interfacial friction function K. These are:

Autruffe et al.[8]

$$K = \lambda_1 \frac{1}{2} \frac{\rho_\ell}{D_h} |u_g - u_\ell| \left\{(1 - \theta_g)[1 + 75(1 - \theta_g)]\right\}^{0.95} \tag{4.6}$$

Here, D_h is the hydraulic diameter and λ_1 is the constant coefficient.

Harlow and Amsden[9]

$$K = \frac{3}{4}\theta_g \frac{1}{r}\left[\frac{6\nu_\ell \rho_g}{r} + \frac{1}{2}\rho_\ell C_D |u_g - u_\ell|\right] \tag{4.7}$$

Here, r is the radius of a bubble and C_D is the drag coefficient.

Rexroth and Starkovich[10]

$$K = \frac{3}{4}\frac{\theta_\ell}{\theta_g^{5.7} r^2}\left[6\frac{\rho_g}{\rho_\ell}\mu_\ell + \frac{1}{2}\rho_\ell r C_D |u_g - u_\ell|\right] \tag{4.8}$$

Rivard and Torrey[11]

$$K = \frac{3}{8}(\rho_g + \rho_\ell)\left[\frac{12\nu}{r} + C_D |u_g - u_\ell|\right]\frac{1}{r} \tag{4.9}$$

Here,

$$\nu = \theta_g \nu_g + \theta_\ell \nu_\ell, \tag{4.10}$$

is the mixture kinematic viscosity,

$$A = \theta_g^{2/3}\left(\frac{4\pi N}{3}\right)^{1/3}, \ \theta_g < 1/2; \quad A = \theta_\ell^{2/3}\left(\frac{4\pi N}{3}\right)^{1/3}, \ \theta_g > 1/2 \tag{4.11}$$

is the area of contact, and

$$r = \left(\frac{4\pi N}{3\theta_g}\right)^{-1/3}, \ \theta_g < 1/2; \quad r = \left(\frac{4\pi N}{3\theta_\ell}\right)^{-1/3}, \ \theta_g > 1/2 \tag{4.12}$$

is the radius of a bubble.

General Form

The general form of all of these correlations is

$$K = \lambda_1\left[\lambda_2\lambda_3 \frac{1}{2}\rho_g |u_\ell - u_g| + \lambda_4\right] \tag{4.13}$$

where,

K = Interfacial friction coefficient, $kg/m^3 \cdot sec$

λ_1 = Constant coefficient

λ_2 = Friction factor

λ_3 = Surface area per unit volume, 1/m

λ_4 = Contribution corresponding to viscous drag; Stokes equation, $kg/m^3 \cdot sec$.

An option has been included to permit the use of constant input value for interfacial drag coefficient K.

4.3 Interfacial Heat Transfer

The following model is used in subroutine RCOEF for computing interfacial energy exchange.

$$\dot{q}_{g\ell} = R(T_g - T_\ell) = \max(\dot{q}_{\ell p}, \dot{q}_{gp}) \tag{4.14}$$

where,

$$\dot{q}_{\ell p} = h_{\ell p} A(T_{sat} - T_\ell) \tag{4.15}$$

is the energy exchange between liquid and interface,

$$\dot{q}_{gp} = h_{gp} A(T_g - T_{sat}) \tag{4.16}$$

is the energy exchange between interface and vapor,

$$h_{gp} = 8.067\ k_g/r, \tag{4.17}$$

is the vapor side heat transfer coefficient, k_g is the thermal conductivity of gas,

$$h_{\ell p} = k_\ell \left[\frac{2|u_\ell - u_g| 0.25\ Pr_\ell^{-0.33}}{\pi \alpha_\ell} + \frac{1}{r} \right] \tag{4.18}$$

is the convective heat transfer coefficient on the liquid side, r is the bubble radius, α is the thermal diffusivity, and A is the interfacial surface area per unit volume.

In addition, an option has been included so that one can specify a desired value for interfacial heat transfer coefficient R.

4.4 Wall Friction

COMMIX-2 has the following two models for computing the effect of wall friction. The resistive forces are calculated in the subroutine FRICTW.

Simplified Mode

$$F_\ell = 2f\rho_\ell \theta_\ell |w_\ell| w_\ell / D_h \tag{4.19}$$

and

$$F_g = 2f\rho_g \theta_g |w_g| w_g / D_h \tag{4.20}$$

Here, F_ℓ and F_g are resistive forces, f is the friction coefficient, and D_h is the hydraulic diameter.

Rivard and Torrey[11]

$$F_g = \theta_g \left\{ f\rho_\ell w_\ell^2 \theta_\ell^2 \Big/ (2D_h) \right\} \phi^2, \tag{4.21}$$

and

$$F_\ell = \theta_\ell \left\{ f\rho_\ell w_\ell^2 \theta_\ell^2 \Big/ (2D_h) \right\} \phi^2, \tag{4.22}$$

Here, friction factor f is given by

$$f = 1.74 - 2\ \mathrm{Log}_{10}\left[2(\varepsilon/D_h) + 18.7 f^{-1/2}/\mathrm{Re} \right], \tag{4.23}$$

the Reynolds number

$$\mathrm{Re} = (\rho \theta w D_h/\mu)_\ell, \tag{4.24}$$

the multiplier

$$\phi^2 = \theta_\ell^{-2}(\rho_g + \rho_\ell)/\rho_\ell, \text{ (Dispersed flow)}$$

$$= 1/\theta_\ell^2, \text{ (Annular flow)} \tag{4.25}$$

and ε/D_h is the wall roughness.

4.5 Wall Heat Transfer

The following heat transfer correlations are provided for computing wall heat transfer for different flow regimes.

4.5.1: Sodium

1. Single Phase Liquid[12]:

$$\mathrm{Nu} = \frac{h_\ell D_h}{k_\ell} = F_{geom}(\mathrm{RePr})^{0.3} \text{ (for RePr > 150)} \tag{4.26}$$

$$\mathrm{Nu} = \frac{h_\ell D_h}{k_\ell} = 4.5\ F_{geom} \text{ (for RePr < 150)} \tag{4.26a}$$

2. Nucleate Boiling: Granziera and Kazimi[12] (Modified Chen Correlation)

$$q'' = F_{Re}^{0.375}\ h_\ell (T_w - T_\ell) + h_{NB}(T_w - T_{sat}) \tag{4.27}$$

Here,

$$h_{NB} = 0.00122 \frac{\left[k^{0.79}(\rho c_p)^{0.45}\right]_\ell (\Delta p)^{0.75} S_f}{\sigma^{0.5} \mu_\ell^{0.29}} \left(\frac{T_w - T_{sat}}{h_{fg}\rho_g}\right)^{0.24}, \tag{4.28}$$

F_{Re} is the Reynolds number factor, F_{geom} is the geometrical factor, and h_ℓ is the single phase heat transfer coefficient for liquid. Here,

$$\Delta p = p_{sat}(T_w) - p_{sat}(T_\ell), \tag{4.29}$$

the suppression factor

$$S_f = \begin{cases} (1 + 0.12Re_{TP}^{1.14})^{-1}; & Re_{TP} < 32.5 \\ (1 + 0.42Re_{TP}^{0.78})^{-1}; & 32.5 < Re_{TP} < 70 \\ 0.1; & Re_{TP} > 70, \end{cases} \tag{4.30}$$

the two-phase Reynolds number

$$Re_{TP} = F_{Re}^{1.25}\left(\frac{\rho\theta u}{\mu}\right)_\ell D_h \cdot 10^{-4}, \tag{4.31}$$

$$F_{Re} = \begin{cases} 2.35\left(0.213 + \frac{1}{x_{tt}}\right)^{0.736}; & x_{tt} < 10 \\ 1; & x_{tt} > 10, \end{cases} \tag{4.32}$$

$$F_{geom} = -16.15 + 24.96(P/D) - 8.55(P/D)^2 \tag{4.33}$$

(Equations 4.26-4.27), P/D is the pitch to diameter ratio, σ is the surface tension and x_{tt} is the Martinelli parameter.

3. Film Boiling: Granziera and Kazimi[12]

$$h_{FB} = h_\ell F_1 + h_g. \tag{4.34}$$

Here,

$$F_1 = F_{Re}^{0.375}(12 - 12.5\theta_g)^3, \tag{4.35}$$

and h_g is the single phase vapor heat transfer coefficient.

4. Single-phase Vapor: Dittus and Boelter[13]

$$(Nu)_g = 0.023(Re)_g^{0.8}(Pr)_g^{0.4} \tag{4.36}$$

5. Condensation:

$$h_{cond} = \begin{cases} h_\ell F_{Re} \text{ for } \theta_g < 0.88 & (4.37) \\ h_\ell F_1 + h_g \text{ for } \theta_g > 0.88 & (4.38) \end{cases}$$

4.5.2: Water

1. Forced Convection: Sieder and Tate[14] (Liquid or Vapor)

$$(Nu) = 0.023(Re)^{0.8}(Pr)^{0.33}\left(\frac{\mu}{\mu_w}\right)^{0.14} \tag{4.39}$$

Fluid properties at bulk fluid temperature, except μ_w at T_w.

2. Free Convection: McAdams[15] (Liquid or Vapor)

$$(Nu) = 0.13\left\{\frac{\rho^2 g\beta(T_w - T)\ PrD^3}{\mu^2}\right\}^{1/3} \tag{4.40}$$

Here,

β is the coefficient of thermal expansion, and is equal to $1/T_g$ for vapor. Fluid properties are evaluated at fluid film temperature. Higher value of h between (4.39) and (4.40) is used.

3. Subcooled Boiling; Nucleate Boiling; Vaporization

$$\dot{q}'' = F_{Re}h_\ell(T_w - T_\ell) + h_{NB}(T_w - T_{sat}) \tag{4.41}$$

Here, h_ℓ is obtained from equation (4.36) but with liquid properties and h_{NB} from equation (4.28).

4. Critical Heat Fluxes

High Flow ($G > G_1$): Biasi[16]

$$\dot{q}''_{CHF} = \frac{2.764 \times 10^7}{(100D)^n}\ G^{-1/6}\{1.468F_2\ G^{-1/6} - x\} \tag{4.42}$$

$$\dot{q}''_{CHF} = \frac{7.086 \times 10^7}{(100D)^n}\ G^{-0.6}\ F_3(1 - x) \tag{4.43}$$

Here,

$$F_2 = 0.7249 + 0.099p\cdot10^{-5}\ \exp(-0.032p\cdot10^{-5}), \tag{4.44}$$

$$F_3 = -1.159 + 0.149p\cdot10^{-5}\ \exp(-0.019p\cdot10^{-5})$$

$$+\ 9p\cdot10^{-5}\left(10 + (p\cdot10^{-5})^2\right)^{-1}, \tag{4.45}$$

and

$$n = \begin{cases} 0.4 \text{ for } D > 0.01 \text{ m} \\ 0.6 \text{ for } D \leq 0.01 \text{ m} \end{cases} \tag{4.46a}$$

We use equation (4.43) for $G < 300$ kg/m^2•sec and use the larger of the two values, equations (4.42) and (4.43), for $G > 300$.

Low Flow ($G \leq 27$): Modified Zuber[17,18]

$$\dot{q}''_{CHF} = 0.131\theta_\ell \rho_g h_{fg} \left\{ \frac{\sigma g(\rho_\ell - \rho_g)}{\rho_g^2} \right\}^{0.25} . \tag{4.46}$$

For $27 < G < G_1$, we use linear interpolation between the Biasi and Modified Zuber correlations. Here $G_1 = 270$ kg/m^2•sec for $p10^{-5} > 83$ and $x > 0.5$, otherwise $G_1 = 1350$ kg/m^2•sec.

5. Minimum Stable Film Boiling Temperature: Berenson[19]

$$T_{MSFB} = T_{HN} + (T_{HN} - T_\ell)[(\rho kc_p)_\ell/(\rho kc_p)_w]^{0.5} - \psi(P) \tag{4.47}$$

Here,

$$T_{HN} = \begin{cases} 581.5 + 0.01876(P - 1.034\cdot10^5)^{0.5}, & P \leq P_0 \quad (4.48) \\ 630.39 + 0.004321(P - P_0)^{0.5} & P > P_0 \quad (4.49) \end{cases}$$

$$P_0 = 68.95 \times 10^5 \text{ Pa} \tag{4.50}$$

$$\Psi(P) = \begin{cases} 0 & P \geq 4.826\cdot10^5 \text{ Pa} \quad (4.51) \\ 127.3 - 26.37\cdot10^{-5}\ p & P < 4.826\cdot10^5 \text{ Pa} \quad (4.52) \end{cases}$$

Note: $(\rho kc_p)_w$ above refers to properties of the wall itself, i.e. clad surface material properties.

6. Transition Boiling

$$h_{TB} = \frac{\delta \dot{q}''_{CHF} + (1 - \delta)\, \dot{q}''_{MSFB}}{T_w - T_{sat}} \tag{4.53}$$

Here,

$$\delta = \left(\frac{T_{MSFB} - T_w}{T_{MSFB} - T_{CHF}}\right)^2 \tag{4.54}$$

We use the following Chen correlation for computing T_{CHF}.

$$\dot{q}''_{CHF} = h_\ell\left(T_{CHF} - T_\ell\right) + h_{NB}\left(T_{CHF} - T_{sat}\right)^{1.24}\left(p_{sat}(T_w) - p\right)^{0.75} \tag{4.55}$$

As h_{NB} (Eq. 4.28) is a function of wall temperature (T_{CHF}), an iteration procedure is required.

7. Film Boiling (Eq. 5.7 of Groeneveld and Delorme[20])
(High pressure; high flow)

$$\frac{hD}{k_g} = a\left(Pr_g\right)^c\left\{Re_g\left(x + \frac{\rho_g}{\rho_\ell}(1 - x)\right)\right\}^b$$
$$\times\left\{1 - 0.1(1 - x)^{0.4}\left(\frac{\rho_\ell}{\rho_g} - 1\right)^{0.4}\right\}^d \tag{4.56}$$

where

$$a = 0.052,$$
$$b = 0.688,$$
$$c = 1.26,$$
$$d = -1.06. \tag{4.57}$$

8. Low Pressure High-Flow Film Boiling: (Dougall and Rohsenow[21])

$$(Nu)_g = 0.023\left(Pr_g\right)^{0.4}\left[Re_g\left(x + \frac{\rho_g}{\rho_\ell}(1 - x)\right)\right]^{0.8} \tag{4.58}$$

9. Low-Flow Film Boiling: (Bjornard)[19]

$$h = \theta_g \max\left\{h_g, h_{hf}\right\} + \left(1 - \theta_g\right) h_{mB} \tag{4.59}$$

Here h_g is the single phase heat transfer coefficient for vapor (Eq. 4.40), h_{hf} is the high flow film heat transfer coefficient (Eq. 4.56) and h_{mB} is the heat transfer coefficient obtained from the modified Bromley[19] relation,

$$h_{MB} = 0.62 \left\{ \frac{g k_g^3 \rho_g (\rho_\ell - \rho_g) h'_{fg} \sqrt{\frac{g(\rho_\ell - \rho_g)}{\sigma}}}{2\pi (T_w - T_{sat}) \mu_g} \right\}^{0.25} . \tag{4.60}$$

$$h'_{fg} = h_{fg} + 0.5 C_p (T_w - T_{sat}) \tag{4.60a}$$

10. Horizontal Film Condensation: Chato[22]

$$h = 0.296 \left\{ \frac{\rho_\ell (\rho_\ell - \rho_g) g h_{fg} k_\ell^3}{D \mu_\ell (T_{sat} - T_w)} \right\}^{1/4} \tag{4.61}$$

11. Vertical Film Condensation: Collier[23]

$$h = 1.132 \left\{ \frac{\rho_\ell (\rho_\ell - \rho_g) h_{fg} k_\ell^3 g \cos\theta}{D \mu_\ell (T_{sat} - T_w)} \right\}^{1/4} \tag{4.62}$$

12. Turbulent Film Condensation: Carpenter and Colburn[24]

$$h = 0.065 \frac{k_\ell \rho_\ell^{1/2}}{\mu_\ell} (Pr)^{1/2} \tau_i^{1/2} , \tag{4.63}$$

where the interfacial shear, τ_i, is

$$\tau_i = \frac{0.046}{(Re_g)} \left(\frac{\rho_g u^2}{2} \right) \tag{4.63a}$$

Equation (4.63) replaces equations (4.61) or (4.62) whenever it yields higher value.

13. When CHF Calculation is Bypassed

$$h = \max (h_{lam}, h_{turb}) \tag{4.64}$$

Here, h_{lam} and h_{turb} are the laminar and turbulent heat transfer coefficients given by the following relations.

$$h_{lam} = 4.0 \frac{k_m}{D} \tag{4.65}$$

$$h_{turb} = 0.023 \frac{k_m}{D} (Re_m)^{0.8} (Pr_\ell)^{0.4} \tag{4.66}$$

Here, the two-phase mixture properties are defined by

$$\phi_m = \frac{1}{\frac{x}{\phi_g} + \frac{1 - x}{\phi_\ell}} . \tag{4.67}$$

The sodium and water wall heat transfer logics are presented in the form of flow charts in Figs. 4.1 and 4.2. The regions of applications of these correlations are shown in Figs. 4.3 and 4.4.

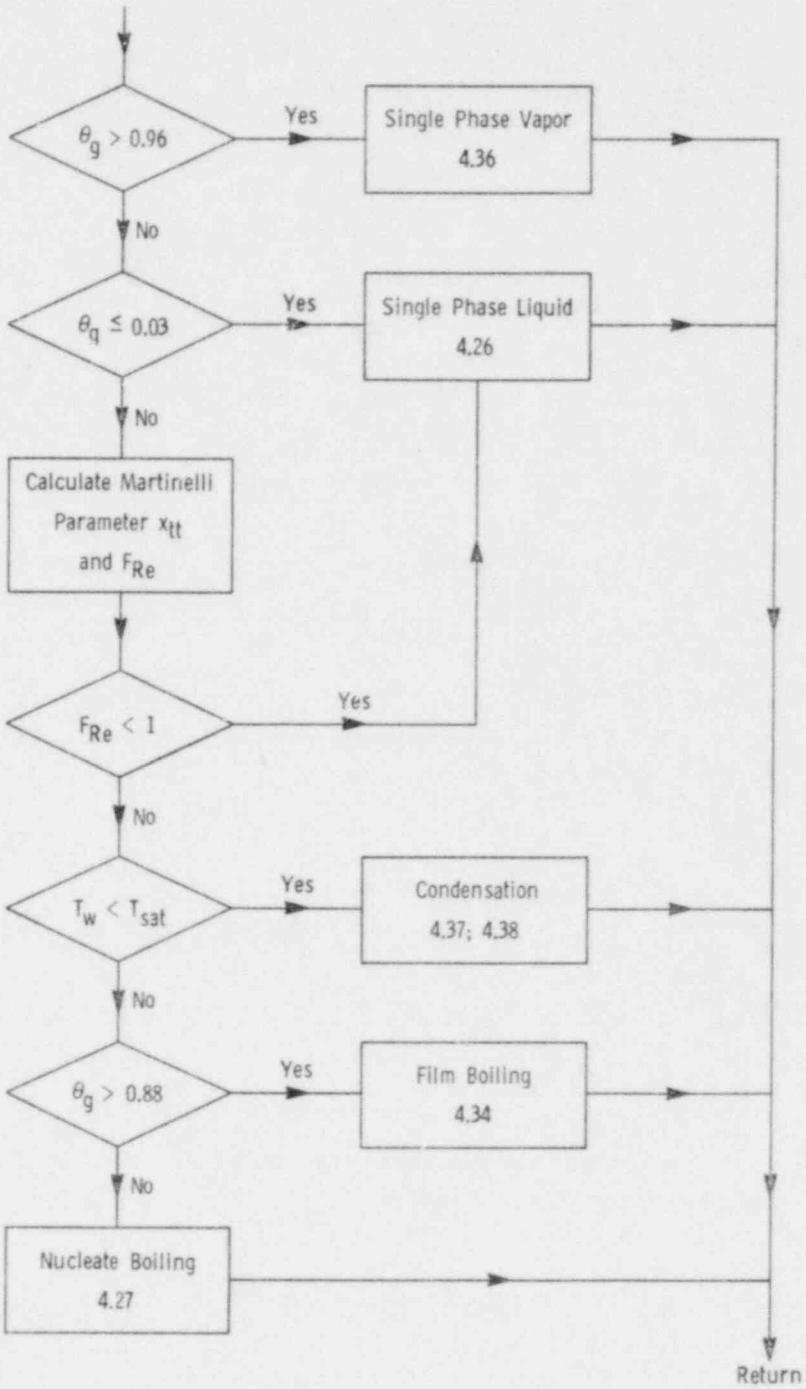

Fig. 4.1. Wall Heat Transfer Logic—Sodium

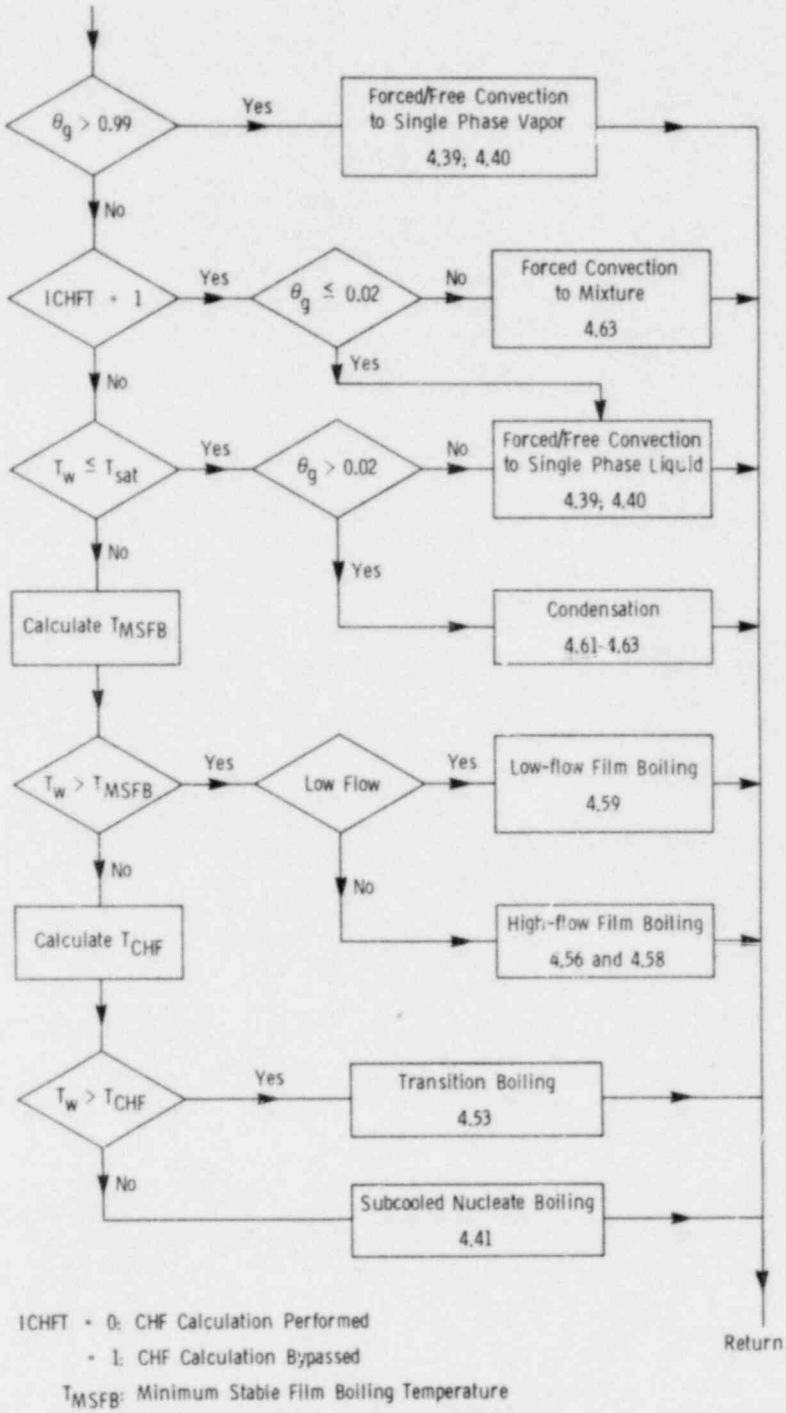

ICHFT = 0: CHF Calculation Performed
= 1: CHF Calculation Bypassed
T_{MSFB}: Minimum Stable Film Boiling Temperature

Fig. 4.2. Wall Heat Transfer Logic—Water

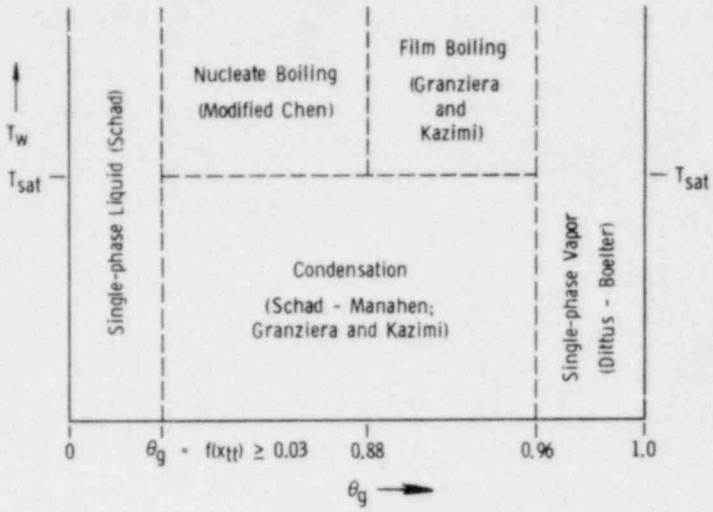

Fig. 4.3

Wall Heat Transfer Correlations and Their Regions of Applications: Sodium

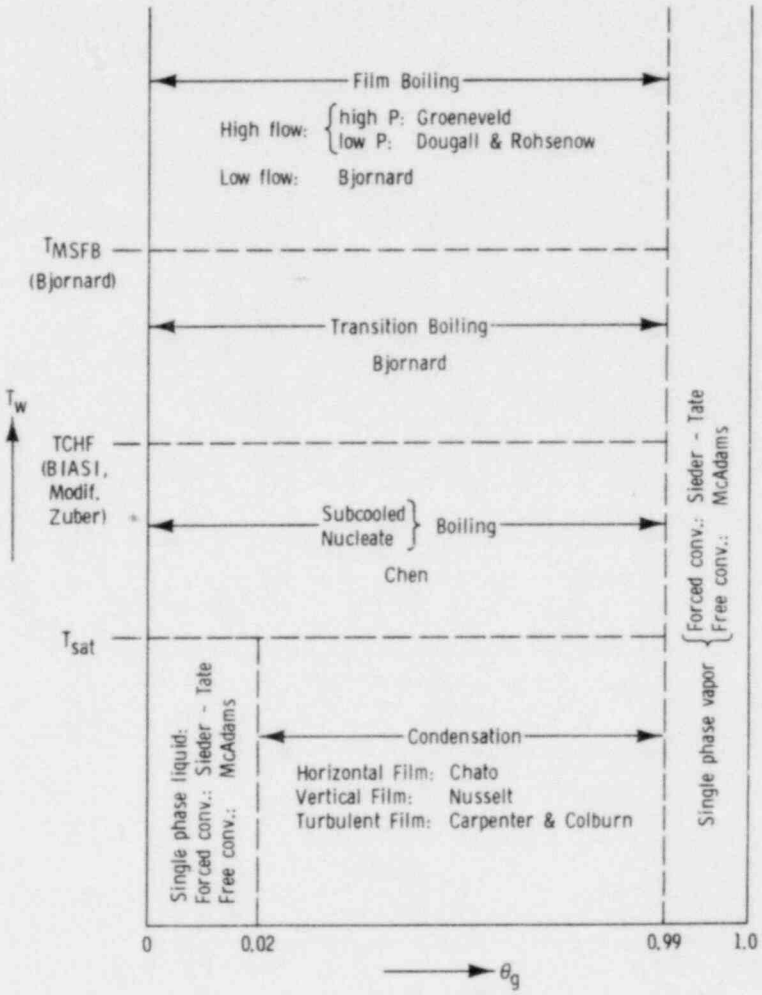

Fig. 4.4

Wall Heat Transfer Correlations and Their Regions of Applications: Water

5. PRELIMINARY CONSIDERATIONS

The numerical solution of the governing differential equations is accomplished by constructing a grid and obtaining the values of the dependent variables at the grid points. Although the principles used can be applied to a grid in any coordinate system, only a Cartesian-coordinate grid is employed here.

The finite-difference equations are derived by integrating the differential equation over a control volume surrounding each grid point. Thus, the derivation process and the resulting equations have direct physical meaning, and the consequent solution satisfies the conservation principles (such as the conservation of mass, the conservation of momentum), over any group of control volumes and, of course, over the whole calculation domain. This desirable feature of the present method exists for any number of grid points, and not just in the limit of a very fine grid.

5.1 Construction of Control Volumes

The control volumes around the grid points can be defined in a number of ways. In one practice, the control volume faces are located midway between neighboring grid points. Figure 5.1 shows the grid points by dots and the control-volume boundaries by dashed lines. Although only a two-dimensional view is shown, the three-dimensional configuration can be easily imagined. It is not necessary for the grid lines to be uniformly spaced.

In another practice, which COMMIX-2 uses, the locations of the control-volume faces are selected first and then a grid point is placed in the geometrical center of each control volume. Again, the control volumes can have nonuniform sizes. This type of construction is shown in Fig. 5.2. The convention used in COMMIX-2 for defining the neighboring control volumes and grid positions is described in Table 5.1.

TABLE 5.1. Convention Used in COMMIX-2 for Defining Neighboring Control Volumes or Grid Positions

Subscript Used	Control Volume or Grid Position Relative to the One under Consideration	i, j, k Notation	x, y, z Notation
0	Under consideration	i, j, k	x, y, z
1	West	i - 1, j, k	$x - \overline{\Delta x}$, y, z
2	East	i + 1, j, k	$x + \overline{\Delta x}$, y, z
3	South	i, j - 1, k	x, $y - \overline{\Delta y}$, z
4	North	i, j + 1, k	x, $y + \overline{\Delta y}$, z
5	Bottom	i, j, k - 1	x, y, $z - \overline{\Delta z}$
6	Top	i, j, k + 1	x, y, $z + \overline{\Delta z}$

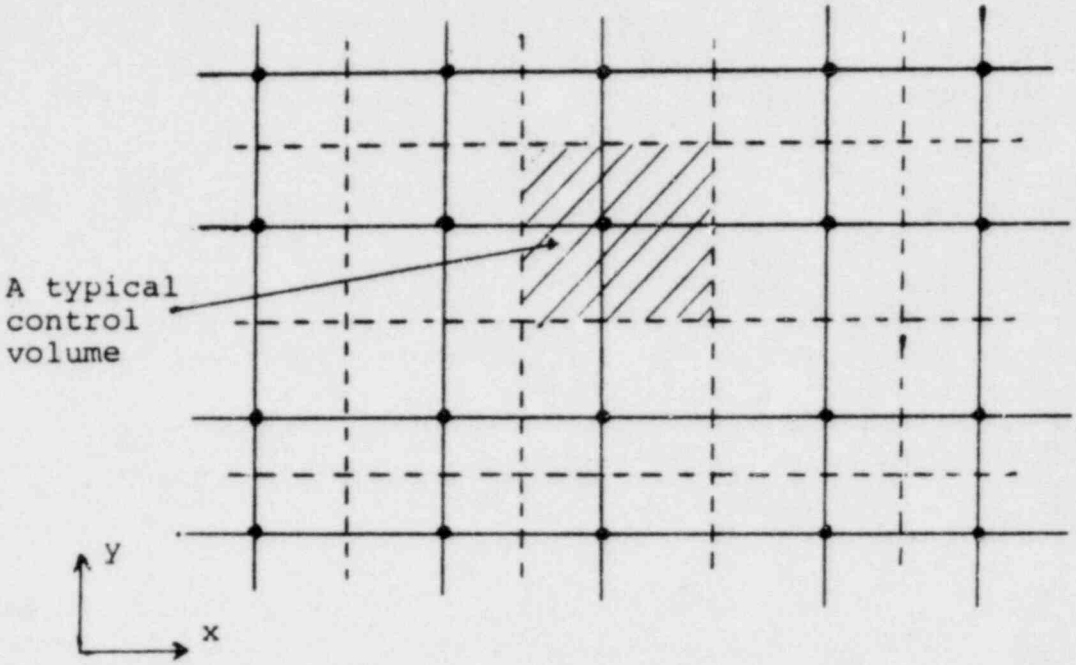

Fig. 5.1. Construction of control volumes (first practice)

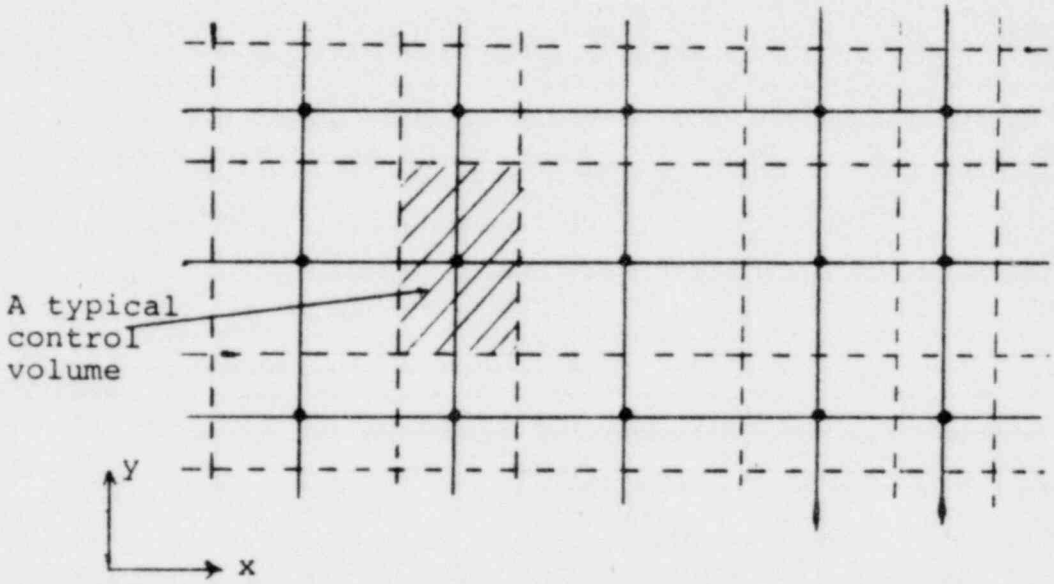

Fig. 5.2. Construction of control volumes (second practice)

This may be a convenient place to remark on the use of nonuniform grids. A misconception seems to prevail that the nonuniform grids lead to lower accuracy than do the uniform grids. This is simply not true. The grid spacing should be directly linked to the way the dependent variable changes in the domain. Obviously, a fine grid is sufficient where the changes are steep, and a coarse grid is sufficient where the changes are rather flat. Indeed, a nonuniform grid enables us to deploy the computing power in an effective way. For most problems, it is desirable to compute exploratory coarse-grid solutions, from which useful guidance can be obtained for designing an appropriate nonuniform grid.

5.2 Unsteady Situations

The solution for an unsteady situation is obtained by marching in time. For every time step, the values of the dependent variables at the beginning of the time step are supposed to be known, and those at the end of the step are to be calculated. A fully implicit scheme is used in this report. This means that the "new" values govern the entire time step, and the "old" values appear only through the term $\partial[\rho\theta\phi]/\partial t$. When the time step Δt is made very large, the calculation procedure automatically reverts to the steady-state formulation.

5.3 Convection and Diffusion Terms

If the sum of convection and diffusion flux of a given phase is expressed by J_ϕ:

$$\left(J_\phi\right)_i = \rho\theta u_i\phi - \Gamma_\phi\theta\left(\frac{\partial\phi}{\partial x_i}\right), \tag{5.1}$$

the convection and diffusion terms in Eq. 2.6 can be written as:

$$\frac{\partial}{\partial x_i}\left[\rho\theta u_i\phi\right] - \frac{\partial}{\partial x_i}\left[\Gamma_\phi\theta\frac{\partial\phi}{\partial x_i}\right] = \frac{\partial\left(J_\phi\right)_i}{\partial x_i}. \tag{5.2}$$

Integration of these terms over the control volume will lead to the balance of the total fluxes entering and leaving the control volume at its faces.

Figure 5.3 shows a control-volume face between grid points 0 and 2. The face is normal to the x-direction and has an area $A_x = \gamma_x\Delta y\Delta z$. The expression for the total flux J_ϕ can be based on the exact solution for a one-dimensional problem given in Ref. 4.

For a one-dimensional case

$$\frac{d}{dx}\left[\rho\theta u\phi\right] = \frac{d}{dx}\left[\Gamma_\phi\theta\frac{d\phi}{dx}\right], \tag{5.3}$$

with the boundary conditions

$$x = 0: \ \phi = \phi_0,$$

$$x = L: \ \phi = \phi_L, \tag{5.4}$$

the solution is

$$\frac{\phi - \phi_0}{\phi_L - \phi_0} = \frac{\exp[Pe\ x/L] - 1}{\exp[Pe] - 1}. \tag{5.5}$$

Here, $Pe = (\rho uL/\Gamma_\phi)$ is the Peclet number. Equation 5.5 leads to:

$$(J_x A_x)_{i+1/2} = a_2(\phi_0 - \phi_2) + F_2\phi_0, \tag{5.6}$$

where

$$a_2 = \left\{F/(\exp(F/D) - 1)\right\}_2, \tag{5.7}$$

$$F_2 = (\rho\theta u A_x)_{i+1/2}, \tag{5.8}$$

and

$$D_2 = \frac{A_{x,i+1/2}}{\left(\frac{0.5\delta x}{\Gamma_\phi \theta}\right)_i + \left(\frac{0.5\delta x}{\Gamma_\phi \theta}\right)_{i+1}}. \tag{5.9}$$

Here, F is the flow rate across the control-volume face, $A_x = (\gamma_x \Delta y \Delta z)$ is the flow cross sectional area, and D represents the strength of diffusion. The ratio F/D is the local Peclet number. We can see from Fig. 5.4 that Eq. 5.7 reduces to the central-difference scheme at low values of the Peclet number and progressively takes on an "upwind" character as the Peclet number is increased.

The definition of D, given in Eq. 5.9, is based on the model that the value Γ_0 prevails in control volume around point 0, and the value Γ_2 rules the behavior in the control volume around 2. That this representation leads to more realistic and accurate solutions has been shown in Ref. 25; also the formulation makes it easy to handle irregular geometries or obstacles, as we shall explain later.

Since the computation of the exponential in Eq. 5.7 is time-consuming, an approximation to the equation has been devised, which, for all practical purposes, performs almost identically to Eq. 5.7. This approximation is:

$$(J_x A_x)_{i+1/2} = a_2(\phi_0 - \phi_2) + F_2\phi_0, \tag{5.10}$$

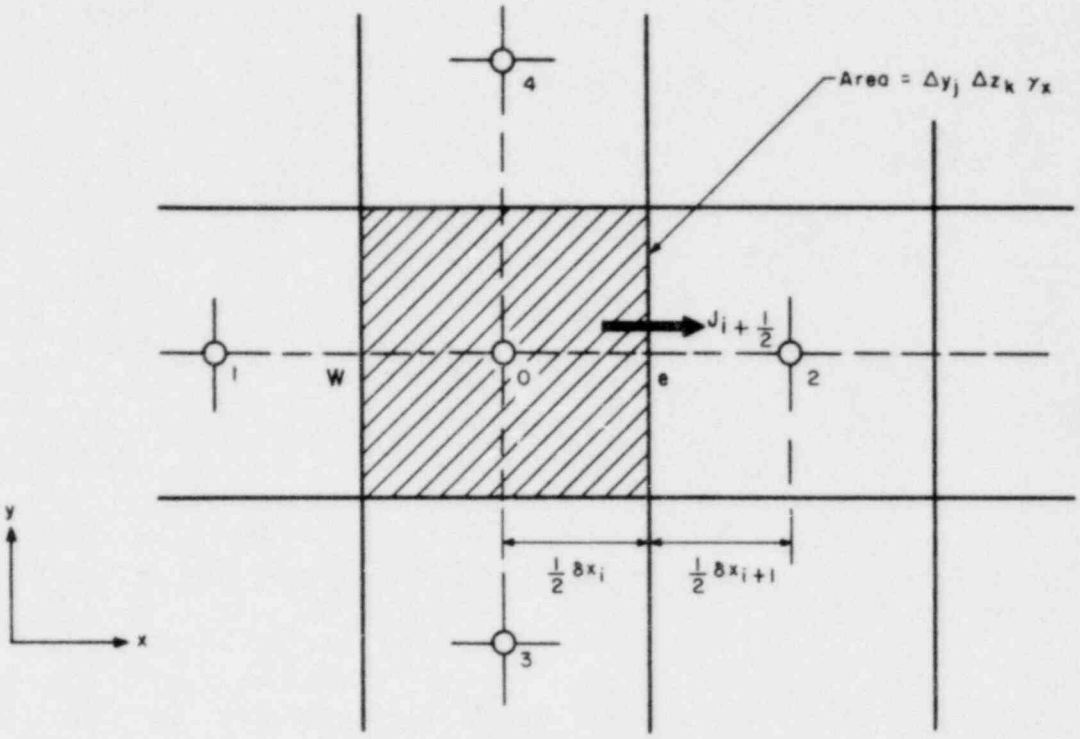

Fig. 5.3. Total flux across a control-volume face

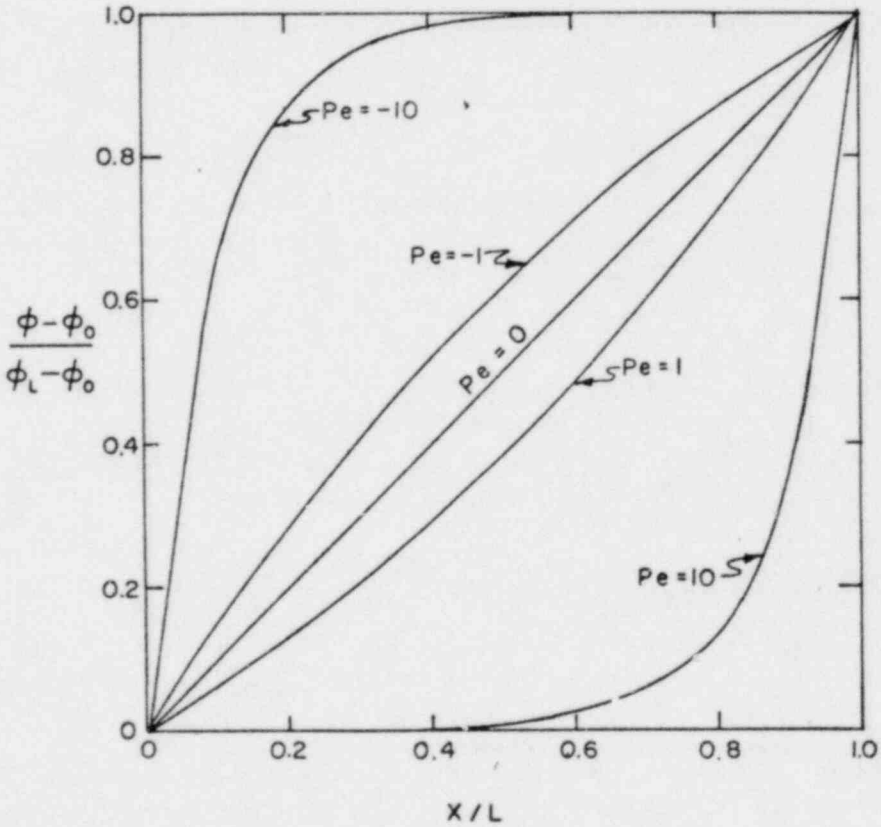

Fig. 5.4. Effect of Peclet number on the variation of ϕ

or

$$\left(J_x A_x\right)_{i+1/2} = a_0\left(\phi_0 - \phi_2\right) + F_2\phi_2, \tag{5.11}$$

where,

$$a_2 = \left\{D_2\left\|0,\left(1 - 0.1|F_2/D_2|\right)^5\right\| + \left\|-F_2,0\right\|\right\}, \tag{5.12}$$

and

$$a_0 = \left\{D_2\left\|0,\left(1 - 0.1|F_2/D_2|\right)^5\right\| + \left\|F_2,0\right\|\right\}. \tag{5.13}$$

Figure 5.5 shows comparison of various finite difference schemes for convection and diffusion terms. We can see that the approximation (Eq. 5.12) is very close to the exact solution.

Here, the new operator $\|\ \|$ is to be interpreted as $\|A,B\|$ = the greater of A and B. It should be noted that $\|A,B\|$ is equivalent to AMAX1 [A,B] in the computer language FORTRAN.

5.4 Source Term

For the finite-difference representation of the source term S in Eq. 2.6, it is convenient to express S as:

$$S_\phi = S_{c\phi} + S_{p\phi}\phi_0, \tag{5.14}$$

where the quantities $S_{c\phi}$, $S_{p\phi}$ and ϕ_0 would be assumed to prevail over the control volume surrounding point 0. This "linearization" of the source term is an effective device for stability and convergence. The exact expressions for $S_{c\phi}$ and $S_{p\phi}$ do depend on the actual form of S_ϕ. Here it may be noted that $S_{p\phi}$ is always kept equal to or less than zero, or else instability, divergence or physically unrealistic solutions would result. When the expression for S_ϕ is rather complicated, we set $S_{p\phi}$ equal to zero, and $S_{c\phi}$ equal to S_ϕ. When the $S_\phi \sim \phi$ variation is nonlinear, and $S_{c\phi}$ and $S_{p\phi}$ are functions of ϕ_p; we calculate them iteratively until convergence is achieved.

5.5 Unsteady Term

For the representation of the term $\partial[\rho\theta\phi]/\partial t$, we assume that the values ρ_0, θ_0, and ϕ_0 prevail over the control volume surrounding point 0. The integration of the unsteady term over the control volume would then give:

$$\int_{c.v.} \partial[\rho\theta\phi]/\partial t\ dx\ dy\ dz = \left\|\rho_0\theta_0\phi_0 - \rho_0^0\theta_0^0\phi_0^0\right\|\gamma_v\Delta x\Delta y\Delta z/\Delta t \tag{5.15}$$

where the superscript 0 denotes the known values at the beginning of the time step.

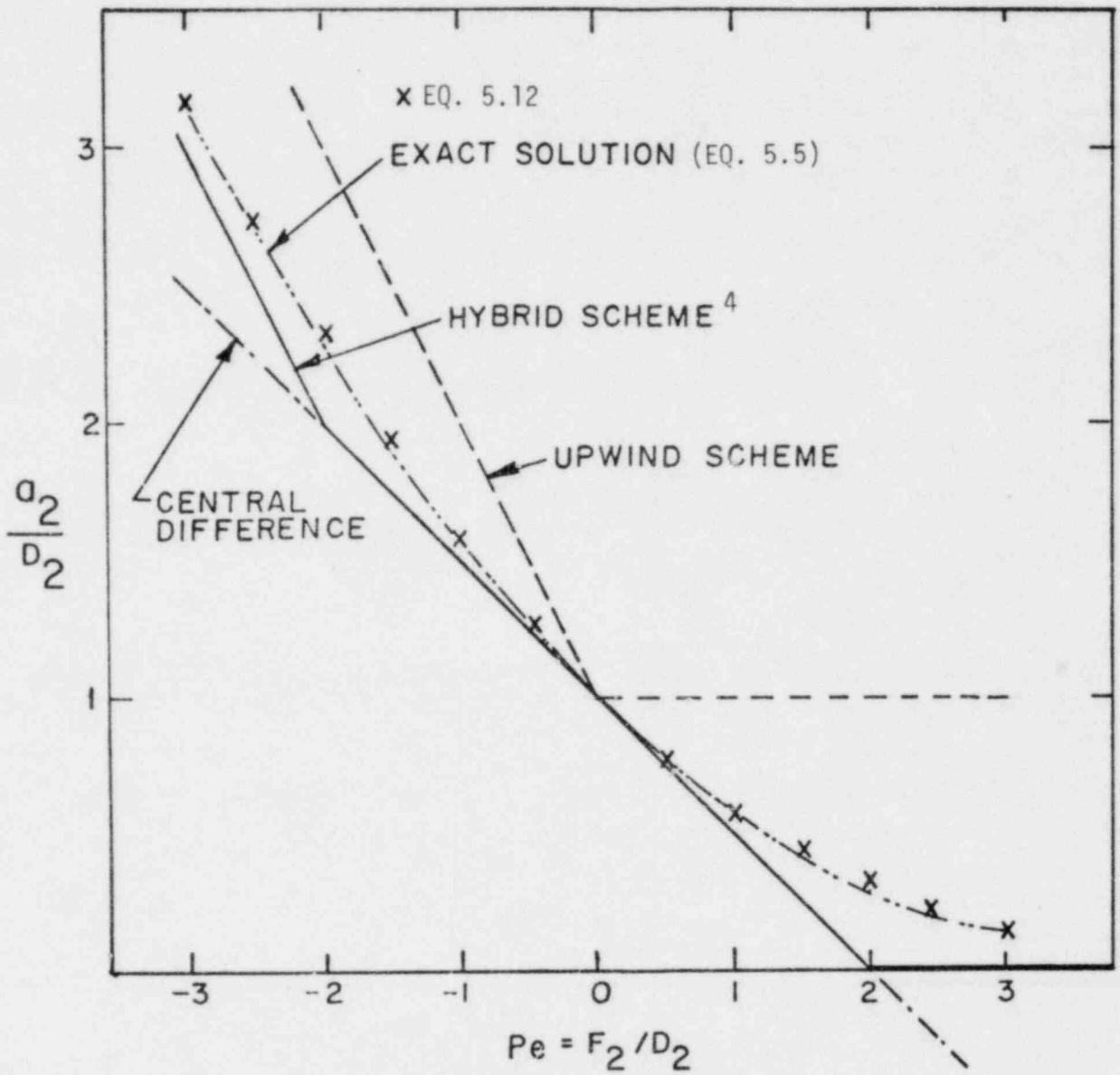

Fig. 5.5. Comparison of various finite difference schemes for convection and diffusion terms

6. GENERAL FINITE-DIFFERENCE EQUATION

6.1 General Form

The basic details outlined so far enable us to obtain the finite-difference form of the general differential equation (2.6). Let us consider the control volume shown in Fig. 6.1. It is constructed around point 0, which has 2 and 1 as its east and west neighbors, 4 and 3 as the north and south neighbors, and 6 and 5 as the top and bottom neighbors representing the z-direction. The control-volume faces are denoted by e, w, n, s, t, and b.

The general finite-difference equation for variable ϕ is arranged as:

$$a_0\phi_0 = a_1\phi_1 + a_2\phi_2 + a_3\phi_3 + a_4\phi_4 + a_5\phi_5 + a_6\phi_6 + a_0^0\phi_0^0 + b_0 \tag{6.1}$$

where

$$a_1 = B_1 + [F_1, 0], \tag{6.2a}$$

$$a_2 = B_2 + [-F_2, 0], \tag{6.2b}$$

$$a_3 = B_3 + [F_3, 0], \tag{6.2c}$$

$$a_4 = B_4 + [-F_4, 0], \tag{6.2d}$$

$$a_5 = B_5 + [F_5, 0], \tag{6.2e}$$

$$a_6 = B_6 + [-F_6, 0], \tag{6.2f}$$

$$a_0^0 = \rho_0^0\theta_0^0(\gamma_v\Delta x\Delta y\Delta z)/\Delta t, \tag{6.2g}$$

$$\begin{aligned} b_0 &= (S_c + S_\Omega)(\gamma_v\Delta x\Delta y\Delta z) \text{ (if } \Omega \text{ is +ve)} \\ &= (S_c + S_\Omega - \Omega\phi)(\gamma_v(\Delta x\Delta y\Delta z) \text{ (if } \Omega \text{ is -ve)} \end{aligned} \tag{6.2h}$$

and

$$\begin{aligned} a_0 &= a_1 + a_2 + a_3 + a_4 + a_5 + a_6 + a_0^0 - (S_p - \Omega)(\gamma_v\Delta x\Delta y\Delta z) \text{ (if } \Omega \text{ is +ve)} \\ &= a_1 + a_2 + a_3 + a_4 + a_5 + a_6 + a_0^0 - S_p(\gamma_v\Delta x\Delta y\Delta z) \text{ (if } \Omega \text{ is -ve)} \end{aligned} \tag{6.2i}$$

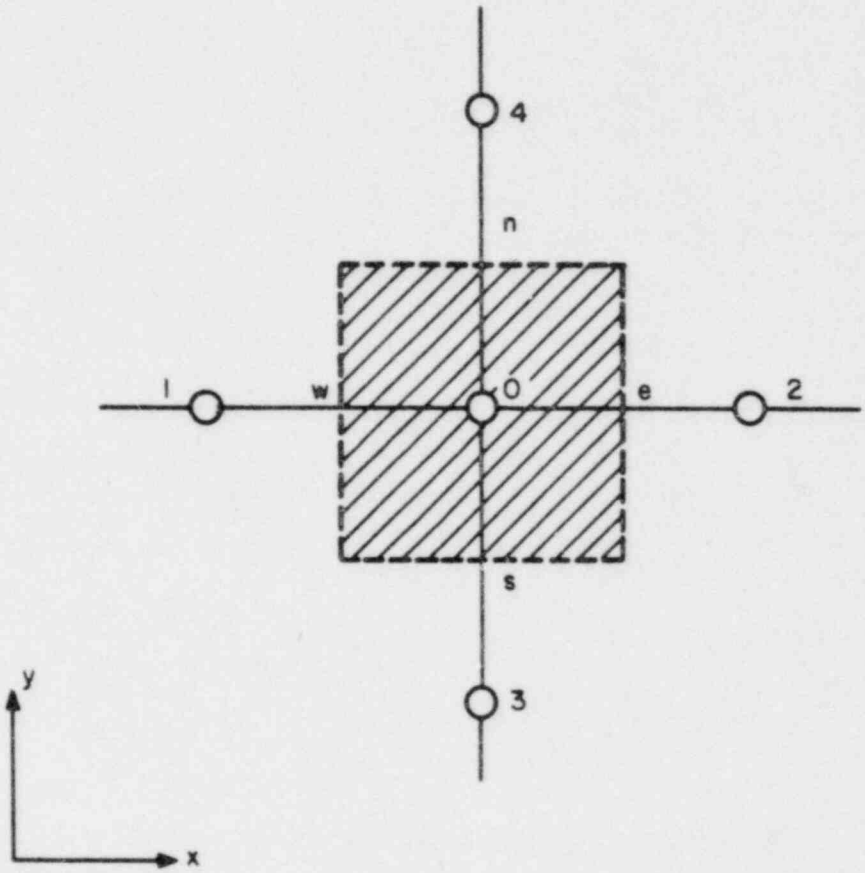

Fig. 6.1. Control volume around point 0

We have two alternative equations for a_0 and b_0 terms, the reason being that the convergence and stability are better if the a_0 term is made larger and more dominant. This can be achieved by retaining the mass source term Ω (evaporation or condensation) in the left-hand side (in a_0) if Ω is -ve and in the right-hand side (in b_0) if Ω is +ve.

The quantities B_1, B_2, B_3, B_4, B_5, B_6 are defined in an identical manner. For example:

$$B_2 = D_2 [\![0, (1 - 0.1|F_2/D_2|)^5]\!], \tag{6.3}$$

where F and D are given by Eqs. 5.8 and 5.9. For any other face, appropriate definitions of F and D are used, such as

$$F_6 = \left(\rho\theta w A_z\right)_{k+1/2}, \tag{6.4}$$

and

$$D_6 = \frac{A_{z,k+1/2}}{\left[\left(\frac{0.5\delta z}{\Gamma_\phi \theta}\right)_k + \left(\frac{0.5\delta z}{\Gamma_\phi \theta}\right)_{k+1}\right]}. \tag{6.5}$$

Therefore,

$$B_6 = D_6 [\![0, (1 - 0.1|F_6/D_6|)^5]\!] \tag{6.6}$$

The derivation of Eq. 6.2i is as follows. If we combine Eqs. 5.10, 6.2b and 6.3, we get:

$$\left(J_x A_x\right)_{i+1/2} = \left\{D_2 [\![0, (1 - 0.1|F_2/D_2|)^5]\!] + [\![-F_2, 0]\!] (\phi_0 - \phi_2) + F_2\phi_0\right\} \tag{6.7}$$

From the definition of a_2 (Eq. 6.2), we can now write Eq. 6.7 as:

$$\left(J_x A_x\right)_{i+1/2} = \left\{B_2 + [\![-F_2, 0]\!]\right\}(\phi_0 - \phi_2) + F_2\phi_0 \tag{6.8}$$

Similar expressions would hold for $(J_y A_y)_{j+1/2}$ and $(J_z A_z)_{k+1/2}$. For the flux crossing the west surface of the control volume, the expression is

$$\left(J_x A_x\right)_{i-1/2} = \left\{B_1 + [\![-F_1, 0]\!]\right\}(\phi_1 - \phi_0) + F_1\phi_1. \tag{6.9}$$

This is obtained from Eq. 6.8 by replacing ϕ_0 by ϕ_1 and ϕ_2 by ϕ_0. A further rearrangement gives:

$$\left(J_x A_x\right)_{i-1/2} = \left\{B_1 + \left[F_1, 0\right]\right\}\left(\phi_1 - \phi_0\right)$$

$$+ \left\{\left[-F_1, 0\right] - \left[F_1, 0\right]\right\}\left(\phi_1 - \phi_0\right) + F_1\phi_1. \tag{6.10}$$

Noting that

$$\left[-F_1, 0\right] - \left[F_1, 0\right] = -F_1, \tag{6.11}$$

we obtain:

$$\left(J_x A_x\right)_{i-1/2} = \left\{B_1 + \left[F_1, 0\right]\right\}\left(\phi_1 - \phi_0\right) + F_1\phi_0. \tag{6.12}$$

With a_1 defined by Eq. 5.2a, we write:

$$\left(J_x A_x\right)_{i-1/2} = a_1\left(\phi_1 - \phi_0\right) + F_1\phi_0. \tag{6.13}$$

Similar expressions can be written for $(J_y A_y)_{j-1/2}$ and $(J_z A_z)_{k-1/2}$. With all these flux expressions for the control volume faces, and with the contributions from Eqs. 5.14 and 5.15, the coefficients of ϕ_0 can be written as

$$a_0 = a_1 - F_1 + a_2 + F_2 + a_3 - F_3 + a_4 + F_4 + a_5 - F_5 + a_6 + F_6$$

$$- S_p\left(\gamma_v \Delta x \Delta y \Delta z\right) + \rho_0\Theta_0\left(\gamma_v \Delta x \Delta y \Delta z/\Delta t\right). \tag{6.14}$$

Substitution of Eq. 6.2g into this gives us

$$a_0 = a_1 + a_2 + a_3 + a_4 + a_5 + a_6 + a_0^0 - S_p\left(\gamma_v \Delta x \Delta y \Delta z\right) + \left\{\left(\rho_0\Theta_0 - \rho_0^0\Theta_0^0\right)\right.$$

$$\left. \cdot \left(\gamma_v \Delta x \Delta y \Delta z/\Delta t\right) + \left(F_2 - F_1\right) + \left(F_4 - F_3\right) + \left(F_6 - F_5\right)\right\}. \tag{6.15}$$

The terms in the curly brackets can be recognized as the discretized form of the left-hand side of the continuity equation and hence can be regarded as equal to the source term $(\Omega)(\gamma_v \Delta x \Delta y \Delta z)$. With the contents of the curly brackets in Eq. 6.15 set equal to the source term, we obtain Eq. 6.2i.

6.2 Formulations in i, j, k Notations

Consider the control volume shown in Fig. 6.2. It is constructed around grid point 0 (i,j,k) which has 2 (i+1,j,k) and 1 (i-1,j,k) as its east and west neighbors, 4 (i,j+1,k) and 3 (i,j-1,k) as the north and south neighbors, and 6 (i,j,k+1) and 5 (i,j,k-1) as the top and bottom neighbors representing the z-direction. The control volume is formed by six planes $x_{i-1/2}$, $x_{i+1/2}$, $y_{j-1/2}$,

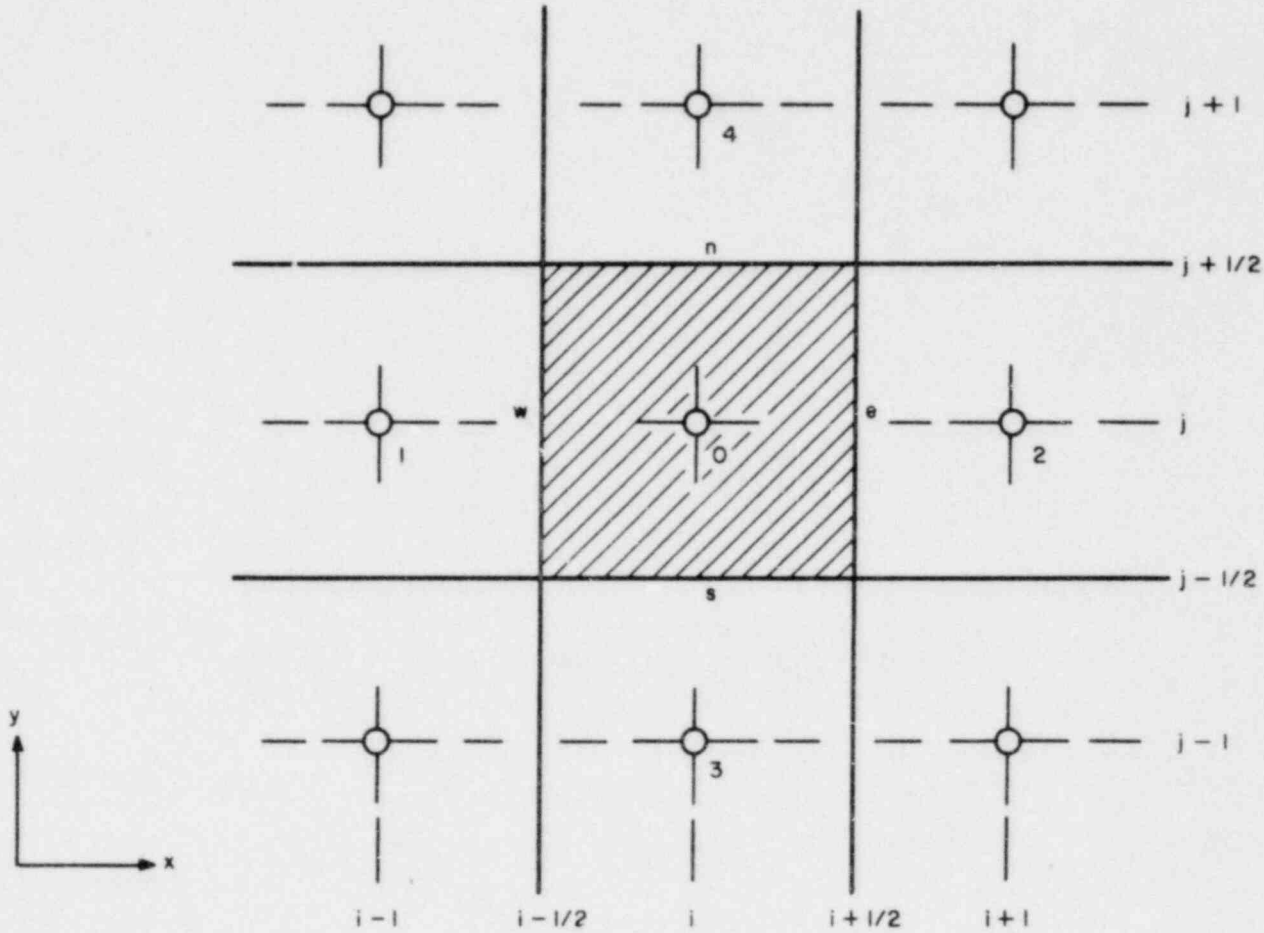

Fig. 6.2. Control volume around point 0 in ijk notation

$y_{j+1/}$, $z_{k-1/2}$, and $z_{k+1/2}$. For simplicity, two of the indices i, j, and k are suppressed. Therefore,

$$\phi_{i+1/2} = \phi_{i+1/2,j,k};\ \phi_{j+1} = \phi_{i,j+1,k} \text{ and so on.}$$

The general finite difference equation can be arranged as

$$a_{ijk}\phi_{ijk} = a_{i+1}\phi_{i+1} + a_{i-1}\phi_{i-1} + a_{j+1}\phi_{j+1} + a_{j-1}\phi_{j-1} + a_{k+1}\phi_{k+1}$$
$$+ a_{k-1}\phi_{k-1} + a^0_{ijk}\phi^0_{ijk} + b_{ijk} \tag{6.16}$$

Here,

$$a_{i+1} = B_{i+1/2} + [-F_{i+1/2}, 0], \tag{6.17a}$$

$$a_{i-1} = B_{i-1/2} + [F_{i-1/2}, 0], \tag{6.17b}$$

$$a_{j+1} = B_{j+1/2} + [-F_{j+1/2}, 0], \tag{6.17c}$$

$$a_{j-1} = B_{j-1/2} + [F_{j-1/2}, 0], \tag{6.17d}$$

$$a_{k+1} = B_{k+1/2} + [-F_{k+1/2}, 0], \tag{6.17e}$$

$$a_{k-1} = B_{k-1/2} + [F_{k-1/2}, 0], \tag{6.17f}$$

$$a^0_{ijk} = (\rho^0\theta^0)_{ijk}(\gamma_v\Delta x_i\Delta y_j\Delta z_k)/\Delta t, \tag{6.17g}$$

$$b_{ijk} = S_c + S_\Omega(\gamma_v\Delta x_i\Delta y_j\Delta z_k), \text{ (if } \Omega \text{ is +ve)}$$
$$= (S_c + S_\Omega - \Omega\phi)(\gamma_v\Delta x\Delta y\Delta z), \text{ (if } \Omega \text{ is -ve)} \tag{6.17h}$$

and

$$a_{ijk} = a_{i+1} + a_{i-1} + a_{j+1}\ a_{j-1} + a_{k+1} + a_{k-1}$$
$$+ a^0_{ijk} - S_p\gamma_v\Delta x_i\Delta y_j\Delta z_k \text{ (if } \Omega \text{ is -ve)}$$
$$= a_{i+1} + a_{i-1} + a_{j+1} + a_{j-1} + a_{k+1} + a_{k-1}$$
$$+ a^0_{ijk} + (\Omega - S_p)(\gamma_v\Delta x\Delta y\Delta z) \text{ (if } \Omega \text{ is +ve)} \tag{6.17i}$$

The quantities $B_{i+1/2}$, $F_{i+1/2}$, etc., in Eqs. 6.17a to 6.17f are defined in the following manner:

$$B_{i+1/2} = D_{i+1/2}\left[0,\ \left(1 - 0.1\left|F_{i+1/2}/D_{i+1/2}\right|\right)^5\right], \tag{6.18}$$

$$D_{i+1/2} = \frac{\left(\Delta y_j \Delta z_k\right)\left(\gamma_x\right)_{i+1/2}}{\left[\dfrac{\Delta x_i}{2\left(\Gamma_\phi \theta\right)_{ijk}} + \dfrac{\Delta x_{i+1}}{2\Gamma_{\phi,i+1}\theta_{i+1}}\right]}, \tag{6.19}$$

and

$$F_{i+1/2} = \left(\rho\theta u\gamma_x\right)_{i+1/2} \Delta y_j \Delta z_k = \left(\rho\theta u A_x\right)_{i+1/2}. \tag{6.20}$$

Similarly for other faces, e.g.

$$B_{k-1/2} = D_{k-1/2}\left[0,\ \left(1 - 0.1\left|F_{k-1/2}/D_{k-1/2}\right|\right)^5\right], \tag{6.21}$$

$$D_{k-1/2} = \frac{\Delta x_i \Delta y_j \left(\gamma_z\right)_{k-1/2}}{\left[\dfrac{\Delta z_k}{2\left(\Gamma_\phi \theta\right)_{ijk}} + \dfrac{\Delta z_{k-1}}{2\Gamma_{\phi,k-1}\theta_{k-1}}\right]}, \tag{6.22}$$

and

$$F_{k-1/2} = \left(\rho\theta w\gamma_z\right)_{k-1/2} \Delta x_i \Delta y_j = \left(\rho\theta w A_z\right)_{k-1/2}. \tag{6.23}$$

7. THE FINITE-DIFFERENCE FORM OF MOMENTUM EQUATIONS

Since the momentum equations conform to the general ϕ equation, no separate derivation of their finite-difference form should be necessary. However, because it is desirable to calculate the velocity components for "staggered" locations, as will be explained shortly, some differences of detail arise in constructing the momentum finite-difference equations.

7.1 Staggered Grid

Although all dependent variables are calculated for the grid points, the velocity components u, v, and w of both phases constitute an exception. They are calculated for displaced or "staggered" locations, and not for the grid points. The displaced locations of the velocity components are such that they are placed on the faces of the control volumes. Thus, the x-direction velocity u is calculated at the faces that are normal to the x direction.

Figure 7.1 shows the locations of u and v, by short arrows, on a two-dimensional grid; the three-dimensional counterpart can be easily imagined. With respect to the grid points, the u locations are displaced only in the x direction, the v locations only in the y direction, and so on. The location for u thus lies on the x-direction link joining two adjacent grid points. It is the pressure difference between these grid points that will be used to "drive" the velocity u located between them. This is the main consequence of the staggered grid.

Except for uniform grids cases, the staggered velocity locations will not lie exactly midway between the adjacent grid points. The velocity components are located on the control-volume faces, and as we are using the second practice outlined in Section 5.1 the velocity components may not be midway between the grid points.

7.2 The Momentum Control Volumes

A direct consequence of the staggered grid is that the control volumes to be used for the conservation of the momentum must also be staggered. The control volumes shown in Figs. 5.1 and 5.2 will now be referred to as the main control volumes. The control volumes for momentum will be staggered in the direction of the momentum such that its faces normal to that direction pass through the grid points (see Fig. 7.1). Thus, the pressures at these grid points can be directly used for calculating the pressure force on the momentum control volume. Figure 7.2 shows the control volumes for the x-direction momentum.

7.3 The Finite-difference Equation for Momentum

All the basic concepts developed in Section 5 and implemented in Section 6 will be applied to the staggered control volumes for momentum. The

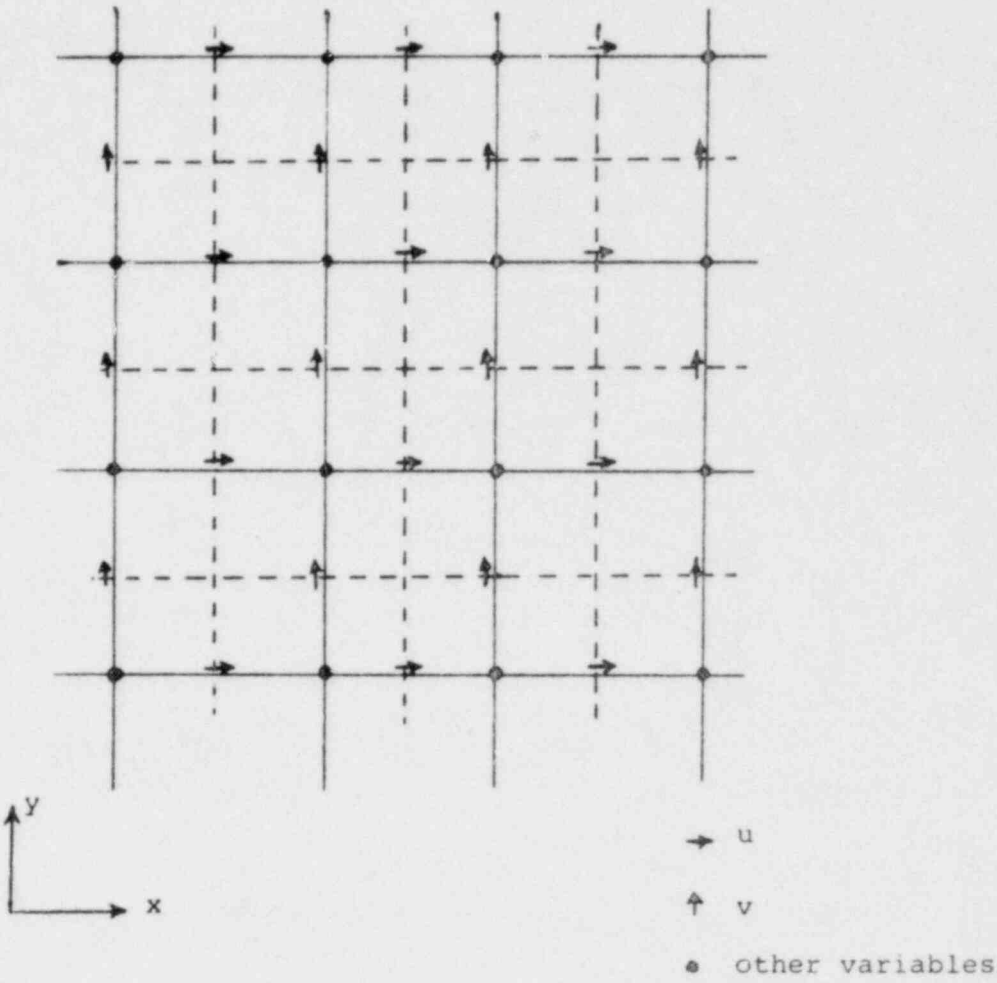

Fig. 7.1. Staggered Grid

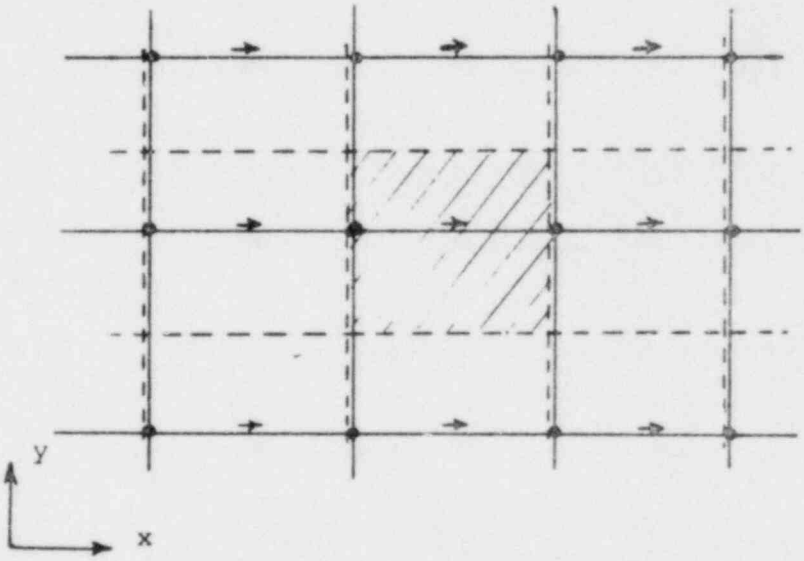

Fig. 7.2. Momentum control volume in x-direction

differences are mainly geometrical and involve the appropriate calculation of the flow rates and diffusion strengths for the faces of the momentum control volume.

We consider the situation shown in Fig. 7.3. Let F_4 and F_{24} denote the flow rates for the two main control volumes which contribute to the momentum control volume around e. We assume that the calculation of F_4 and F_{24} is already performed. The part of F_4 that contributes to the y-direction flow rate at the upper face of the momentum control volume is:

$$F_4 \times (\text{distance } 0e)/(\text{distance } we) = F_4/2$$

Similarly, the contribution of F_{24} is:

$$F_{24} \times (\text{distance } e2)/(\text{distance } e\text{-}ee) = F_{24}/2,$$

where ee is the point on the right side of 2 where an arrow is shown in Fig. 7.3. Thus, the total y-direction flow rate at the upper face of the momentum control volume is:

$$\frac{1}{2}\left(F_4 + F_{24}\right).$$

The diffusion quantity for the same face is calculated from

$$D_4 \cdot \frac{\text{distance } 0e}{\text{distance } we} + D_{24} \cdot \frac{\text{distance } e2}{\text{distance } e\text{-}ee} = \frac{1}{2}\left(D_4 + D_{24}\right).$$

The evaluation of the main-control-volume diffusion strengths D_4 and D_{24} is performed in the manner stated in Eq. 5.9.

The x-direction flow rate entering the momentum control volume at 0 is obtained by linear interpolation:

$$F_0 = F_1 \cdot \frac{\text{distance } 0e}{\text{distance } we} + F_2 \cdot \frac{\text{distance } w0}{\text{distance } we} = \frac{1}{2}\left(F_1 + F_2\right).$$

The diffusion strength at 0 is wholly governed by $\Gamma_{\phi 0}$ and hence calculated as:

$$D_0 = \left(\gamma_x \Delta y \Delta z\right)\Gamma_{\phi 0}\theta_0/(\delta x)_i. \tag{7.1}$$

The quantity $\left[\rho_0^0\theta_0^0\left(\gamma_v \Delta x \Delta y \Delta z\right)\right]$ in Eq. 6.2g stands for the mass of fluid contained in the main control volume around point 0. The corresponding quantity for the momentum control volume shown in Fig. 7.3 is obtained by taking the appropriate mass contributions from the control volumes surrounding points 0 and 2. In our case, it is

$$\frac{1}{2}\left[\rho^0\theta^0\left(\gamma_v \Delta x \Delta y \Delta z\right)_0 + \rho^0\theta^0\left(\gamma_v \Delta x \Delta y \Delta z\right)_2\right].$$

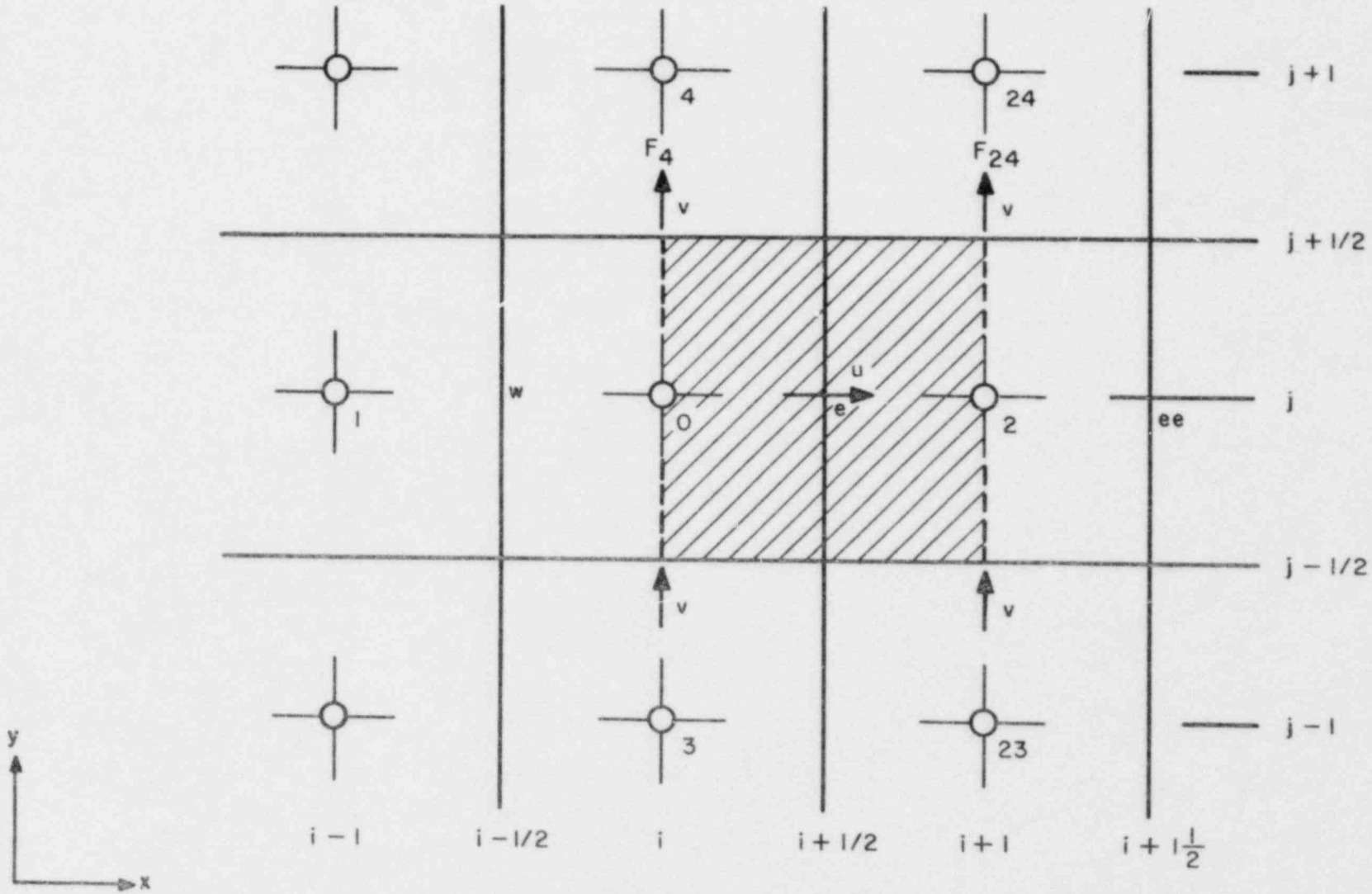

Fig. 7.3. Momentum control volume in relation to the main control volumes

With these details, the momentum finite-difference counterpart of Eq. 6.1 is constructed. One additional feature, however, should now be introduced. As seen from Eq. 2.3, the pressure gradient appears in the momentum equation, but the pressure field is neither known beforehand nor directly obtainable from some sort of "conservation equation for pressure." Thus, pressure is regarded as unknown and determined indirectly from the constraint that the velocity field satisfies the continuity equation 2.2. For this reason, the pressure-containing term in the finite-difference form of the momentum equation is displayed separately.

From these considerations, we write the finite-difference equation for the control volume shown in Fig. 7.3 as:

$$a_0 u_0 = \Sigma a_{nb} u_{nb} + a_0^0 u_0^0 + b_0 + (\gamma_x \theta \Delta y \Delta z)(p_0 - p_2), \tag{7.2}$$

where the subscript nb denotes a neighbor u and the summation is taken over the six neighbors surrounding u_0. The term $a_0^0 u_0^0$ arises from the unsteady term in the differential equation; a_0^0 is calculated similar to a_0^0 defined in Eq. 6.2g. The definitions of the neighbor coefficients a_{nb} and the center coefficient a_0 are identical to those in Eq. 6.2, with appropriate calculations of the flow rates F and diffusion strength D.

The contributions of the source term that enter a_0 and b_0 do not contain the pressure gradient; the effect of the pressure gradient is expressed by the last term in Eq. 7.2, where $(\gamma_x \Delta y \Delta z)$ is the area on which the pressure drop $(p_0 - p_2)$ acts. The momentum equations for the y- and z-directions are obtained in a similar manner.

7.4 Velocity-Pressure Relationships

In order to convert the indirect specification of pressure contained in the continuity equation into a direct algorithm for calculating pressure, we establish relationships between the velocity components and corresponding pressure drops. For this purpose, we define a pseudo-velocity by:

$$\hat{u}_0 \equiv [\Sigma a_{nb} u_{nb} + a_0^0 u_0^0 + b_0]/a_0. \tag{7.3}$$

This enables us to write Eq. 7.2 as:

$$u_0 = \hat{u}_0 + d_0[p_0 - p_2], \tag{7.4}$$

where

$$d_0 \equiv [\gamma_x \theta \Delta y \Delta z]/a_0. \tag{7.5}$$

Pseudo-velocities $\hat{v}$ and $\hat{w}$ are similarly obtained from the corresponding momentum equations.

We now imagine that the pressure changes from a guessed value p* to a new value p. The corresponding change in the velocity is expressed as

$$u_0 - u_0^* = d_0[(p_0 - p_0^*) - (p_2 - p_2^*)] \tag{7.6}$$

where we have assumed that the change in $\hat{u}_0$ is unimportant. The change in pressure is denoted by the "pressure correction" p', i.e.,

$$p = p^* + p', \tag{7.7}$$

and we derive a velocity-correction formula from Fq. 7.6 as:

$$u_0 = u_0^* + d_0[p_0' - p_2']. \tag{7.8}$$

Here u_0^* is the value of u_0 given by Eq. 7.2 when the guessed value p* is substituted for the pressure p.

The similarity between Eqs. 7.4 and 7.8 should be noted.

7.5 Solution of the Momentum Equation

There are two ways one can solve the momentum equation for velocity field. One procedure is to use a set of equations (7.2) and solve them simultaneously by either line-by-line or plane-by-plane solution procedure as described in Section 11. This is a more implicit procedure as all the neighboring velocities in Eq. 7.2 are considered unknown. The second procedure is to use the velocity-pressure relations, Eq. 7.4, after solving pressure equation derived in Section 9. This is an explicit procedure as all the neighboring velocities are considered to be known. The COMMIX-2 has, at present, an option that permits the use of either of the above two described procedures.

8. FINITE-DIFFERENCE FORMS OF THE CONTINUITY EQUATIONS

8.1 Phase Continuity Equation

We can see that the phase continuity equation has the same form as the general Eq. 2.6 without the diffusion term. We can therefore, make $\Gamma_\theta = 0$ and use the formulations described in Section 6. It may be noted here that due to the absence of the diffusion term, the final finite-difference equations that we obtain correspond to the equations that we obtain by upwind differencing.

The finite-difference equation for fluid volume fraction θ can be arranged as:

$$a_0\theta_0 = a_1\theta_1 + a_2\theta_2 + a_3\theta_3 + a_4\theta_4 + a_5\theta_5 + a_6\theta_6 + a_0^0\theta_0^0 + b_0, \tag{8.1}$$

where

$$a_1 = [\![F_1, 0]\!], \tag{8.2a}$$

$$a_2 = [\![-F_2, 0]\!], \tag{8.2b}$$

$$a_3 = [\![F_3, 0]\!], \tag{8.2c}$$

$$a_4 = [\![-F_4, 0]\!], \tag{8.2d}$$

$$a_5 = [\![F_5, 0]\!], \tag{8.2e}$$

$$a_6 = [\![-F_6, 0]\!], \tag{8.2f}$$

$$a_0^0 = [\rho^0\gamma_v]_0[\Delta x_i \Delta y_j \Delta z_k]/\Delta t, \tag{8.2g}$$

$$b_0 = \Omega(\gamma_v \Delta x_i \Delta y_j \Delta z_k), \tag{8.2h}$$

$$\bar{a}_1 = [\![-F_1, 0]\!], \tag{8.2i}$$

$$\bar{a}_2 = [\![F_2, 0]\!], \tag{8.2j}$$

$$\bar{a}_3 = [\![-F_3, 0]\!], \tag{8.2k}$$

$$\bar{a}_4 = [\![F_4, 0]\!], \tag{8.2l}$$

$$\bar{a}_5 = [-F_5, 0], \tag{8.2m}$$

$$\bar{a}_6 = [F_6, 0], \tag{8.2n}$$

$$\bar{a}_0^0 = (\rho_v \gamma_v)_0 (\Delta x_i \Delta y_j \Delta z_k)/\Delta t, \tag{8.2o}$$

and

$$a_0 = \bar{a}_1 + \bar{a}_2 + \bar{a}_3 + \bar{a}_4 + \bar{a}_5 + \bar{a}_6 + \bar{a}_0^0. \tag{8.2p}$$

The coefficients without overscore represent "inflows" while the coefficients with overscore represent "outflows." It may be noted here that only one of the two coefficients (with or without overscore) exists. That is, if a_1 exists, then $\bar{a}_1$ is equal to zero or vice versa. The quantities F appearing in Eq. 8.2 are as defined previously but without fluid volume fraction. Thus

$$F_2 = (\rho u \gamma_x)_{i+1/2} (\Delta y_j \Delta z_k) = (\rho u A_x)_{i+1/2} \tag{8.3}$$

8.2 Combined Continuity Equation

The combined continuity equation, Eq. 2.2b is integrated over the control volume as shown in Fig. 6.1 to yield:

$$\begin{aligned}
&\left\{\left[(\rho_\ell \theta_\ell u_\ell + \rho_g \theta_g u_g)\gamma_x\right]_w - \left[(\rho_\ell \theta_\ell u_\ell + \rho_g \theta_g u_g)\gamma_x\right]_e\right\} (\Delta y \Delta z) \\
&+ \left\{\left[(\rho_\ell \theta_\ell v_\ell + \rho_g \theta_g v_g)\gamma_y\right]_s - \left[(\rho_\ell \theta_\ell v_\ell + \rho_g \theta_g v_g)\gamma_y\right]_n\right\} (\Delta z \Delta x) \\
&+ \left\{\left[(\rho_\ell \theta_\ell w_\ell + \rho_g \theta_g w_g)\gamma_z\right]_b - \left[(\rho_\ell \theta_\ell w_\ell + \rho_g \theta_g w_g)\gamma_z\right]_t\right\} (\Delta x \Delta y) \\
&+ \left[(\rho_\ell \theta_\ell + \rho_g \theta_g)^0 - (\rho_\ell \theta_\ell + \rho_g \theta_g)\right](\gamma_v \Delta x \Delta y \Delta z/\Delta t) = 0
\end{aligned} \tag{8.4}$$

We use one of the two phase continuity equations to compute the void fractions, and the combined continuity equation (8.4) for determining the pressure correction. Since the pressure or the pressure correction does not appear here, further manipulation is needed to derive the finite-difference equations for p and p'.

9. PRESSURE AND PRESSURE-CORRECTION EQUATIONS

As mentioned earlier, the pressure appearing in the momentum equation is unknown and has to be determined from the continuity equation. There are a number of possible ways to derive pressure and pressure-correction equations from the continuity and momentum equations. An important thing is to note that the equations derived must satisfy the following three equations.

Liquid continuity, (9.1)

Gas continuity, (9.2)

and

$$\theta_\ell + \theta_g = 1. \tag{9.3}$$

In COMMIX-2, we have provided two alternative procedures for pressure-correction equations. At present, we do not have enough testing and comparison to favor any one of the two procedures. Further experimentation is planned to determine the computational efficiencies of these two procedures. Meantime, an option has been included in the code to select either one of the two procedures.

In procedure 1, we use the liquid continuity equation (9.1) to compute the liquid volume fraction, $\theta_\ell + \theta_g = 1$ relation (9.3) to obtain gas volume fraction and the combined continuity equation (sum of Eqs. 9.1 and 9.2) to obtain the pressure-correction equation. In the alternative procedure 2, we have used the liquid continuity equation (9.1) to obtain the liquid volume fraction and the gas continuity equation (9.2) to obtain the gas volume fraction. The pressure correction equation is derived from the constraint that the sum of θ_ℓ and θ_g must be equal to unity (Eq. 9.3). The pressure equation for both procedures is obtained from the combined continuity equation. The derivations of pressure and pressure-correction equations are given in the following sections.

9.1 Pressure Equation

Substitution of the velocity-pressure relations such as Eq. 7.4 into Eq. 8.4 leads to:

$$a_0 P_0 = a_1 P_1 + a_2 P_2 + a_3 P_3 + a_4 P_4 + a_5 P_5 + a_6 P_6 + b_0, \tag{9.4}$$

where

$$a_1 = \{(\rho_\ell \theta_\ell d_\ell + \rho_g \theta_g d_g)\gamma_x\}_w (\Delta y \Delta z), \tag{9.5a}$$

$$a_2 = \{(\rho_\ell \theta_\ell d_\ell + \rho_g \theta_g d_g)\gamma_x\}_e (\Delta y \Delta z), \tag{9.5b}$$

$$a_3 = \left\{(\rho_\ell\theta_\ell d_\ell + \rho_g\theta_g d_g)\gamma_y\right\}_s (\Delta x\Delta z), \tag{9.5c}$$

$$a_4 = \left\{(\rho_\ell\theta_\ell d_\ell + \rho_g\theta_g d_g)\gamma_y\right\}_n (\Delta x\Delta z), \tag{9.5d}$$

$$a_5 = \left\{(\rho_\ell\theta_\ell d_\ell + \rho_g\theta_g d_g)\gamma_z\right\}_t (\Delta x\Delta y), \tag{9.5e}$$

$$a_6 = \left\{(\rho_\ell\theta_\ell d_\ell + \rho_g\theta_g d_g)\gamma_z\right\}_b (\Delta x\Delta y), \tag{9.5f}$$

$$a_0 = a_1 + a_2 + a_3 + a_4 + a_5 + a_6, \tag{9.5g}$$

and

$$\begin{aligned} b_0 = &\left\{\left[(\rho_\ell\theta_\ell\hat{u}_\ell + \rho_g\theta_g\hat{u}_g)\gamma_x\right]_w - \left[(\rho_\ell\theta_\ell\hat{u}_\ell + \rho_g\theta_g\hat{u}_g)\gamma_x\right]_e\right\}(\Delta y\Delta z) \\ &+ \left\{\left[(\rho_\ell\theta_\ell\hat{v}_\ell + \rho_g\theta_g\hat{v}_g)\gamma_y\right]_w - \left[(\rho_\ell\theta_\ell\hat{v}_\ell + \rho_g\theta_g\hat{v}_g)\gamma_y\right]_n\right\}(\Delta x\Delta z) \\ &+ \left\{\left[(\rho_\ell\theta_\ell\hat{w}_\ell + \rho_g\theta_g\hat{w}_g)\gamma_z\right]_b - \left[(\rho_\ell\theta_\ell\hat{w}_\ell + \rho_g\theta_g\hat{w}_g)\gamma_z\right]_t\right\}(\Delta x\Delta y) \\ &+ \left[(\rho_\ell\theta_\ell + \rho_g\theta_g)^0 - (\rho_\ell\theta_\ell + \rho_g\theta_g)\right](\gamma_v\Delta x\Delta y\Delta z/\Delta t) \end{aligned} \tag{9.5h}$$

9.2 Pressure-correction Equation 1

In this section we have derived the pressure-correction equation for two-phase flow by extending the 'SIMPLER' procedure for single phase. If we substitute Eq. 7.8 (and similar velocity-correction formulas for v and w) into Eq. 8.4, we get the pressure-correction equation

$$a_0p_0' = a_1p_1' + a_2p_2' + a_3p_3'\ a_4p_4' + a_5p_5' + a_6p_6' + b_0 \tag{9.6}$$

where a_1, a_2, a_3, a_4, a_5, a_6, and a_0 are given by Eqs. 9.5a to 9.5g, and b_0 is given by

$$\begin{aligned} b_0 = &\left\{\left[(\rho_\ell\theta_\ell u_\ell^* + \rho_g\theta_g u_g^*)\gamma_x\right]_w - \left[(\rho_\ell\theta_\ell u_\ell^* + \rho_g\theta_g u_g^*)\gamma_x\right]_e\right\}(\Delta y\Delta z) \\ &+ \left\{\left[(\rho_\ell\theta_\ell v_\ell^* + \rho_g\theta_g v_g^*)\gamma_y\right]_s - \left[(\rho_\ell\theta_\ell v_\ell^* + \rho_g\theta_g v_g^*)\gamma_y\right]_n\right\}(\Delta x\Delta z) \\ &+ \left\{\left[(\rho_\ell\theta_\ell w_\ell^* + \rho_g\theta_g w_g^*)\gamma_z\right]_b - \left[(\rho_\ell\theta_\ell w_\ell^* + \rho_g\theta_g w_g^*)\gamma_z\right]_t\right\}(\Delta x\Delta y) \\ &+ \left[(\rho_\ell\theta_\ell + \rho_g\theta_g)^0 - (\rho_\ell\theta_\ell + \rho_g\theta_g)\right](\gamma_v\Delta x\Delta y\Delta z/\Delta t). \end{aligned} \tag{9.7}$$

The similarity between Eqs. 9.5h and 9.7 should be noted. The only difference between the two equations is that, whereas the b_0 for the pressure equation is calculated in terms of $\hat{u}$, $\hat{v}$, and $\hat{w}$, the corresponding quantity for the pressure correction equation is obtained in terms of $\overset{*}{u}$, $\overset{*}{v}$, and $\overset{*}{w}$.

9.3 Pressure-correction Equation 2

The pressure correction equation derived in this section is based on the procedure very similar to the numerical procedure known as IPSA.[5] In this procedure we differentiate the phase continuity equations and momentum equations and combine them with the condition

$$\theta_\ell + \theta_g = 1 \tag{9.8}$$

to obtain the pressure correction equation.

Let us assume that we have an estimated pressure field p*. We can then solve the momentum equations to obtain velocity fields u_ℓ^*, v_ℓ^* and w_ℓ^* for liquid phase and u_g^*, v_g^*, and w_g^* for gas phase. These velocity fields can be used in the continuity equations to obtain fluid volume fractions θ_ℓ^* and θ_g^*. As the fluid volume fractions are based on estimated pressure field p*, they will, in general, not add up to 1. We, therefore, require the corrections to fluid volume fractions θ_ℓ' and θ_g' such that

$$\left(\theta_\ell^* + \theta_\ell'\right) + \left(\theta_g^* + \theta_g'\right) = 1, \tag{9.9}$$

or

$$\theta_\ell' + \theta_g' = 1 - \theta_\ell^* - \theta_g^*. \tag{9.9a}$$

Now from Eq. 8.1, the fluid volume fraction is given by

$$\theta^* = \frac{\beta}{\alpha}, \tag{9.10}$$

where,

$$\beta = \left(\sum a_{nb}\theta_{nb}^*\right)_{in} + a_0^0\theta_0^0 + b_0 \tag{9.10a}$$

$$\alpha = \left(\sum \bar{a}_{nb}\right)_{out} + \bar{a}_0, \tag{9.10b}$$

The subscript nb refers to six neighboring points, "in" represents inflow, and "out" represents outflow. From Eq. 9.10 we derive a fluid volume fraction correction formula.

$$\theta' = \frac{\alpha\beta' - \beta\alpha'}{\alpha^2}, \tag{9.11}$$

or

$$\theta' = \frac{\alpha\left(\sum a'_{nb}\theta^{*}_{nb}\right)_{in} - \beta\left(\sum \bar{a}'_{nb}\right)_{out}}{\alpha^{2}}, \tag{9.11a}$$

or

$$\theta' = \frac{\left(\sum a'_{nb}\theta^{*}_{nb}\right)_{in} - \Theta^{*}\left(\sum \bar{a}'_{nb}\right)_{out}}{\alpha}. \tag{9.11b}$$

Here a' and $\bar{a}'$ are the changes in coefficients due to pressure correction p'.

In order to determine a' and $\bar{a}'$, we look at the coefficients a_2 and $\bar{a}_2$ (Eq. 8.2) making note that the coefficients a_{nb} and $\bar{a}_{nb}$ exist only for inflows and outflows, respectively;

$$a_2 = |F_2|_{in} = -\rho_{i+1}\left(u^{*}A_x\right)_{i+1/2}, \tag{9.12a}$$

and

$$\bar{a}_2 = \left(F_2\right)_{out} = \rho_i\left(u^{*}A_x\right)_{i+1/2}. \tag{9.12b}$$

Combining Eq. 9.12 with Eq. 7.8 we get

$$a'_2 = \rho_{i+1}\left(A_x d\right)_{i+1/2}\left(p'_{i+1} - p'_i\right), \text{ (in)} \tag{9.13a}$$

and

$$\bar{a}'_2 = \rho_i\left(A_x d\right)_{i+1/2}\left(p'_i - p'_{i+1}\right), \text{ (out)} \tag{9.13b}$$

Equations for other neighboring coefficients can be obtained in an identical manner. We now substitute all these coefficients in Eqs. 9.9a and 9.11b. After simplification we get

$$\theta' = \frac{1}{\alpha}\left\{\sum_{in} (\rho A d\theta^{*})_{nb}\left(p'_{nb} - p'_p\right) - (\rho\theta^{*})_{ijk} \sum_{out} (Ad)_{nb}\left(p'_p - p'_{nb}\right)\right\}, \tag{9.14}$$

and

$$\{1 - (\theta_\ell^* + \theta_g^*)\} = \sum \left\{ \left[\frac{(\rho_\ell A d_\ell \theta_\ell^*)_{nb}}{\alpha_\ell} + \frac{(\rho_g A d_g \theta_g^*)_{nb}}{\alpha_g} \right]_{in} \right.$$

$$\left. + \left[\frac{(A d_\ell)_{nb}}{\alpha_\ell} (\rho_\ell \theta_\ell^*)_{ijk} + \frac{(A d_g)_{nb}}{\alpha_g} (\rho_g \theta_g^*)_{ijk} \right]_{out} \right\} p'_{nb}$$

$$- p'_{ijk} \left\{ \sum_{in} \left[\frac{(\rho_\ell A d_\ell \theta_\ell^*)_{nb}}{\alpha_\ell} + \frac{(\rho_g A d_g \theta_g^*)_{nb}}{\alpha_g} \right] \right.$$

$$\left. + \sum_{out} \left[\frac{(A d_\ell)_{nb}}{\alpha_\ell} (\rho_\ell \theta_\ell^*)_{ijk} + \frac{(A d_g)_{nb}}{\alpha_g} (\rho_g \theta_g^*)_{ijk} \right] \right\}. \quad (9.15)$$

Here A represents the cross sectional area, e.g.,

$$A_{i+1} = (\gamma_x)_{i+1/2} \Delta y_j \Delta z_k, \quad (9.16a)$$

$$A_{i-1} = (\gamma_x)_{i-1/2} \Delta y_j \Delta z_k. \quad (9.16b)$$

Equation 9.15 is our final pressure correction equation. After solving for pressure corrections (Eq. 9.15) we use Eqs. 9.14 for computing fluid volume fraction corrections. The velocities and fluid volume fractions are then modified to account for these corrections.

10. INITIAL AND BOUNDARY CONDITIONS

10.1 Initial Conditions

Generally, before the solution sequence can begin, all values of variables must be assigned. This can be accomplished by either continuing a previous run via the restart capability or by specifying the initial temperature, pressure, and velocity distribution throughout the interior points of the space under consideration. When the initialization is not a restart, density and enthalpy can be claculated from equations of state, using the specified pressures and temperatures. The determination of these distributions and their subsequent input into the code are generally tedious. Options are provided in the code to ease this initialization task. When a steady-state solution is being sought, an initialization as close as possible to the expected solution should be used to reduce computer running time.

Pressure Initialization for Static Head

When gravity is acting along any one of the three principal coordinate axes and there is either constant or one-dimensional temperature variation in that same direction, an option has been provided to reduce the initialization task. This option is exercised by specifying a pressure at a point and either the constant or one-dimensional temperature variation. The entire temperature field can be generated from the input temperature information. The density field is then computed from the equation of state. With this density field and the point pressure, a pressure field is generated to account for the static head. From the pressure and temperature fields, the enthalpy is obtained, thus completing this initialization option.

Pressure-drop Initialization

A linear variation or constant-pressure-gradient initialization option is also provided as in COMMIX-1 (Ref. 2). This can be used when the constant pressure gradient is along any one of the three principal axes. It is accomplished by specifying the constant pressure gradient as either $\partial P/\partial x$, $\partial P/\partial y$, or $\partial P/\partial z$, and a point pressure. This option can be used along with the static-head initialization. However, if the constant pressure gradient is along the same axis as gravity, the pressure gradient due to gravity must be included in the specification of the constant pressure gradient.

10.2 Boundary Conditions

The options are provided in the code for the following boundary conditions.

Velocity

1. No slip
2. Slip
3. Continuative velocity boundary

4. Continuative momentum boundary
5. Constant or prescribed transient velocity boundary

Temperature

1. Constant or transient temperature boundary
2. Constant or transient heat flux boundary
3. Adiabatic surface

Pressure

1. Constant pressure boundary
2. Transient pressure boundary

10.3 Boundary Conditions for Pressure and Pressure-correction Equations

Since the continuity equation has been reformulated as the pressure equation and the pressure-correction equation, special attention is given to the boundary conditions for these equations. Normally, either the velocity normal to the boundary is specified or the pressure at the boundary is given.

Given Normal Velocity at the Boundary

A control volume adjacent to a boundary is shown in Fig. 10.1. If the velocity u_W entering the control volume at the boundary face is known, then, in the derivation of the pressure and pressure-correction equations, we do not substitute u_W in terms of $\hat{u}_W$ or u_W^*; instead we use the known value of u_W. Thus, p_W or p_W' does not appear in the p or p' equations. In other words, the coefficient a_W will be zero in these equations. Since this boundary coefficient is zero, no information about the boundary pressure is needed.

The given velocity boundary condition occurs at walls, symmetry planes, and inflow boundaries with known flow rate. Also the outflow boundaries can be treated as known-velocity boundaries by specifying the normal velocity there by reference to overall mass conservation. Only when the flow rates are unknown, but the pressure drop is specified, do we turn to the given-pressure boundary condition.

Given Pressure at the Boundary

When the pressure at the boundary point 1 in Fig. 10.1 is known, the situation is straightforward. For the pressure equation, the known value p_1 is used in the appropriate neighbor term. Further, if p_1^* is set equal to p_1, we have $p_1' = 0$, which serves as the known boundary value for the pressure-correction equation.

10.4 Irregular Geometries

When the actual boundaries of the calculation domain do not coincide with the boundaries of the nominal (rectangular) domain, special treatment is needed

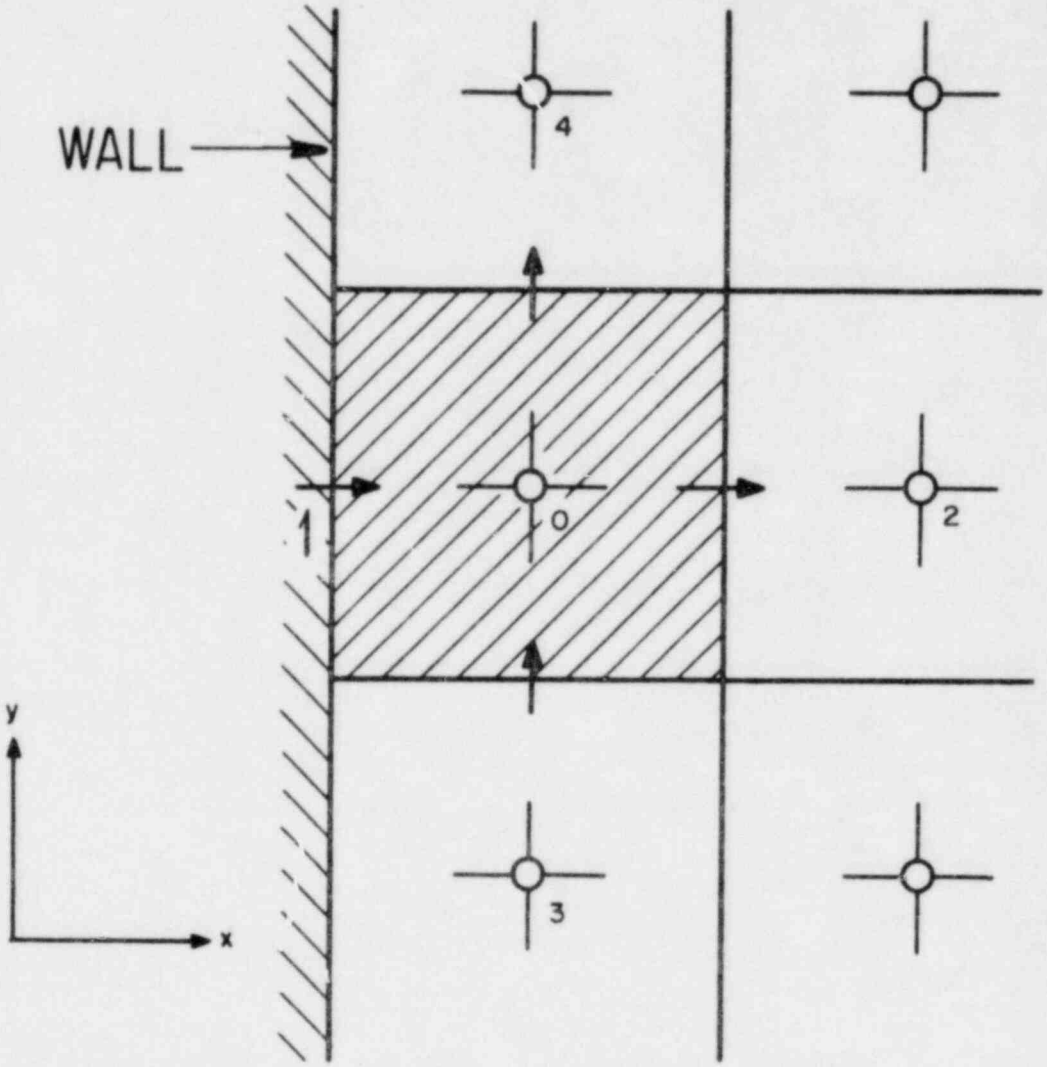

Fig. 10.1. Near-boundary control volume

to incorporate the "internal" boundaries. When the boundary is internal to the nominal calculation domain, the grid should be so designed that the actual boundary is suitably approximated by a succession of control-volume faces. Figure 10.2 illustrates this for a solid obstacle projecting into the nominal calculation domain. The dashed lines indicate the control-volume faces, while the shaded area denotes the obstacle.

The irregular boundaries can be treated through appropriate choice of the Γ's as described in Ref. 25. When ϕ stands for velocity, the corresponding values of Γ for the control volumes that lie in the solid can be made very large. This results in very small (essentially zero) values of velocity predicted for the solid region. A given value of ϕ, such as temperature, can also be arranged at the internal boundary by making the Γ values for the solid large and by specifying the given value of ϕ at the nominal boundary adjacent to the solid. An adiabatic surface, on the other hand, can be simulated by the use of a very low Γ_h for the solid.

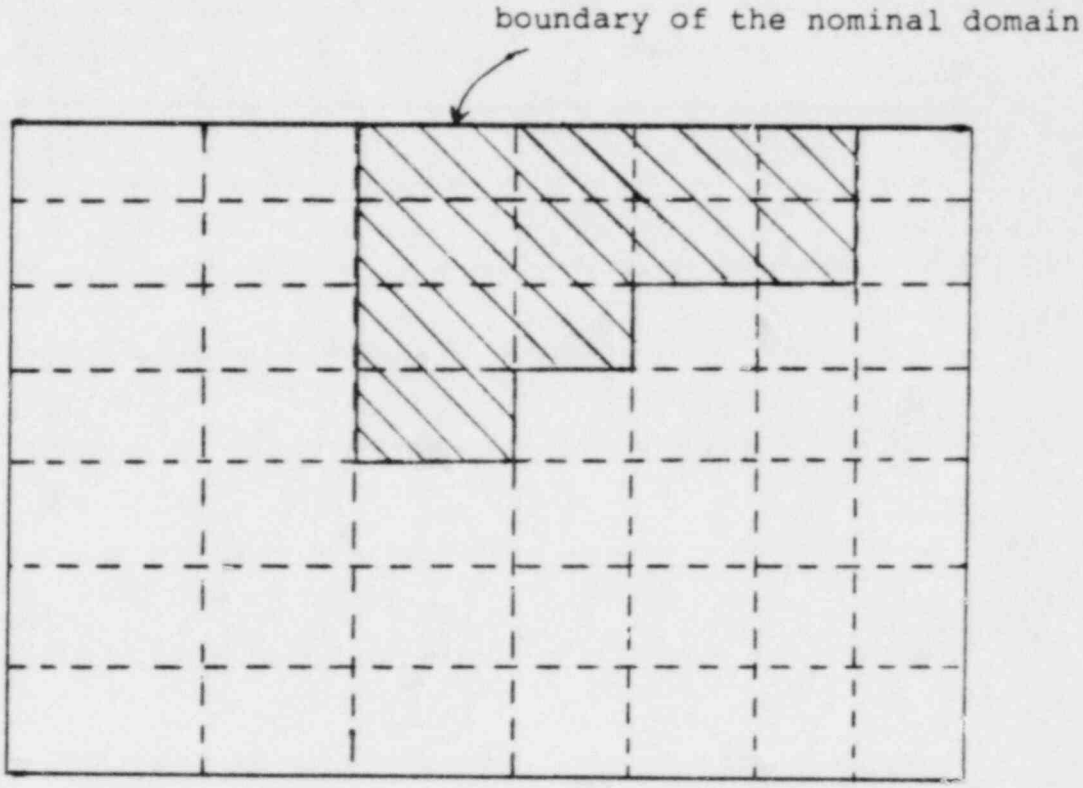

Fig. 10.2. Design of control volumes for irregular geometry

11. SOLUTION OF THE FINITE-DIFFERENCE EQUATIONS

The finite-difference equations derived for the general variable ϕ, for the velocity components, for pressure, and for the pressure correction have a common form. They all relate the value of the variable at 0 to the values at the six neighbor points.

The form of the equation is such that it permits various numerical solution schemes, e.g., cell-by-cell, line-by-line, plane-by-plane, block iterative, direct inversion etc. The cell-by-cell procedure generally requires less storage but takes a longer time to converge. The direct inversion procedure, at the other end, requires prohibitively large computer storage but provides stability and efficiency. We have provided two solution procedure options in the code. One is the cell-by-cell solution procedure with successive over-relaxation and second is the line-by-line solution procedure. The line-by-line solution procedure, for the solution of the algebraic equations of the general form is described here.

Although the general finite-difference equation contains seven unknowns, the equations for the near-boundary control volumes have fewer unknowns. This results from the fact that either the boundary values are known or their influence has been set equal to zero through our boundary-condition practice. Thus, we may always regard the boundary values as known for the purpose of solving the equations.

11.1 Tri-Diagonal-Matrix Algorithm

The primary building block in the solution method is the Tri-Diagonal-Matrix Algorithm (TDMA). It enables us to solve directly for all the values along one line.

Let the system of equations be represented by

$$A_i\phi_i = B_i\phi_{i+1} + C_i\phi_{i-1} + D_i, \tag{11.1}$$

for $i = 2, 3, \ldots, N$, with ϕ_1 and ϕ_{N+1} being the known values.

The first step is to calculate the transformed coefficients P_i and Q_i from

$$P_2 = B_2/A_2,\ Q_2 = \left(C_2\phi_1 + D_2\right)/A_2, \tag{11.2}$$

and, for $i = 3, 4, \ldots, N$

$$P_i = B_i/\left(A_i - C_iP_{i-1}\right),$$

$$Q_i = \left(D_i + C_iQ_{i-1}\right)/\left(A_i - C_iP_{i-1}\right). \tag{11.3}$$

The second and final step is the "back substitution," i.e., the calculation of ϕ_i from

$$\phi_i = P_i \phi_{i+1} + Q_i. \tag{11.4}$$

for i = N, N - 1, N - 2, ..., 4, 3, 2:

This step gives the solution of the system of equations (11.1).

11.2 Line-by-line Scheme

The line-by-line procedure for solving the finite-difference equations is a logical extension of the Gauss-Seidel point-by-point method. Instead of visiting a point and solving for the value there by the use of the available values at the neighbor points, we choose a line and solve for all the values along it by the TDMA.

The procedure is schematically illustrated in Fig. 11.1. A grid line is chosen for the application of the TDMA. In the finite-difference equations for all the points along this line will appear the values of the variable along the four neighboring lines (two of which are shown in Fig. 11.1; the other two contain the z-direction neighbors). If these neighbor-line values are assumed to be known, then the finite-difference equations along the chosen line will take the form of Eq. 11.1 and can be solved by the TDMA. The main advantage of this procedure is that the boundary-condition information from the ends of the line is at once transmitted to the interior of the domain, no matter how many grid points lie on the line. In the point-by-point procedure, on the other hand, the influences from the boundary travel only one grid interval per iteration.

When all the lines in a given direction are visited, the basic operation of the line-by-line procedure is complete.

11.3 Traverse and Sweep Directions

The basic operation just mentioned does not, however, give the final solution of the algebraic equations. The reason is that guessed values from neighboring lines are used in the procedure. Only after many repetitions of the basic operation, do we get the correct solution of the equations. Of course, it is desirable to seek ways of reducing the number of required repetitions.

The direction of the line chosen for the TDMA is called the traverse direction. In many problems, geometrical and other factors result in a situation where the coefficients in a particular direction are much larger than those in other directions. In this situation, a TDMA traverse in the direction of large coefficients is particularly effective; because the guessed values from the neighboring lines enter with only weak coefficients. When such a preferred traverse direction is not available, it is best to conduct three successive repetitions of the basic operation by choosing a new traverse direction each time.

Having chosen the direction of traverse, we need to decide the sequence in which the lines are visited. This will be called the sweep direction. It is

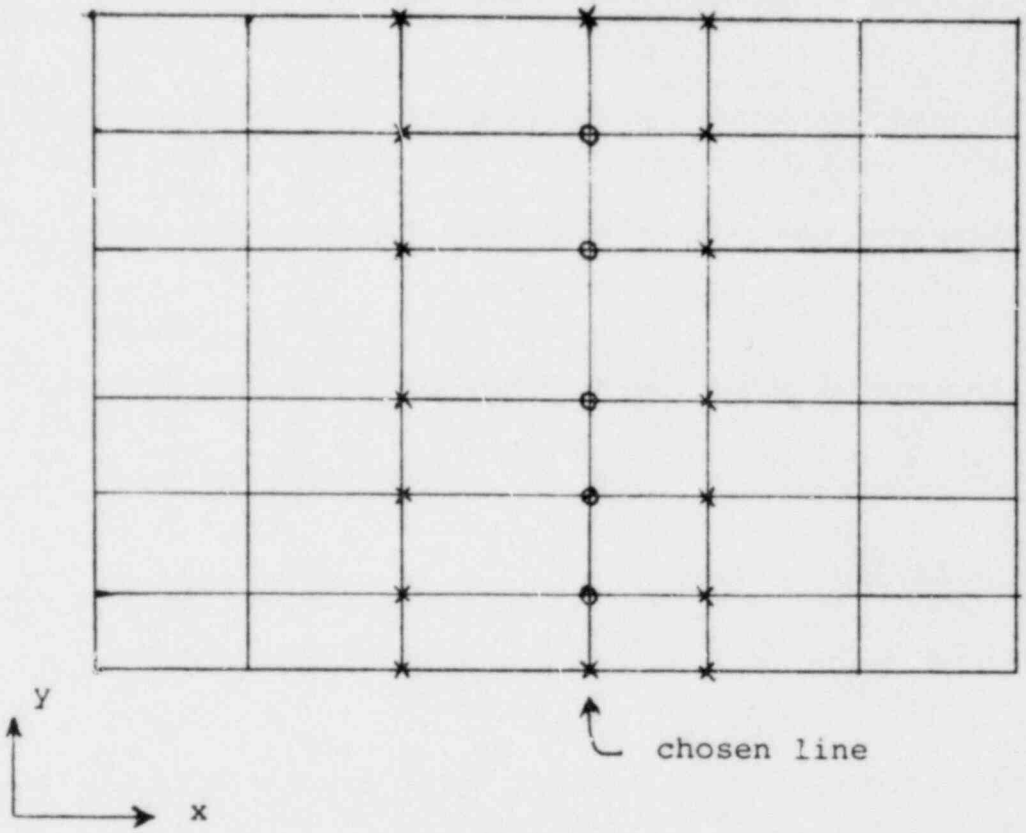

Fig. 11.1. Illustration of the line-by-line scheme

convenient to start at one end of the calculation domain and proceed to the other end, so that the boundary-condition influence is quickly brought in. If the fluid flow in the domain has a predominant direction, it is very beneficial to make the sweep direction the same as the predominant flow direction. Then the upstream information rapidly gets conveyed to the downstream locations. In the absence of a major flow direction, it is best to alternate the sweep direction in the successive repetitions of the algorithm.

Presently, the COMMIX-2 uses the following sequence of operations. The calculation starts at k = 1 (z-plane) and proceeds to the other end, k = kmax plane. In each plane two alternate traverses and sweeps are performed, i.e., first x-traverse and y-sweep, and then y-traverse and x-sweep. This sequence of operation (sweeping of planes in the k-direction) can be repeated several times. An input parameter has been provided for selecting the number of times this sweeping of planes in the k-direction is desired.

11.4 Optimization of the Equation-solving Effort

The equation-solving algorithm described so far is used for one variable at a time. Further, it regards the finite-difference equations as linear. The nonlinearity of the equations and the interlinkage between the variables are handled by the iteration scheme outlined in the next section. During any given iteration we have only tentative values of the coefficients in the finite-difference equations. The coefficients must be recalculated for every iteration to reflect the changes that have occurred in the relevant dependent variables. Therefore, the repetitions of the line-by-line procedure, which is working on merely the tentative values of the coefficients, need not be carried to ultimate convergence. It is sufficient to obtain a reasonably good solution of the algebraic equations before the coefficients are recalculated. The optimum equation-solving effort should be determined by experience and experimentation, but a simple rule is that the work required for calculating the coefficients should be roughly comparable to the work involved in solving the equations.

12. ITERATION SCHEME

For every time step in an unsteady situation, a number of iterations must be performed to account for the interlinkages and nonlinearities. Also, the solution for a steady-state problem is achieved after a number of iterations. A given iteration starts with a set of values of all the dependent variables (obtained from an initial guess for the first iteration and from the previous iterations for subsequent iterations) and proceeds to obtain a new set of values. When subsequent iterations cease to produce any significant change in the values, the iteration sequence is said to have reached convergence. The COMMIX-2 has the following sequence of operations.

12.1 Sequence of Operations

a. Initialize all the dependent variables. This is performed either by providing input data or reading the values from the restart tape.

b.† Compute density field from the equations of state.

c.†† The fluid volume fractions θ_ℓ^* and θ_g^* are then obtained by

(i) solving the liquid continuity for θ_ℓ and evaluating θ_g from the relation $\theta_\ell + \theta_g = 1$ (extended SIMPLER procedure),

or

(ii) solving the two-phase continuity equations (similar to the IPSA procedure).

d.† Compute coefficients and pseudovelocities ($\hat{u}$, $\hat{v}$, and $\hat{w}$) of the momentum equations.

e. Set up and solve the pressure equation, using line-by-line or cell-by-cell SOR procedures, to obtain new values of pressure p.

f. Using this pressure field p*, solve the momentum equations (7.2) or (7.4) to yield u*, v*, and w*.

g. Set up and solve pressure correction equations (9.3) or (9.15) to obtain the values of p'.

h.† Modify

(i) pressure field,

---

†Liquid phase, or vapor phase, or both phase variables are computed.

††For two-phase only.

(ii) void fractions using the void fraction-correction formula (Eq. 9.11) in IPSA type procedure, and

(iii) velocity field using the velocity-correction formula (Eq. 7.8).

i. Modify pressure and velocity fields to satisfy plane-by-plane integral mass balance (Section 12.5).

j.† Set up and solve the energy equation.

k. Return to step b with the new values obtained during this iteration as improved guesses and continue the procedure until convergence is achieved.

12.2 Under-relaxation

The finite-difference equations and the line-by-line scheme have been constructed such that, if there were no interlinkages and nonlinearities, convergence would be certain. However, because the equations of interest almost always contain nonlinear and interlinked influences, care has to be taken to prevent divergence. One simple strategy is to slow down the changes in the coefficients that would occur from iteration to iteration. This is accomplished via under-relaxation.

Under-relaxation of the Dependent Variables

The general finite-difference equation, Eq. 6.1 is

$$a_0\phi_0 = \sum a_{nb}\phi_{nb} + a_0^0\phi_0^0 + b_0, \tag{12.1}$$

where the subscript nb denotes the neighbor points. This equation can be modified as follows: From Eq. 12.1 we can write

$$\phi_0 = \sum \frac{a_{nb}}{a_0}\phi_{nb} + \frac{a_0^0\phi_0^0}{a_0} + b_0/a_0. \tag{12.1a}$$

Also, let

$$\phi_0^{new} = \omega\phi_0 + (1 - \omega)\phi_0^*, \tag{12.1b}$$

where ϕ_0^* denotes the last iteration value of ϕ_0, ϕ_0 denotes the value obtained directly if Eq. 12.1 is solved; and ω is the under-relaxation factor. Substitution of Eq. 12.1a in Eq. 12.1b and rearrangement give

†Liquid phase, or vapor phase, or both phase variables are computed.

$$(a_0/\omega)\phi_0^{new} = \Sigma a_{nb}\phi_{nb} + a_0^0\phi_0^0 + b_0 + (1 - \omega)(a_0/\omega)\phi_0^* . \tag{12.2}$$

It is easy to see that, when ϕ_0 becomes equal to ϕ_0^* (i.e., the iterations converge), Eq. 12.2 becomes identical to Eq. 12.1. In the meantime, however, Eq. 12.2 would have a tendency to keep the resulting ϕ_0^{new} closer to ϕ_0^* (than Eq. 12.1 would do) provided the relaxation factor ω is less than 1. A value of ω close to zero would indicate a very heavy under-relaxation.

A value of $\omega = 0.5$ usually provides sufficient under-relaxation for most variables. For the velocity components, a value of $\omega = 0.7$ may be used. The pressure equation may be under-relaxed by using $\omega = 0.8$. These values should be regarded as only initial suggestions; a proper set of ω values should be obtained by actual experience for a given class of problems. In COMMIX-2, input parameters OMEGAP, OMEGAV, OMEGAT and OMEGAE are provided for under-relaxing pressure, velocity, fluid volume fraction and energy, respectively.

Under-relaxation of Auxiliary Quantities

In addition to under-relaxing the dependent variables, a number of other quantities can be under-relaxed with advantage. For example, the density ρ and the diffusion coefficient Γ can be calculated from

$$\rho = \omega\rho_{new} + (1 - \omega)\rho_{old}, \tag{12.3}$$

$$\Gamma = \omega\Gamma_{new} + (1 - \omega)\Gamma_{old}. \tag{12.4}$$

Often the source terms can be a cause of divergence. Under-relaxation of the source terms in the form

$$S = \omega S_{new} + (1 - \omega)S_{old}, \tag{12.5}$$

can be helpful to prevent divergence. Even some boundary values can be introduced in a controlled manner via

$$\phi_B = \omega\phi_{B,given} + (1 - \omega)\phi_{B,old}, \tag{12.6}$$

where ϕ_B denotes a boundary value.

It should be obvious that the values of ω appearing in Eqs. 12.2 to 12.6 can all be different; indeed, it is possible, though inconvenient, to choose a separate value of ω for each grid point. Further, the values of ω can be changed as the iterations proceed.

In order to minimize the number of input variables, we have not included under-relaxation factors for auxiliary quantities. However, if one desires, this can be incorporated in the code very easily.

12.3 Linearization of the Source Term

In the derivation of the finite-difference equations, we have expressed the source term S via Eq. 5.14 in a linearized form. This form is an attempt to anticipate the change in S resulting from the change in the value of ϕ_0. In order to obtain a diagonally dominant matrix, S_p in Eq. 5.14 is allowed to become positive. This is achieved by linearizing the source term in the following way.

Let S_1 and S_2 denote the positive and negative parts of the source term such that

$$S = S_1 - S_2 \; (S_1 > 0, \; S_2 > 0). \tag{12.7}$$

We then set S_C and S_p according to

$$S_C = S_1, \tag{12.8}$$

and

$$S_p = -(S_2/\phi_0^*), \tag{12.9}$$

where ϕ_0 denotes the last-iteration value of ϕ_0.

Source due to Phase Change

For the source term due to phase change in the momentum equation we have assumed that evaporating mass from liquid has a velocity equal to the liquid velocity. Thus, for x-momentum equations

$$S_{m\Omega\ell} = \Omega_\ell u_\ell = -\dot{m}'''_{evap} u_\ell, \tag{12.10}$$

and

$$S_{m\Omega g} = \Omega_g u_\ell = \dot{m}'''_{evap} u_\ell \tag{12.11}$$

Similar expressions are assumed for y and z directions. With this assumption, Eqs. 6.2h and 6.2i become:

Liquid Momentum:

$$b_0 = S_c(\gamma_v \Delta x \Delta y \Delta z) \tag{12.12}$$

$$a_0 = a_1 + a_2 + a_3 + a_4 + a_5 + a_6 + a_0^G - S_p(\gamma_v \Delta x \Delta y \Delta z) \tag{12.13}$$

<u>Gas Momentum</u> $(\dot{m}'''_{evap} > 0)$

$$b_0 = (S_c + \dot{m}'''_{evap}\phi_\ell)(\gamma_v \Delta x \Delta y \Delta z) \tag{12.14}$$

$$a_0 = a_1 + a_2 + a_3 + a_4 + a_5 + a_6 + a_0^0 - (S_p - \dot{m}'''_{evap})(\gamma_v \Delta x \Delta y \Delta z) \tag{12.15}$$

<u>Gas Momentum</u> $(\dot{m}'''_{evap} < 0)$

$$b_0 = [S_c + \dot{m}'''_{evap}(\phi_\ell - \phi_g)](\gamma_v \Delta x \Delta y \Delta z), \tag{12.16}$$

$$a_0 = a_1 + a_2 + a_3 + a_4 + a_5 + a_6 + a_0^0 - S_p(\gamma_v \Delta x \Delta y \Delta z) \tag{12.17}$$

Here ϕ stands for u, v and ω velocity components.

For the source term due to phase change in the energy equation, we have assumed that condensing mass from gas has enthalpy equal to gas enthalpy. With this assumption, the source terms in the energy equations are

$$S_{h\Omega\ell} = \Omega_\ell h_g = -\dot{m}'''_{evap} h_g, \tag{12.18}$$

and

$$S_{h\Omega g} = \Omega_g h_g = \dot{m}'''_{evap} h_g. \tag{12.19}$$

Thus, Eqs. 6.2h and 6.2i are:

<u>Liquid:</u> $(\dot{m}'''_{evap} \ (= -\Omega_\ell) < 0)$

$$b_0 = (S_c - \dot{m}'''_{evap} h_g)(\gamma_v \Delta x \Delta y \Delta z) \tag{12.20}$$

$$a_0 = a_1 + a_2 + a_3 + a_4 + a_5 + a_6 + a_0^0 - (S_p + \dot{m}'''_{evap})(\gamma_v \Delta x \Delta y \Delta z) \tag{12.21}$$

<u>Liquid:</u> $(\dot{m}'''_{evap} \ (= -\Omega_\ell) > 0)$

$$b_0 = (S_c - \dot{m}'''_{evap}(h_g - h_\ell))(\gamma_v \Delta x \Delta y \Delta z) \tag{12.22}$$

$$a_0 = a_1 + a_2 + a_3 + a_4 + a_5 + a_6 + a_0^0 - S_p(\gamma_v \Delta x \Delta y \Delta z) \tag{12.23}$$

Gas:

$$b_0 = S_c(\gamma_v \Delta x \Delta y \Delta z) \tag{12.24}$$

$$a_0 = a_1 + a_2 + a_3 + a_4 + a_5 + a_6 + a_0^0 - S_p(\gamma_v \Delta x \Delta y \Delta z) \tag{12.25}$$

12.4 Distinction between Steady and Unsteady Situations

The calculation method outlined in this report makes only a small distinction between the steady and unsteady problems. The suggested calculation sequence for one time step in an unsteady situation is almost identical to the sequence for obtaining the steady-state solution. If the time step Δt is made very large, our finite-difference equations for an unsteady problem reduce to those for a steady problem.

The main difference between the two situations turns out to be in the number of the required iterations. In an unsteady situation, the "initial" values of ϕ for any time step are either given or known from the previous time step. If the value of Δt is reasonable, the ϕ values do not change very drastically within one time step. Thus, the values ϕ_0^0 at the start of the time step serve as good guesses for the new values ϕ_0, and therefore, only a few iterations may be sufficient to attain convergence for the time step. On the other hand, if the guesses available for a steady-state problem are rather "wild," then many iterations might be necessary before convergence is obtained.

12.5 Performance of Integral Balances

During the iterative process, because of partial convergence of the continuity equations, it is possible that the total (or individual phase) mass flow out of a slab of cells (across a plane) is not equal to the known, correct value. In order to make the solution at subsequent slabs of cells more accurate, it is advantageous to correct the velocity and pressure fields to satisfy the integral mass balance. This section explains such a practice, and describes its merits.

Consider first a flow in which there is a predominant flow direction (e.g., pipe flow). For a pipe flow, we recognize that the total flow outwards of any plane perpendicular to the pipe axis must be equal to the inflow at the entrance of the pipe. Mathematically, this means

$$\sum_i \sum_j \rho_{ij} w_{ij} A_{ij} = \dot{m} \tag{12.26}$$

where ρ is density, w is the axial velocity, and A is the area perpendicular to the pipe axis. The summation is made over all cells in the cross-sectional plane. Since the above equation is not always satisfied until convergence, we wish to correct w_{ij} by an amount Δw_{ij} to meet this criteria. There are a few

different ways to perform the corrections to the w field and associated pressure field; here two methods found often superior to others are described. Only the first method described here is included in COMMIX-2.

Uniform Pressure Correction

Let Δp be a uniform correction (over the cross-section) to the pressure affecting the w velocity at the given plane. Also, let D_w be $\partial w/\partial p$ for each cell. We can then write

$$\Delta p \sum_i \sum_j \rho_{ij} (D_w)_{ij} A_{ij} = \Delta \dot{m}, \tag{12.27}$$

where $\Delta \dot{m}$ is the error (required minus actual). This leads to the relation for Δp, as follows:

$$\Delta p = \frac{\Delta \dot{m}}{\sum \sum \rho_{ij} (D_w)_{ij} A_{ij}}, \tag{12.28}$$

and

$$\Delta w_{ij} = (D_w)_{ij} \Delta p. \tag{12.29}$$

Note that the Δp correction is uniform, but Δw is different for each cell.

The above expressions can be extended to two-phase flows, considering the total mass flow as the quantity to be balanced. Thus,

$$\sum_i \sum_j (\rho_\ell \theta_\ell w_\ell A)_{ij} + \sum_i \sum_j (\rho_g \theta_g w_g A)_{ij} = \dot{m}_\ell + \dot{m}_g = \dot{m}_t. \tag{12.30}$$

We can derive in a straightforward way, that

$$\Delta p = \frac{(\dot{m}_t)_{req} - (\dot{m}_t)_{actual}}{\sum_i \sum_j \left[\left(\theta_\ell \rho_\ell D_{w_\ell} \right)_{ij} + \left(\theta_g \rho_g D_{w_g} \right)_{ij} \right] A_{ij}}, \tag{12.31}$$

$$(\Delta w_\ell)_{ij} = \left(D_{w_\ell} \right)_{ij} \Delta p, \tag{12.32}$$

and

$$(\Delta w_g)_{ij} = \left(D_{w_g} \right)_{ij} \Delta p. \tag{12.33}$$

The Δw corrections are applied at the slab concerned, but the Δp corrections are made to all downstream planes in the domain. This practice avoids the creation of artificial pressure gradients at subsequent planes.

The COMMIX-2 has incorporated the uniform pressure correction approach. The integral mass balance is checked across a z plane. The sweeping of z-planes begins at k = 1 and proceeds to k = kmax.

Uniform Velocity Correction

Let Δw be a uniform correction (over the cross-section) to the axial velocity at a given plane. We can then write

$$\Delta w \sum_i \sum_j \rho_{ij} A_{ij} = \Delta \dot{m}, \tag{12.34}$$

or

$$\Delta w = \frac{\Delta \dot{m}}{\sum_i \sum_j \rho_{ij} A_{ij}} . \tag{12.35}$$

Having computed Δw, we can easily derive the relation for Δp_{ij}.

$$\Delta p_{ij} = \frac{\Delta w}{\left(D_w\right)_{ij}} = \frac{1}{\left(D_w\right)_{ij}} \frac{\Delta \dot{m}}{\sum_i \sum_j \rho_{ij} A_{ij}} \tag{12.36}$$

In this procedure, we have uniform Δw for all cells in a plane, but Δp is different for each cell. We extend this procedure to two phase flows in the following way. Let $\Delta \dot{m}_\ell$ and $\Delta \dot{m}_g$ be the errors in mass flow rates and Δw_ℓ and Δw_g be the velocity corrections of liquid phase and gas phase, respectively. We then have

$$\Delta w_\ell = \frac{\Delta \dot{m}_\ell}{\sum_i \sum_j \left(\rho_\ell \theta_\ell A_\ell\right)_{ij}} , \tag{12.37}$$

and

$$\Delta w_g = \frac{\Delta \dot{m}_g}{\sum_i \sum_j \left(\rho_g \theta_g A_g\right)_{ij}} . \tag{12.38}$$

The pressure correction Δp_{ij} can be obtained by averaging the pressure corrections required for balancing of each phase of the two phases. Thus

$$\Delta p_{ij} = \frac{1}{2}\left(\left(\Delta p_{ij}\right)_{\ell} + \left(\Delta p\right)_{ij_g}\right) = \frac{1}{2}\left[\frac{\Delta \dot{m}_{\ell}}{D_{w_{ij}} \sum_i \sum_j \left(\rho_{\ell}\theta_{\ell}A_{\ell}\right)_{ij}} + \frac{\Delta \dot{m}_g}{D_{w_{ij}} \sum_i \sum_j \left(\rho_g\theta_g A_g\right)_{ij}}\right] \tag{12.39}$$

The Δw corrections are applied at the slab concerned, but the Δp corrections are made to all downstream planes in the domain.

13. FLOW CHARTS

The calculation method of COMMIX-2 described so far can be visualized through the flow charts presented in this section. It may be recognized that a number of decisions taken while designing the computer program have some effect on the details of the flow charts. The description here is given for an unsteady situation; the specialization to a steady-state problem has already been dealt with.

13.1 Time-step and Iteration Loops

The main structure of the computer program can be seen from Fig. 13.1 We begin by specifying the grid and, if desired, calculating a number of geometrical quantities which are frequently needed in later work. This is done in subroutines HOWBIG, GEOM3D, BOX, QTRPIN, and FULPIN. The subroutines QTRPIN and FULPIN are specifically designed for hexagonal fuel assemblies with desired quarter pin partitioning and full pin partitioning respectively, while the subroutine BOX is for all other geometries. Next the initial value of all variables are specified or calculated. This is done in the subroutine INITAL. At this stage, the subroutine OUTPUT is called to print initial values of all desired variables. Boundary conditions are then specified. The iteration sequence, for which further details will be given below, is then repeated a number of times until convergence is obtained. The subroutine TIMSTP determines the sequence of calling of all subroutines required during iteration. When the convergence is achieved, we return to MAIN where we update all variables and proceed to the next time step. When the required number of time steps has been performed, or the required maximum computation time is reached, the computation is terminated and, if requested, the restart data are written on a tape.

13.2 Iteration Sequence

The details of the iteration sequence are shown in Fig. 13.2. They follow the steps listed in Section 12.1. The sequence presented here is for the two-phase case. If a problem to be analyzed is single-phase only (liquid or gas) then all the subroutines for the second phase (gas or liquid) are bypassed.

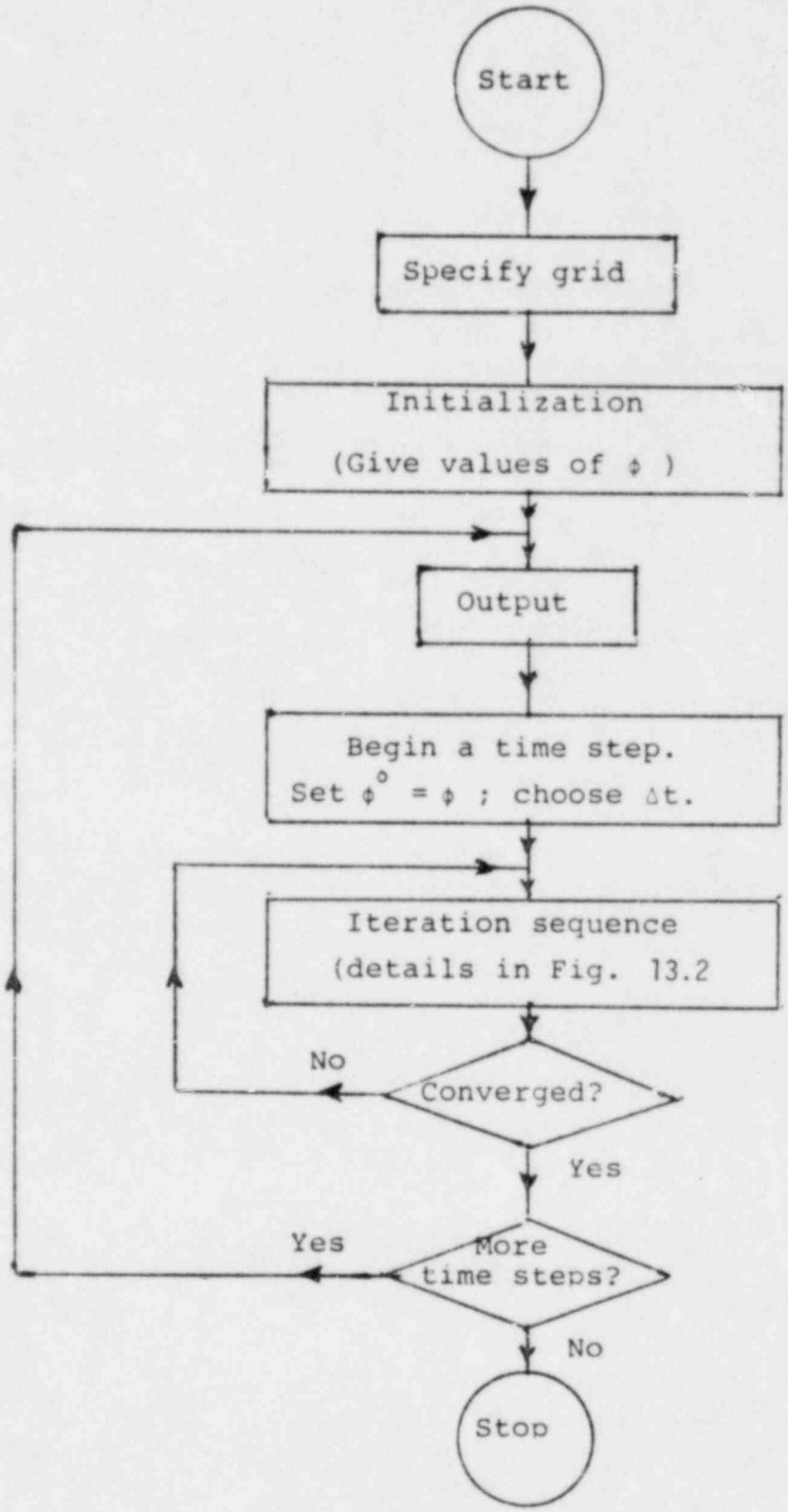

Fig. 13.1. The overall flow chart

1. Compute evaporation rate Ω (BOIL)
2. Set up coefficients of liquid volume fraction θ_ℓ equation (LVOID)
3. Solve liquid continuity equation to get θ_ℓ^* (SOLVEF)
4. Obtain θ_g^*

   (i) Use $\theta_g + \theta_\ell = 1$

   or

   (i) Coefficients of gas volume fraction θ_g equation (GVOID)

   (ii) Solve gas continuity equation to get θ_g^* (SOLVEF)
5. Compute density (PROPTY)
6. Compute liquid momentum source terms S_c and S_p (VSORCL)
7. Set up coefficients and compute pseudo velocities of the liquid momentum equations (XMOM; YMOM; ZMOM)
8. Compute gas momentum source terms S_c and S_p (VSORCG)
9. Set up coefficients and compute pseudo velocities of the gas momentum equations (XMOM; YMOM; ZMOM)

   Set up coefficients of pressure equation (PEQN)

11. Solve pressure equation to get p* using either line-by-line (SOLVEF) or cell-by-cell SOR (SOLVIT) procedure
12. Solve momentum equations to get u*, v*, w*

    Eq. 7.2 (VELMOM; SOLVEU; SOLVEV; SOLVEW)

    or

    Eq. 7.4 (MOMENT)
13. Update boundary flow values (BCFLOW)
14. Set up coefficients of pressure correction equation

    Eq. 9.6 (PCEQN1) (SIMPLER Procedure)

    or

    Eq. 9.15 (PCEQN2) (IPSA Procedure)
15. Solve pressure correction equation to get p' (SOLVEF)
16. Modify pressure $p = p^* + p'$
17. Modify liquid fractions (IF PCEQN2 is used) $\theta = \theta^* + \theta'$ (DELTAT)
18. Modify velocity $u = u^* + u'$ (DELTAV)
19. Perform integral balance (REBAL)
20. Compute density (PROPTY)
21. Compute source terms S_c and S_p of the energy equation (ESORCE)
22. Set up coefficients of the energy equation (ENERGY)
23. Solve energy equation to obtain h (SOLVEF)
24. Update temperature and density boundary values (BCTEMP)
25. Check the convergence

Fig. 13.2. Iteration Sequence

14. CONCLUDING REMARKS

This report has described the numerical procedure of COMMIX-2 for the solution of three-dimensional, single-phase/two-phase, steady/unsteady flow problems with heat transfer. The method is based on the control-volume approach, which is easy to interpret in physical terms and which ensures overall conservation. Calculation practices and iteration sequences, which have been found to be accurate and efficient have been used in COMMIX-2. The structure of the computer program has been outlined by way of flow charts.

We have developed this code retaining similarity with COMMIX-1A. All special features of COMMIX-1A have also been incorporated in the code. COMMIX-1A users will have, therefore, no difficulty in adopting COMMIX-2.

APPENDIX A

Thermodynamic and Transport Properties

The thermodynamic and transport properties of sodium are obtained from Golden and Tokar[26] and of water from Brookhaven National Laboratory.

A.1 Sodium-Liquid Properties

Density (kg/m^3)

$$\rho(T) = 9.50076E2 + T[-2.2976E-1 + T(-1.46049E-5 + 5.63788E-9\ T)]. \quad (A.1)$$

Viscosity (pascal-second) or (Pa•s)

$$\mu(T) = 3.2419E-3 \exp[5.0807E2/(T + 273.15) -0.4925\ \ell n(T + 273.15)]. \quad (A.2)$$

Specific Heat (J/kg•K)

$$c_p(T) = 1.43605E3 + T(-5.802E-1 + 4.62506E-4\ T). \quad (A.3)$$

Conductivity (W/m•K)

$$k(T) = 92.948 - 5.809E-2\ T + 1.1727E-5\ T^2. \quad (A.4)$$

In the above, T is temperature, in degrees Celsius.

Enthalpy (J/kg)

The enthalpy of liquid H(p,T) is calculated from the enthalpy of saturated liquid and the enthalpy change relation

$$dH = \frac{K}{\rho_\ell}\left[1 + \frac{T_K}{\rho_\ell}\left(\frac{\partial \rho_\ell}{\partial T_K}\right)_p\right]dp. \quad (A-5)$$

Here K is the ratio of gas constants in joules/pascal•m^3, and T_K is the temperature in kelvins.

Temperature (°C)

The temperature of sodium liquid T(H,p,T) is calculated using an iterative procedure. Initially the liquid temperature T* is assumed. The enthalpy H*(T*,p) is calculated. If the enthalpy H* is not in agreement

with the specified enthalpy H, then T* is modified. The procedure is repeated until H*(T*,p) is in close agreement with the prescribed enthalpy.

Saturation Pressure (pascals)

$$p_{sat}(T) = 1.01325E5 \left(\frac{3.03266E6}{\sqrt{T_R}}\right) e^{-2.30733E4/T_R}. \quad (\text{for } T_R < 2059.7) \qquad (A.6)$$

$$p_{sat}(T) = 1.01325E5 \left(\frac{6.8817602E6}{(T_R)^{0.61344}}\right) e^{-22981.96/T_R}. \quad (\text{for } T_R > 2059.7) \qquad (A.7)$$

Here, T_R is the temperature in degrees Rankine.

Saturation Enthalpy (J/kg)

$$H_{sat}(T) = 2.32444E3\{-29.02 + [T_R [0.389352 + T_R(-0.5529955E-4 + 0.113726E-7\ T_R)]]\}. \qquad (A.8)$$

Saturation Temperature (°C)

The saturation temperature $T_{sat}(p)$ is obtained by iterative solution of Eqs. A.6 and A.7.

A.2. Sodium Vapor Properties

Specific Heat (J/kg•K)

$$C_p(T) = 3821 - 1.952T + 6.347E-4\ T^2. \qquad (A.9)$$

Conductivity (W/m•K)

$$k(T) = 1.72958\{0.1639E-2 + 0.3977E-4\ T_F - 0.9697E-8\ T_F^2\}. \qquad (A.10)$$

Viscosity (Pa•sec)

$$\mu(T) = 4.133789E-4[0.03427 + 8.176E-6\ T_F]. \qquad (A.11)$$

Density (kg/m^3)

The density of sodium is calculated assuming that the vapor is made up of the monomer, dimer and tetramer and that these are all perfect gases.

$$\rho(p,T) = \frac{p\overline{M}}{RT_R} = \frac{16.01846\ \overline{M}p_{atm}}{0.730229\ T_R}. \qquad (A.12)$$

$$\bar{M} = M_1(N_1 + 2N_2 + 4N_4),$$

$$= 22.991(N_1 + 2N_2 + 4N_4). \tag{A.13}$$

The mole fractions N_1, N_2 and N_4 are obtained by solving

$$p_{atm}^3 k_4 N_1^4 + p_{atm} k_2 N_1^2 + N_1 - 1 = 0, \tag{A.14}$$

$$N_2 = k_2 p N_1^2, \tag{A.15}$$

and

$$N_4 = 1 - N_1 - N_2. \tag{A.16}$$

The equilibrium constants are

$$k_2 = e^{[-9.95845 + 16588.3/T_R]}, \tag{A.17}$$

and

$$k_4 = e^{[-24.59115 + 37589.7/T_R]}. \tag{A.18}$$

Here, p_{atm} is the pressure in atmospheres.

<u>Enthalpy</u> (J/kg)

$$H(p,T) = H_{g,sat} + 2328.9\{716.54[B_2(p_{sat}) - B_2(p)]$$

$$+ 811.85[B_4(p_{sat}) - B_4(p)]\}. \tag{A.19}$$

Here,

$$B_2 = \frac{2N_2}{N_1 + 2N_2 + 4N_4}, \tag{A.20}$$

$$B_4 = \frac{4N_4}{N_1 + 2N_2 + 4N_4}, \tag{A.21}$$

and

$H_{g,sat}$ is the saturation enthalpy.

Temperature (°C)

The temperature of sodium vapor is calculated by an iterative procedure. We start with assumed temperature T* and calculate the enthalpy $H^*(T^*,\rho)$. If H* is not in agreement with the specified enthalpy then the temperature is modified. The iterative procedure is continued until the calculated enthalpy is in close agreement with the prescribed enthalpy.

Saturation Enthalpy (J/kg)

$$H_{g,sat}(T_{sat}) = H_{\ell sat} + h_{fg}, \tag{A.22}$$

where

h_{fg} is the latent heat of vaporization.

$$h_{fg} = 2328.9\left\{\frac{1.8}{\bar{M}}\left[N_1\Delta H_1 + N_2\Delta H_2 + N_4\Delta H_4\right]\right\}. \tag{A.23}$$

$$\Delta H_1 = 25980.7 - 2.21312T_R + 7.06278E\text{-}4\ T_R^2 - 1.4526E7\ T_R^3. \tag{A.24}$$

$$\Delta H_2 = 2\Delta H_1 - 18304.0. \tag{A.25}$$

$$\Delta H_4 = 4\Delta H_1 - 41478.0. \tag{A.26}$$

A.3 Water-Liquid Properties

Density

$$\rho(p,H) = 16.018463\left\{a_1 + a_2H_R^2 + a_3H_R^4\right\}. \quad (H \leq 6.4477E5) \tag{A.27}$$

$$\rho(p,H) = 16.018463\left\{\left(a_1 + a_2H_R^2 + a_3H_R^4\right)f(y) + [1 - f(y)]\left(b_1 + \frac{b_2}{H_R - b_3}\right)\right\}.$$

$$(6.4477E5 < H \leq 6.57793E5) \tag{A.28}$$

$$\rho(p,H) = 16.018463\left\{b_1 + \frac{b_2}{H_R - b_3}\right\}. \quad (H > 6.57793E5). \tag{A.29}$$

Here,

$$a_1 = 62.4 + 2.14E\text{-}4\ p_R, \tag{A.30}$$

$$a_2 = -8.73E\text{-}5 + 1.438E\text{-}9\ p_R,, \tag{A.31}$$

$$a_3 = 2.32E\text{-}10 - 6.20E\text{-}15\ p_R, \tag{A.32}$$

$$b_1 = 92.924 + 5.761E\text{-}4\ p_R, \tag{A.33}$$

$$b_2 = 3.94402E4 + 1.6386\ p_R, \tag{A.34}$$

$$b_3 = 1.37735E3 + 3.5704E\text{-}2\ p_R, \tag{A.35}$$

$$y = \frac{H_R - 280}{2.8}, \tag{A.36}$$

$$f(y) = \frac{1}{16}\{8 - 15y + 10y^3 - 3y^5\}, \tag{A.37}$$

$$H_R = 4.299226E\text{-}4\ H, \tag{A.38}$$

$$p_R = 1.4503774E\text{-}4\ p, \tag{A.39}$$

H is the enthalpy in J/kg, and p is the pressure in pascals.

<u>Viscosity</u> (Pa•sec)

$$\mu(p,H) = (a_1 + a_2x + a_3x^2 + a_4x^3 + a_5x^4)$$

$$-(b_1 + b_2\eta + b_3\eta^2 + b_4\eta^3)(p - 6.8945753E5).$$

$$(H \geq 2.76E5) \tag{A.40}$$

$$\mu(p,H) = (e_1 + e_2H + e_3H^2 + e_4H^3)$$

$$+ (f_1 + f_2H + f_3H^2 + f_4H^3)(p - 6.8945753E5).$$

$$(2.76E5 < H \leq 3.94E5) \tag{A.41}$$

$$\mu(p,H) = (d_1 + d_2y + d_3y^2 + d_4y^3 + d_5y^5). \ (H > 3.94E5) \tag{A.42}$$

Here,

$$a_1 = 1.29947E\text{-}3, \qquad a_2 = -9.2640321E\text{-}4,$$
$$a_3 = 3.8104706E\text{-}4, \qquad a_4 = -8.2194445E\text{-}5,$$
$$a_5 = 7.022438E\text{-}6, \qquad b_1 = -6.5959E\text{-}12,$$
$$b_2 = 6.763E\text{-}12, \qquad b_3 = 2.88825E\text{-}12,$$
$$b_4 = 4.4525E\text{-}13, \qquad d_1 = 3.0260323E\text{-}4, \tag{A.43}$$
$$d_2 = -1.8366069E\text{-}4, \qquad d_3 = 7.5670758E\text{-}5,$$

(Contd.)

$d_4 = -1.6478789E-5, \quad d_5 = 1.4164576E-6,$ (Contd.)

$e_1 = 1.4526053E-3, \quad e_2 = -6.9880085E-9,$ (A.43)

$e_3 = 1.5210230E-14, \quad e_4 = -1.2303195E-20,$

$f_1 = -3.8063508E-11, \quad f_2 = 3.9285208E-16,$

$f_3 = -1.2585799E-21, \quad f_4 = 1.2860181E-27$

$$x = \frac{H - 42658.84}{116532.6}, \tag{A.44}$$

$$\eta = \frac{H - 55358.8}{154213.8}, \tag{A.45}$$

and

$$y = \frac{H - 401467.6}{256953.22}. \tag{A.46}$$

<u>Specific Heat</u> (J/kg•K)

$$c_p(p,H) = \left\{x_1 - \frac{x_2}{(H - 1.7556418E6)^2}\right\}^{-1}. \quad (H \leq 8.12E5) \tag{A.47}$$

$$c_p(p,H) = \left\{x_1 - \frac{x_2}{(H - 1.7556418E6)^2}\right\}^{-1} f(y)$$

$$+ \left\{Z_1 + Z_2H + Z_3H^2\right\}^{-1} \{1 - f(y)\}.$$

$$(8.12E5 < H \leq 8.16E5) \tag{A.48}$$

$$c_p(p,H) = \left\{Z_1 + Z_2H + Z_3H^2\right\}^{-1}. \quad (H > 8.16E5) \tag{A.49}$$

Here,

$x_1 = 2.4688303E-4 + 1.24419E-13\ p,$

$x_2 = 1.8790464E7 - 5.634438E-2\ p,$

$Z_1 = 1.1964506E-5 + 6.291758E-12\ p,$

$Z_2 = 4.58929E-10 - 1.1980206E-17\ p,$

$Z_3 = -2.5763436E-16 + 6.046356E-24\ p,$ (A.50)

$$f(y) = \frac{1}{16}\{8 - 15y + 10y^3 - 3y^5\}, \tag{A.51}$$

and

$$y = \frac{H - 8.14E5}{2000}. \tag{A.52}$$

Conductivity (W/m•K)

$$k(H) = a_1 + a_2\, x + a_3x^2 + a_4x^3. \tag{A.53}$$

Here,

$$a_1 = 0.57373862, \quad a_2 = 0.25361036,$$
$$a_3 = -0.14546827, \quad a_4 = 0.013874725,$$

and

$$x = H/5.815E5. \tag{A.54}$$

Enthalpy: (J/kg)

The enthalpy H(p,T) is calculated iteratively. We start with an assumed value of enthalpy. Liquid temperature is calculated. If the calculated liquid temperature is not in agreement with the prescribed temperature then enthalpy is modified. The modification is continued until the agreement in temperatures is achieved.

Temperature (°C)

$$T(p,H) = x_1 + x_2H + \frac{x_3}{H - 1.7556418E6} - 273.15. \quad (H > 8.12E5) \tag{A.55}$$

$$T(p,H) = \left\{x_1 + x_2H + \frac{x_3}{H - 1.7556418E6}\right\}f(y)$$
$$+ \left\{Z_1 + Z_2H + Z_3H^2 + Z_4H^3\right\}[1-f(y)] - 273.15.$$
$$(8.12E5 < H \leq 8.16E5) \tag{A.56}$$

$$T(p,H) = \left\{Z_1 + Z_2H + Z_3H^2 + Z_4H^3\right\} - 273.15. \quad (H > 8.16E5) \tag{A.57}$$

Here,

$$x_1 = 2.8378E2 - 2.752333E-7\ p,$$

$$x_2 = 2.4688303E-4 + 1.24419E-13\ p,$$

$$x_3 = 1.8790464E7 - 5.634438E-2\ p,$$

$$Z_1 = 3.49661E2 - 2.364921E-6\ p,$$

$$Z_2 = 1.1964506E-5 + 6.291758E-12\ p,$$

$$Z_3 = 2.294645E-10 - 5.990103E-18\ p,$$

$$Z_4 = -8.587812E-17 + 2.015452E-24\ p, \tag{A.58}$$

and y and f(y) are given by Eqs. A.51 and A.52 respectively.

<u>Saturation Temperature</u> (°C)

$$T_{sat}(p) = \frac{1}{1.8}\left\{C_1 + C_2 p_R + C_3 p_R^2 - \frac{226805}{p_R + 768.85}\right\}.$$

$$(p_R > 1090.8) \tag{A.59}$$

$$T_{sat}(p) = \frac{1}{1.8}\left\{\frac{a_1}{a_2 - x} + a_3 + a_4 x\right\}.$$

$$(p_R < 43.4302) \tag{A.60}$$

$$T_{sat}(p) = \frac{1}{1.8}\left\{\frac{a_1}{a_2 - x} + a_3 - a_4 x\right\} f(y)$$

$$+ \frac{1}{1.8}\left\{b_1 + b_2 x + b_3 x^2 + b_4 x^3 + b_5 x^4\right\}(1 - f(y)).$$

$$(43.4302 < p_R < 45.4298) \tag{A.61}$$

$$T_{sat}(p) = \frac{1}{1.8}\left\{b_1 + b_2 x + b_3 x^2 + b_4 x^3 + b_5 x^4\right\}.$$

$$(p_R < 1069.2) \tag{A.62}$$

$$T_{sat}(p) = \frac{1}{1.8}\left\{b_1 + b_2x + b_3x^2 + b_4x^3 + b_5x^4\right\}f(y_1)$$

$$+ \frac{1}{1.8}\left\{c_1 + c_2p_R + c_3p_R^2 - \frac{226805}{p_R + 768.85}\right\}(1 - f(y_1)),$$

$$(1069.2 < p_R < 1090.8) \tag{A.63}$$

Here,

$c_1 = 588.994,$ $c_2 = 0.055386,$

$c_3 = -3.516E-16,$ $a_1 = 2634.7,$

$a_2 = 6.026,$ $a_3 = -367.486,$

$a_4 = 4.484,$ $b_1 = 73.802,$

$b_2 = 65.14,$ $b_3 = 24.859,$

$b_4 = -4.3391,$ $b_5 = 1.6889,$ (A.64)

$$p_R = 1.4503774E-4\ p, \tag{A.65}$$

$$y = \frac{p_R - 44.98}{0.4498}, \tag{A.66}$$

$$y_1 = \frac{p_R - 1080}{10.80}, \tag{A.67}$$

and

f(y) is given by Eq. A.51.

A.4. Steam-Vapor Properties

Specific Heat (J/kg•K)

$$c_p(p,H) = \frac{1}{\left(b_0 + b_1p + b_2p^2\right) + \left(c_0 + c_1p + c_2p^2\right)H}. \tag{A.68}$$

Here,

$b_0 = -5.2568962E-4,$ $b_1 = -3.4405779E-11,$

$b_2 = 7.0081327E-19,$ $c_0 = 3.2441688E-10,$

$c_2 = 3.734813E-18,$ $c_2 = -2.9133521E-26.$ (A.69)

and the enthalpy H is in J/kg and pressure p is in pascals.

Conductivity (W/m•k)

$$k(T,\rho) = x_1 + \rho\left\{x_2 + \frac{2.1482E5}{T^{4.2}}\rho\right\}. \tag{A.70}$$

Here,

$$x_1 = a_1 + a_2T + a_3T^2 + a_4T^3, \tag{A.71}$$

$$x_2 = b_1 + b_2T + b_3T^2, \tag{A.72}$$

$$a_1 = 1.76E-2, \qquad a_2 = 5.87E-5,$$
$$a_3 = 1.04E-7, \qquad a_4 = -4.51E-11,$$
$$b_1 = 1.0351E-4, \qquad b_2 = 4.198E-7,$$
$$b_3 = -2.771E-11, \tag{A.73}$$

ρ is the density in kg/m^3 and T is the temperature in degree Celsius.

Viscosity (Pa•sec)

$$\mu(\rho,T) = v_1 - \rho\{1.858E-7 - 5.9E-10\ T\}. \quad (T < 300) \tag{A.74}$$

$$\mu(\rho,T) = v_1 + \rho\left\{\left(f_1 + f_2T + f_3T^2 + f_4T^3\right) + \left(g_1 + g_2T + g_3T^2 + g_4T^3\right) + \left(a_1 + a_2T + a_3T^2\right)\right\}.$$

$$(300 < T < 375) \tag{A.75}$$

$$\mu(\rho,T) = v_1 + \rho\left\{a_1 + a_2\rho + a_3\rho^2\right\}.$$

$$(T > 375) \tag{A.76}$$

Here,

$$a_1 = 3.53E-8, \qquad a_2 = 6.765E-11,$$
$$a_3 = 1.021E-14, \qquad f_1 = -2.885E-6,$$
$$f_2 = 2.427E-8, \qquad f_3 = -6.789333E-11,$$
$$f_4 = 6.317037E-14, \qquad g_1 = 1.76E2,$$
$$g_2 = -1.60, \qquad g_3 = 4.80E-3,$$
$$g_4 = -4.7407407E-6, \tag{A.77}$$

and

$$v_1 = 8.04E\text{-}6 + 4.07E\text{-}8\ T. \tag{A.78}$$

Density (kg/m^3)

$$\rho(p,H) = \left\{\left(a_1 + a_2 p + \frac{a_3}{p}\right) + \left(b_1 + b_2 p + \frac{b_3}{p}\right) H\right\}^{-1}. \tag{A.79}$$

Here,

$$a_1 = -5.1026024E\text{-}5, \quad a_2 = 1.1208014E\text{-}10,$$
$$a_3 = -4.4505598E5, \quad b_1 = -1.6893038E\text{-}10,$$
$$b_2 = -3.3980179E\text{-}17, \quad b_3 = 2.3057608E\text{-}1. \tag{A.80}$$

Enthalpy (J/kg)

The enthalpy of vapor H(p,T) is calculated iteratively. The enthalpy is first assumed and temperature is calculated. If the calculated temperature is not in agreement with the prescribed temperature, then, enthalpy is modified. The procedure is repeated until the calculated and specified temperatures are in close agreement.

Temperature (°C)

$$T(p,H) = \{-972 + 5.0E\text{-}4\ H\} - 273.15. \quad (p < 1.0E4) \tag{A.81}$$

$$T(p,H) = \{(-930 + 4.88E\text{-}4\ H)\ x_1 + (-972 + 5.0E\text{-}4\ H)(1 - x_1)\}$$
$$- 273.15. \quad (1.0E4 \leq p < 1.0E5) \tag{A.82}$$

$$T(p,H) = \left\{(-930 + 4.88E\text{-}4\ H)x_2 + \left(d_1 + d_2 H + d_3 H^2\right)(1 - x_2)\right\}$$
$$- 273.15. \quad (1.0E5 \leq p < 1.0E6) \tag{A.83}$$

$$T(p,H) = \left\{d_1 + d_2 H + d_3 H^2\right\} - 273.15. \quad (1.0E6 \leq p) \tag{A.84}$$

Here,

$$d_1 = a_1 + a_2 p + a_3 p^2,$$
$$d_2 = b_1 + b_2 p + b_3 p^2,$$
$$d_3 = c_1 + c_2 p + c_3 p^2, \tag{A.85}$$

$$x_1 = \frac{1}{0.9}[-0.1 + 1.0E\text{-}5\ p], \tag{A.86}$$

$$x_2 = \frac{1}{9.0}[-1.0 + 1.0E\text{-}5\ p], \tag{A.87}$$

and

$$\begin{aligned} a_1 &= 6.5658906E2, & a_2 &= 9.9065859E\text{-}5, \\ a_3 &= -2.1878607E\text{-}12, & b_1 &= -5.2568969E\text{-}4, \\ b_2 &= -3.4405784E\text{-}11, & b_3 &= 7.0081336E\text{-}19, \\ c_1 &= 1.6220848E\text{-}10, & c_2 &= 1.86704069E\text{-}18, \\ c_3 &= -1.4566764E\text{-}26. \end{aligned} \tag{A.88}$$

APPENDIX B

Thermal Structure Module

B.1. Introduction

The thermal structure module is designed to determine the heat transfer interaction between an immersed structure and surrounding fluid. The following five subroutines form the thermal structure module.

INPSTR: Input and computation of geometric variables.

HSTRUC: Determination of surface heat transfer coefficient

TSTRUC: Calculation of temperature distribution in structures

QSTRUC: Computation of heat transfer rate to surrounding fluid

PSTRUC: Printing of variables.

It is assumed that the axial and angular conduction are negligible compared to radial conduction. Only a one-dimensional (radial) heat-conduction equation is, therefore, used to determine the temperature distribution in a structure and heat transfer rate to the surrounding fluid. The numerical model has the following features.

1. The model considers all internal axial structures. The input NSTRUC determines the total number of structures.

2. Each structure is divided into a desired number of axial elements NTSEL(N).

3. A set of discretization equations is obtained for each element using the proper boundary conditions. The derivation of these equations is presented in Section B.3. The equations are solved using the Tri-Diagonal Algorithm.

4. Radial variation and temperature dependence of thermal conductivity and specific heat are incorporated.

5. The effect of gap between two material regions is also accounted for in the model. The gap width and heat transfer coefficient across a gap are input parameters.

6. The heat source is included in the transient heat conduction equation for the structure element.

B.2. Governing Equation

The transient, one-dimensional heat conduction equation is

$$\rho c_p \frac{\partial T}{\partial r} = \frac{1}{A} \frac{\partial}{\partial r}\left(kA \frac{\partial T}{\partial r}\right) + \dot{q}''' \tag{B.1}$$

Here, ρ, c_p and k are the density, specific heat and conductivity of the material, $\dot{q}'''$ is the heat source per unit volume and A is the cross sectional area.

B.3. Finite Difference Formulation

Figure B.1 shows the cross section of a typical structure element under consideration. Each element is divided into a number of material regions (NTSMAT(N)), and each material region is divided into a number of partitions (NMPAR(MR)). DRPAR(MR) = δR is the partition size of the material region. Let ℓ = NTSPAR(N) be the total number of thermal structure partition cells. For simplicity in calculations, the element height of δz is taken as unity.

Cell Surrounded by the Cells of Same Material

Let us consider the energy balance of a partition cell i, as shown in Fig. B.2. The integration of Eq. B.1 over the control volume of cell i gives,

$$\left(\frac{\rho c_p V}{\delta t}\right)\left\{T_i^{t+\delta t} - T_i^t\right\} = (kA)_{i-1/2} \frac{(T_{i-1} - T_i)}{\delta R} - (kA)_{i+1/2}\left\{\frac{T_i - T_{i+1}}{\delta R}\right\} + \dot{q}'''V. \tag{B.2}$$

Here A is the cross sectional area per unit height, V is the cell volume. Rearranging Eq. B.2, we get

$$(a_i + b_i + b_{i+1})T_i = b_i T_{i-1} + b_{i+1} T_{i+1} + d_i, \tag{B.3}$$

where,

$$a_i = (\rho c_p V/\delta t)_i, \tag{B.4}$$

$$b_i = (kA)_{i-1/2}/\delta R, \tag{B.5}$$

$$b_{i+1} = (kA)_{i+1/2}/\delta R, \tag{B.6}$$

$$d_i = (\dot{q}'''V + \rho c_p V T^0/\delta t), \tag{B.7}$$

and T^0 and T are the temperatures at time t and (t + δt) respectively.

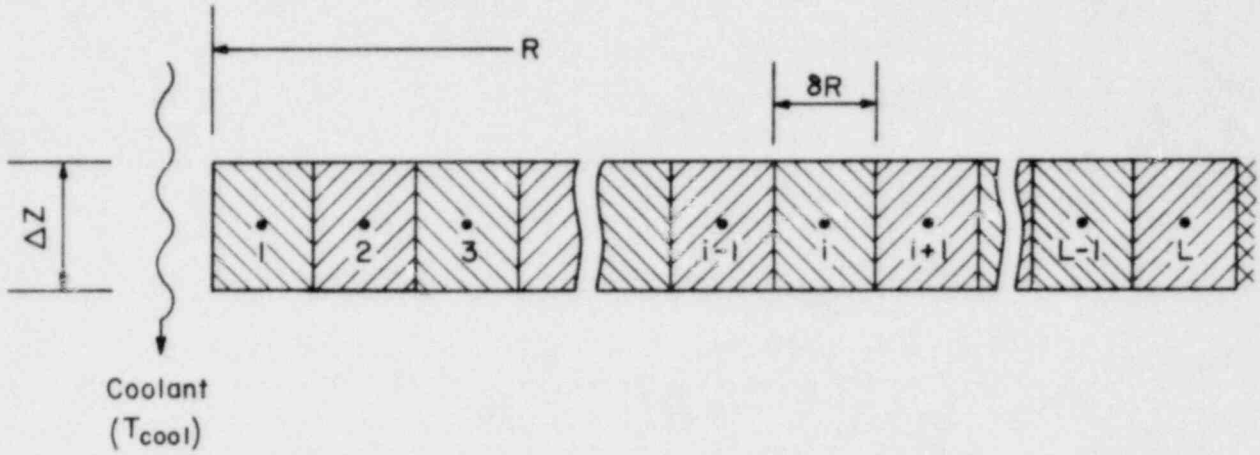

Fig. B.1. Cross section of a thermal structure element

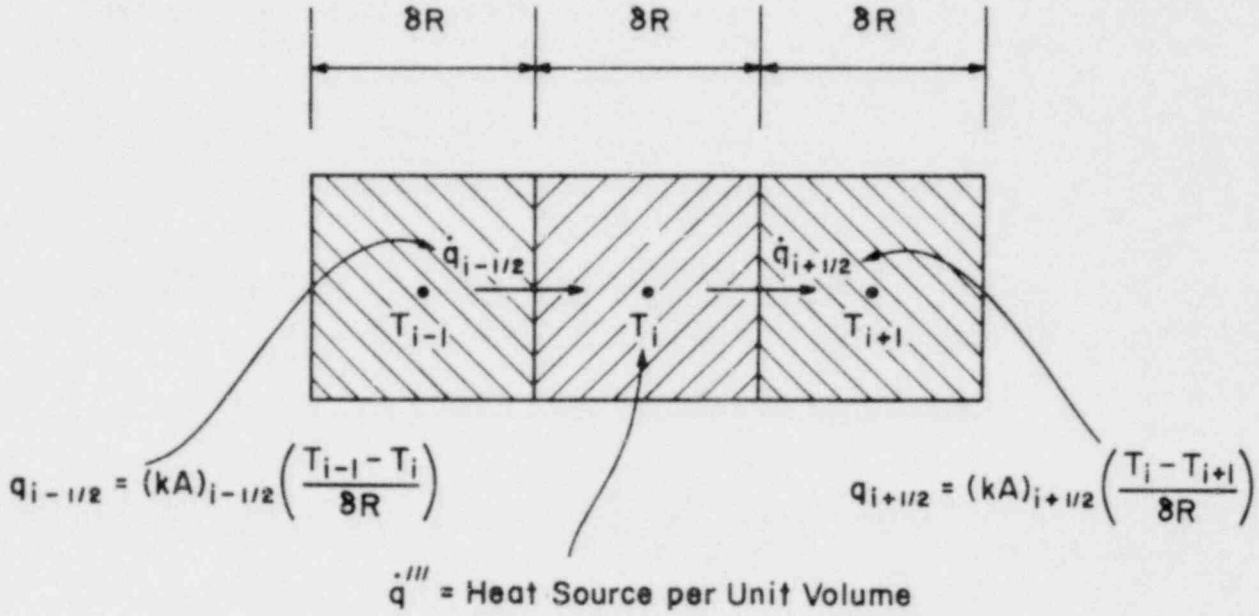

Fig. B.2. Energy balance of partition cell i

Cell 1 Adjacent to Coolant

For the case of cell 1, adjacent to the fluid (coolant) (as shown in Fig. B.3), after integrating the energy equation and simplifying we get

$$(a_1 + b_1 + b_2)T_1 = b_1 T_{cool} + b_2 T_2 + d_1. \tag{B.8}$$

Here a, b, and d have the same meaning, except that b_1 now includes the convective contribution. Therefore,

$$b_1 = \frac{A_1}{\left\{\frac{1}{h_{cool}} + \frac{\delta R}{2k_1}\right\}}. \tag{B.9}$$

Similarly, if the other end of the thermal structure, say cell ℓ, is in contact with fluid, we obtain

$$(a_\ell + b_\ell + b_{\ell-1})T_\ell = b_{\ell-1}T_{\ell-1} + d_\ell, \tag{B.8a}$$

where

$$d_\ell = \{\dot{q}'''v + \rho c_p V T^0/\delta t + b_\ell T_{cool}\}$$

and

$$b_\ell = \frac{A_\ell}{\frac{1}{h_{cool}} + \frac{\delta R}{2k_\ell}}.$$

Cell Surrounded by a Cell of Different Material

For the case of a cell surrounded by a different material cell, as shown in Fig. B.4, we get

$$(a_j + b_j + b_{j+1})T_j = b_j T_{j-1} + b_{j+1}T_{j+1} + d_j \tag{B.10}$$

Equation B.10 is similar to Eq. B.3, except that the term b_{j+1} includes the gap resistance. Thus,

$$b_{j+1} = \frac{A}{\left\{\left(\frac{\delta R}{2k}\right)_j + \frac{1}{h_{gap}} + \left(\frac{\delta R}{2k}\right)_{j+1}\right\}} \tag{B.11}$$

The End Cell with Adiabatic Boundary Condition

For the end cell, Fig. B.5, the second boundary condition option we have is the adiabatic boundary condition. As we have no heat transfer, the resistance is infinite, and the term b_{i+1} goes to zero. The final equation, therefore is

$$(a_\ell + b_\ell)T_\ell = b_\ell T_{\ell-1} + d_\ell \tag{B.12}$$

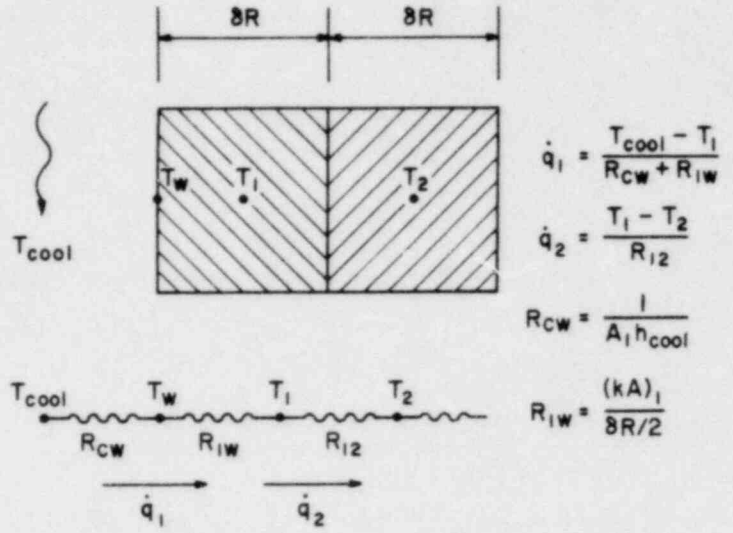

Fig. B.3. Energy balance of cell 1 adjacent to coolant

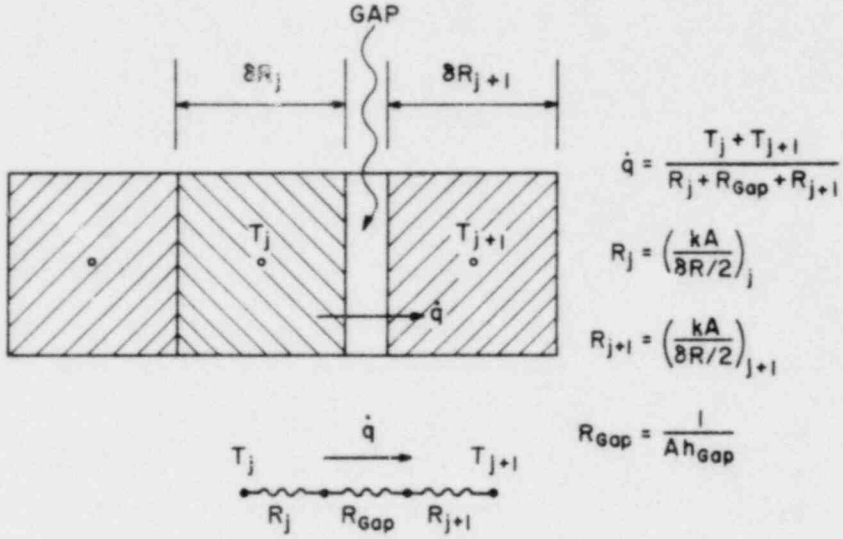

Fig. B.4. Cell surrounded by different materials with air gap between them

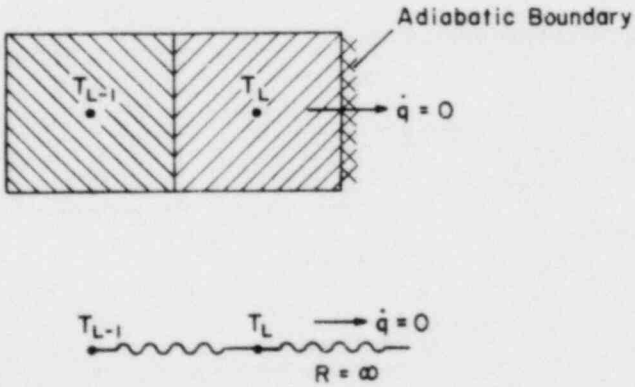

Fig. B.5

Cell with adiabatic boundary

B.4 Solution of the Discretization Equations

We see, from the above derivation that we have ℓ number of equations for ℓ (number of partitions) number of unknown temperatures. The general form of all equations is

$$(a_i + b_i + b_{i+1})T_i = b_i T_{i-1} + b_{i+1} T_{i+1} + d_i. \tag{B.13}$$

We can transform this equation to

$$C_i T_i = b_{i+1} T_{i+1} + A_i, \tag{B.14}$$

where,

$$A_i = d_i + b_i A_{i-1}/C_{i-1}, \tag{B.15}$$

and

$$C_i = a_i + b_i + b_{i+1} - b_i^2/C_{i-1}. \tag{B.16}$$

The first set of coefficients are

$$A_1 = d_1 + b_1 T_{cool}, \tag{B.17}$$

and

$$C_1 = a_1 + b_1 + b_2. \tag{B.18}$$

As,

$$b_{\ell+1} = 0,$$

we first get

$$T_\ell = A_\ell / C_\ell, \tag{B.19}$$

The rest of the temperatures are then computed using Eq. B.14.

B.5. Heat Transfer to Coolant

Once the temperature distribution in a structure element is computed, the heat transfer rate to surrounding fluid is computed from

$$\dot{q}'_{cool} = b_1 (T_1 - T_{cool}). \tag{B.20}$$

Here $\dot{q}'$ is the heat transfer rate in W/meter, because the cross sectional area in term b_1 is per unit height of the element. The volumetric heat source is then computed using

$$\dot{q}'''_{cool} = \dot{q}'_{cool}/(\delta x \delta y). \tag{B.21}$$

The computation of heat transfer rate is carried out in the subroutine QSTRUC.

APPENDIX C

Wire Wrap and Resistance Models

C.1. Introduction

The presence of helical wire wrapping around a fuel pin has two effects on fluid flow. One is the geometrical effect; here the presence of wire wrap influences the fluid flow by reducing the available flow space. This effect is accounted for by modifying the volume porosities and surface permeabilities. The second is the physical effect; here the presence of wire produces additional drag on the fluid flow. This effect is accounted for by including additional resistance terms in the momentum equation.

There are four subroutines related to wire wrap models. These are

1. INTWIR: This subroutine modifies volume porosities and surface permeabilities; locates positions of wire wraps through subroutine WIRE; and computes, through subroutine GETWIR, the wire drag coefficients for x, y, and z directions.

2. WIRVOL: This subroutine computes volume occupied by wire wrap in a computational cell.

3. WIRE: This subroutine determines wire wrap locations, axial areas and blocked lengths along cell edges.

4. GETWIR: This subroutine computes wire wrap drag coefficients for wire wrap model No. 4. Four wire wrap models were developed. The model No. 4 was found to be the most satisfactory, predicting results in agreement with the experimental measurements.

The flag IWIRE is used for the wire wrap model.

IWIRE = 0: No wire wrap option.
= 1: Smeared wire option; geometrical effects are accounted approximately; physical effects are neglected.

= 4: Geometrical effects are calculated locally and in detail; physical effects are accounted for by incorporating wire wrap force Model No. 4.

C.2. Smeared Wire Option

In this model, the volume porosities and surface permeabilities are modified uniformly across the section. This is done by distributing total wire volume equally over all cells and total wire wrap cross-sectional area equally over all cells in each axial plane. Physical effects are neglected.

C.3. Wire Wrap Model

C.3.1. Geometrical Effects.

The geometrical effects due to the presence of wire wrap are accounted for by modifying volume porosities and surface permeabilities. This is done using the following relations.

$$\gamma_v^w = \gamma_v - \frac{1}{(\Delta x \Delta y \Delta z)} \int_{z_1}^{z_2} A_z^w \delta z, \tag{C.1}$$

$$\gamma_{x,i+(1/2)}^w = \gamma_{x,i+(1/2)} - \frac{1}{(\Delta y \Delta z)} \int_{z_1}^{z_2} \delta A_{x,i+(1/2)}^w \tag{C.2}$$

$$\gamma_{y,j+(1/2)}^w = \gamma_{y,j+(1/2)} - \frac{1}{(\Delta x \Delta z)} \int_{z_1}^{z_2} \delta A_{y,j+(1/2)}^w \tag{C.3}$$

$$\gamma_{z,k+(1/2)}^w \doteq \gamma_{z,k+(1/2)} - \frac{A_{z,k+(1/2)}^w}{(\Delta x \Delta y)} \tag{C.4}$$

Here, superscript w refers to wire wrap and A is the cross-sectional area of wire wrap. The right-hand sides of equations (C.1-C.3) are integrated numerically. At each axial position, A^w is computed by determining its proper location in a cell. The step size for numerical integration is taken to be equal to three degrees of angular rotation, i.e.

$$\delta z = \frac{\text{Wire Pitch}}{120} \tag{C.5}$$

C.3.2. Wire Drag Model

The resistance force due to wire wrap is modeled as

$$\vec{F}_w = \frac{c\rho |w| \vec{wA}}{(\Delta x \Delta y \Delta z)} \tag{C.6}$$

Here,

$$\vec{F}_w = f_x \vec{i} + f_y \vec{j} + f_z \vec{k} \tag{C.7}$$

is the resistance force per unit volume,

$$\vec{c} = c_x\vec{i} + c_y\vec{j} + c_z\vec{k} \tag{C.8}$$

is the drag coefficient, and

$$\vec{A} = A_x\vec{i} + A_y\vec{j} + A_z\vec{k} \tag{C.9}$$

is the projected area of wire wrap. The calculation of $\vec{A}$ is briefly described here.

Figure C.1 shows a typical wire wrap arrangement. Let us consider the wire wrap as a spiral ring of width d_w attached to the fuel pin and located at position 0 (x,y,z) as shown in Fig. C.2. The projected area is

$$d\vec{A} = d\vec{S} \times d_w\vec{n}$$

$$= (dx\vec{i} + dy\vec{j} + dz\vec{k}) \times d_w(\vec{i}\cos\alpha + \vec{j}\sin\alpha), \tag{C.10}$$

where,

$$\vec{n} = \vec{i}\cos\alpha + \vec{j}\sin\alpha \tag{C.11}$$

is the unit normal vector,

$$\vec{S} = (x\vec{i} + y\vec{j} + z\vec{k})$$

$$= \vec{i}r_p\cos\alpha + \vec{j}r_p\sin\alpha + \vec{k}\left(z_0 + \frac{\alpha}{2\pi}W_p\right). \tag{C.12}$$

is the wire wrap position vector, r_p is the radius of fuel pin and W_p is the wire pitch. Differentiating and substituting Eq. C.12 into Eq. C.10, we get, after simplification,

$$d\vec{A} = \frac{W_p d_w}{2\pi}\left(\vec{i}(-\sin\alpha) + \vec{j}\cos\alpha - \vec{k}\tan\theta\right)d\alpha. \tag{C.13}$$

Here,

$$\theta = \tan^{-1}\left(\frac{2\pi r_p}{W_p}\right) \tag{C.14}$$

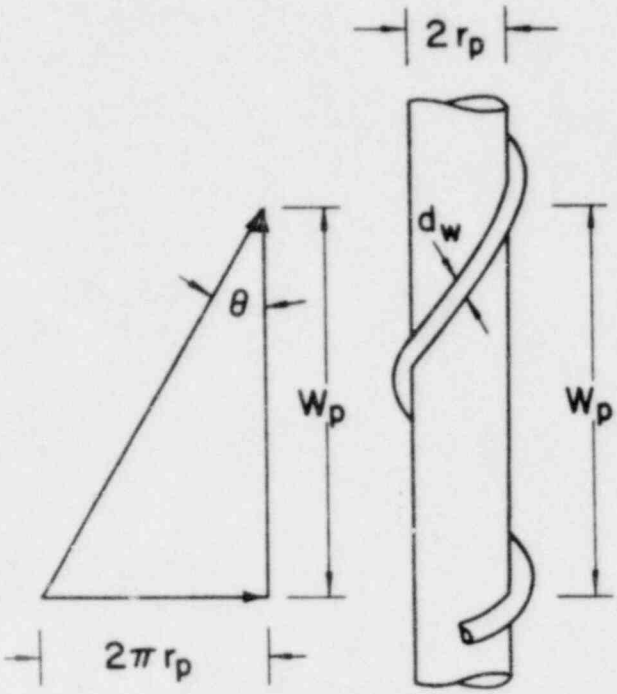

Fig. C.1

Typical Wire Wrap Arrangement

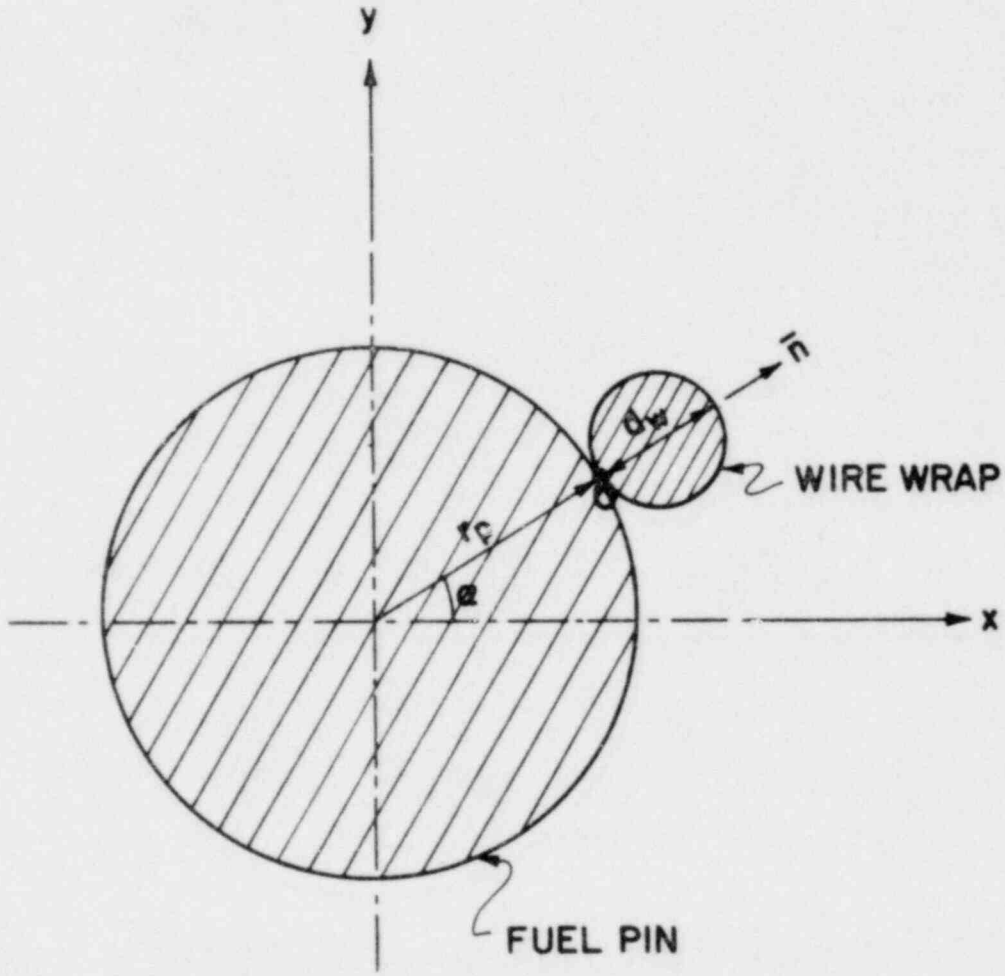

Fig. C.2. Cross Section of Helical Wire Wrap Around a Fuel Pin

is the angle between wire wrap centerline and fuel pin centerline. Integrating Eq. C.13 between two z-planes (k - (1/2) and k + (1/2)) for a given cell, we obtain

$$\vec{A} = \frac{W_p d_w}{2\pi} \{\vec{i}(\cos \alpha_2 - \cos \alpha_1) + \vec{j}(\sin \alpha_2 - \sin \alpha_1) - \vec{k}(\alpha_2 - \alpha_1)\tan \theta\}. \tag{C.15}$$

Here,

$$\alpha = \frac{2\pi(z - z_0}{W_p}, \tag{C.16}$$

$$\alpha_2 - \alpha_1 = \frac{2\pi}{W_p}(z_{k+(1/2)} - z_{k-(1/2)}), \tag{C.17}$$

and z_0 is the axial location, when wire wrap position is on x axis passing through the centerline of a fuel pin. The projected wire wrap areas A_x, A_y and A_z are named in COMMIX-2 as UWIRE, VWIRE and WWIRE respectively, and are computed in subroutine GETWIR.

C.4. Resistance Model

We model the distributed resistance forces defined in Eq. 3.9 in the following way.

$$R_x = \frac{1}{\gamma_v} \frac{1}{2} f_x \rho u^2. \tag{C.18}$$

Here, R_x is the resistance force per unit volume, f_x is the friction factor per unit length, and subscript x refers to x-direction.

When a rod bundle is aligned along the z axis, the crossflow friction factor, f_x, is given by[2]

$$f_x = 2 \frac{u}{|u|} \bar{f}_x \frac{\gamma_v^2 W_p}{\left[1 - \left(\frac{d}{P_y}\right)^2\right]}, \tag{C.19}$$

where,

W_p = wetted perimeter per unit cross-sectional area,

d = rod diameter,

P_y = pitch in y direction,

and

$\bar{f}_x$ = the largest of the following three expressions:

$$\bar{f}_x = 3Re_x^{-1}\left[\frac{P_y - d}{P_y - 0.93d}\right]^2, \tag{C.20}$$

$$\bar{f}_x = 0.6\frac{P_y}{d}\left(0.25 + \frac{0.118}{(P_y/d - 1)^{1.08}}\right)Re_x^{*-0.15}, \tag{C.21}$$

and

$$\bar{f}_x = 3\left(\frac{P_y - d}{P_y - 0.93d}\right)^2\left[\frac{\mu}{\mu_{eff}}Re_x\left(1 + \frac{2.16d}{P_y - d}\right)\right]^{-1}. \tag{C.22}$$

In these expressions,

$$Re_x = \frac{\rho|u|P_y\gamma_V}{\mu} \tag{C.23}$$

and

$$Re_x^* = \frac{\rho|u|d\gamma_V}{\mu(1 - d/P_y)}. \tag{C.24}$$

Analogous expressions are used for f_y, replacing u by v and P_y by P_x in the above definitions.

The axial friction factor, f_z, is given by

$$f_z = 2\frac{w}{|w|}W_p(aRe_z^b + c), \tag{C.25}$$

where

$$Re_z = \frac{\rho|w|D_h}{\mu}, \tag{C.26}$$

D_h = equivalent hydraulic diameter,

and the constants a, b, and c are:

a	b	c	Re_z
8	-1	0	<940
0.07	-0.32	0.0007	>940

APPENDIX D

Input Description

```
* * * * * * * * * * * * * * * * * * * * * * * * * * * * * * * * * * * * * * *
* * * * * * * * * * * * * * * * * * * * * * * * * * * * * * * * * * * * * * *
* * * * * * * * * * * * * * * * * * * * * * * * * * * * * * * * * * * * * * *
* * * * * * * * * * * * * * * * * * * * * * * * * * * * * * * * * * * * * * *
* * * * *                                                   * * * * *
* * * *                                                       * * * *
* * *                 C O M M I X - 2                           * * *
* *                                                               * *
* *                                                               * *
* *        A Three-Dimensional, Transient, Two Phase              * *
* *        Computer Program for Thermal Hydraulic Analysis        * *
* *                                                               * *
* *                                                               * *
* *                                                               * *
* *                     developed by                              * *
* *                                                               * *
* *              Analytical Modelling Section                     * *
* *             Components Technology Division                    * *
* *              Argonne National Laboratory                      * *
* *                                                               * *
* *                                                               * *
* *                   under sponsorship of                        * *
* *                                                               * *
* *        United States Nuclear Regulatory Commission            * *
* *                                                               * *
* *                                                               * *
* *                                                               * *
* *                 contact          phone                        * *
* *                                                               * *
* *             H. M. Domanus       312-972-5931                  * *
* *             R. C. Schmitt       312-972-5914                  * *
* *             W. T. Sha           312-972-5910                  * *
* *             V. L. Shah          312-972-8049                  * *
* *                                                               * *
* *                                 at                            * *
* *                                                               * *
* *               Building 308                                    * *
* *               Argonne National Laboratory                     * *
* *               9700 South Cass Avenue                          * *
* *               Argonne, Illinois  60439                        * *
* *                                                               * *
* *                                                               * *
* *            Version 7.0        January 30, 1981                * *
* *                                                               * *
* *                                                               * *
* * *                                                           * * *
* * * *                                                       * * * *
* * * * * * * * * * * * * * * * * * * * * * * * * * * * * * * * * * * * * * *
* * * * * * * * * * * * * * * * * * * * * * * * * * * * * * * * * * * * * * *
* * * * * * * * * * * * * * * * * * * * * * * * * * * * * * * * * * * * * * *
* * * * * * * * * * * * * * * * * * * * * * * * * * * * * * * * * * * * * * *
```

Input for COMMIX-2 can be described in one of two ways:

1. Box geometry: IGEOM=0 or IGEOM=-1
2. Hex geometry: IGEOM>0

The Box geometry option allows the user to describe the geometry in terms of the cells formed by the X, Y, and Z grid planes. In this case the input structure is as follows:

```
Two problem description cards.
NAMELIST /GEOM/
Surface identification cards.
NAMELIST /DATA/
NAMELIST /FLAG/
NAMELIST /INPUTQ/                    (Optional)
NAMELIST /STRUCT/                    (Optional)
Structure specification cards.       (Optional)
Boundary initialization cards.       (Optional)
Internal cell initialization cards.  (Optional)
```

The hex geometry option is used when analyzing hexagonal fuel assemblies only. Several conventions must be noted:

1. Axial length is along the Z-direction and one hex flat lies on the X-axis.
2. IMAX, JMAX, DX(I), and DY(J) are automatically determined by quarter pin and full pin partitioning.
3. Surfaces have the following locations:

Surface number	Surface location
1	Lower left diagonal in X-Y plane.
2	Upper left diagonal in X-Y plane.
3	Lower right diagonal in X-Y plane.
4	Upper right diagonal in X-Y plane.
5	Lower flat along X-axis.
6	Upper flat.
7	Entrance plane (Z=0.0).
8	Exit plane.

The input structure for this option is as follows:

```
Two problem description cards.
NAMELIST /GEOM/
NAMELIST /DATA/
NAMELIST /INPUTQ/
NAMELIST /STRUCT/
Structure specification cards  (Optional)
Boundary initialization cards  (Optional)
Internal cell initialization cards (Optional)
```

Default values are indicated either by an asterisk or a value in parentheses after the variable description. Arrays are indicated by the use of a subscript following the variable name. The range of the subscripts are indicated

in the table below.

Index	Range	
I	IMAX	
J	JMAX	
K	KMAX	
N	NSURF	
NM	NMATER	
NH	NHEATC	
NS	NSTRUC	
IND	IMAX*JMAX	IND=I+(J-1)*IMAX

```
* * * * * * * * * * * * * * *
*    NAMELIST /GEOM/        *
* * * * * * * * * * * * * * *
```

The restart option used two Argonne system routines called TLEFT and LOCF. TLEFT returns the amount of time left in the current run in units of 0.01 seconds. LOCF returns the absolute address of the variable passed as the argument. Minor modifications are probably necessary to implement this on other systems.

IFRES
- 0--New case with no restart written. (*)
- 1--New case with restart written to tape 10.
- 2--Restart of previous run read from tape 9 with no restart written.
- 3--Restart of previous run read from tape 9 with restart written to tape 10.

IGEOM
- 0--Regular box geometry option. (*)
- -1--Cylindrical geometry option using box geometry input.
- >0--Hex geometry option. Set IGEOM to the number of pins in the hexagonal fuel assembly. The following values are acceptable: 7,19,37,61,91,127,169,217,271.

LMPRNT
- 0--Cell and surface number arrays are not printed. (*)
- 1--Cell number array is printed.
- 2--Cell and surface number arrays are printed.

The following variables must be input when IGEOM = 0.

IMAX — The maximum number of cells in the X-direction.

JMAX — The maximum number of cells in the Y-direction.

KMAX — The maximum number of cells in the Z-direction.

NSURF — The number of unique surfaces on the figure. Unique surfaces are determined by a unique combination of the following three characteristics:
1. Velocity boundary condition
2. Temperature boundary condition
3. Unit normal vector to the surface

DX(I) — The calculational cell sizes along the X-axis, m.

DY(J) — The calculational cell sizes along the Y-axis, m or rad.

DZ(K) — The calculational cell sizes along the Z-axis, m.

The unit normal vectors referred to by the following three variables are those pointing into the configuration.

XNORML(N) The X-component of the unit normal vector to surface N.
YNORML(N) The Y-component of the unit normal vector to surface N.
ZNORML(N) The Z-component of the unit normal vector to surface N.

The following variables must be input when IGEOM > 0.

CLADOD Fuel pin diameter, m.
PITCH Distance between pin centers, m.
WALLCL Wall clearance or distance between pin wall and duct wall, m.
WODIN Wire wrap outside diameter (O.D.) for all wire wraps except those next to the duct wall, m.
WODOUT Wire wrap O.D. of wire wraps next to the duct wall, m.
KMAX The maximum number of cells in the Z-direction.
DZ(K) The calculational cell sizes along the Z-axis, m.
IWIRE 0--No wire wrap option used. (*)
1--Smeared wire wrap option used. This option is suggested for low Reynolds number cases. The total wire wrap area and total wetted perimeter over an axial cross section are distributed over the cross section such that there are two mean hydraulic diameters, one for cells not adjacent to a side wall and one for cells adjacent to side walls. The effect of wire wrap induced flow is ignored.
4--Wire wrap force model used.
5--Wire wrap force model used and force distributions printed.
CWIREI Scal[illegible]tor for wire wrap force model for cells not adj[illegible] to a side wall.
CWIREC Sca[illegible]actor for wire wrap force model for cells adjacent to a side wall.

In the following three variables the index IJ is computed from the following relationship: IJ=I+(I-1)*IMAX.

ALXN(IJ) Surface porosity adjustment subtracted for irregularities in hex in the X-direction.
ALYN(IJ) Surface porosity adjustment subtracted for irregularities in hex in the Y-direction.
ALZN(IJ) Surface porosity adjustment subtracted for irregularities in hex in the Z-direction.

For pictorial representation of the following variable see figures C.1 and C.2 in the COMMIX-2 report.

IPART 0--Quarter pin partitioning is used. (*)
1--Full pin partitioning is used. (Inoperative 1/81 RCS)
ZATO Axial (Z) height where wire wrap is positioned along the positive X-axis relative to the rod center, m.
WIREP Wire wrap pitch, m. Positive WIREP indicates counter-clockwise rotation when looking in the negative Z direction. Negative WIREP indicates clockwise

rotation.

```
* * * * * * * * * * * * * * * * * * *
*   SURFACE IDENTIFICATION CARDS    *
* * * * * * * * * * * * * * * * * * *
```

This set of input is required only if IGEOM=0 or -1. When present its purpose is as follows:

1. Identify each surface element.
2. Conditionally give the area of each surface element.
3. Identify the surface number corresponding to each surface element.

Each surface identification card contains the following variables using FORMAT (A4,F10.3,7I4).

NAME REG The surface element(s) identified lie on a regular surface.

IREG The surface element(s) identified lie on an irregular surface.

AREA .LT.0--Either DX*DY, DY*DZ, or DX*DY, whichever is appropriate is used for the area of the surface element(s) identified.

.GE.0--The value input is used for the area of the surface element(s) identified.

The following six variables define a rectangular solid composed of one or more cells. The rectangular solid required must be totally interior to and adjacent to or partially interior to and containing the surface element(s) under consideration.

IB,IE The beginning and ending I-index limits.

JB,JE The beginning and ending J-index limits.

KB,KE The beginning and ending K-index limits.

N The surface number.

All surfaces with the same combination of the following three items can be assigned the same surface number:

1. Velocity boundary condition.
2. Temperature boundary condition.
3. Unit normal vector to the surface.

Note. It is possible for two surface elements to lie in the same surface and have either the same or different surface numbers as well as for two surface elements to lie in different surfaces and have the same or different surface numbers. The order of the surface identification cards must be as follows:

1. All IREG cards must precede all REG cards.
2. The surface numbers, N, of all IREG cards and all REG cards must be in order or increasing value.

```
* * * * * * * * * * * * * * *
*    NAMELIST /DATA/        *
* * * * * * * * * * * * * * *
```

The following variables allow easy specification of uniform property values at boundaries. Non uniform distributions can also be specified with the boundary array initialization cards.

VELOCL(N) Initial liquid velocity normal to surface N in the direction indicated by XNORML(N), YNORML(N), ZNORML(N). (0.0 m/s)
VELOCG(N) Initial gas velocity normal to surface N in the direction indicated by XNORML(N), YNORML(N), ZNORML(N).
TEMP(N) Inital temperature at surface N, C. (0.0)
PRES(N) Inital pressure at surface N, Pa.

The following three variables are used to initialize a pressure gradient along an axis to speed convergence. Only one value is allowed to be nonzero.
DPDX Pressure drop along the X-axis, Pa/m. (0.0)
DPDY Pressure drop along the Y-axis, Pa/m. (0.0)
DPDZ Pressure drop along the Z-axis, Pa/m. (0.0)

Steady State is reached when the following conditions are met:

1. MAX(RESIDUE)/DCONV < 1.0
   where DCONV=EPS1*(UVWMAX+EPS2) and
   UVWMAX is computed in SUBROUTINE CUTOFF.
2. The change of the U-velocity component divided by the maximum velocity magnitude in the entire field is less than EPS3.
3. The change of the V-velocity component divided by the maximum velocity magnitude in the entire field is less than EPS3.
4. The change of the W-velocity component divided by the maximum velocity magnitude in the entire field is less than EPS3.
5. MAX(DH/H) < EPS3
   where H is the current enthalpy and
   DH is the change in enthalpy over two consecutive time steps.

EPS1 Convergence criteria parameter. (0.0001)
EPS2 Convergence criteria parameter. (0.000001)
EPS3 Convergence criteria parameter. (0.00001)

All transient driving functions are input into the following three variables. Each function is defined by a user specified set of points. Cubic spline fit coefficients are then generated in SUBROUTINE FITIT. Fifty equally spaced values are printed to allow the user to check the adequacy of the input distribution. Ten to fifteen values with points concentrated at rapidly changing Y-values should be adequate.

TVAL The independent variable (usually time) for the transient functions.
FVAL The dependent variable for the transient functions. The first value of the second function immediately follows

	the last value of the first function. The same pattern must be followed for all subsequent functions. The endpoints, or beyond, of the range of values used in the transient functions must be input as the fitting routine does not extrapolate. Discontinuities are indicated by specifyingthe same X-coordinate twice with the same or different Y-coordinate values.
NEND(NF)	The number of points in the NFth transient function.
NTIME	Time step number at beginning of current run.
TIME	Time at beginning of current run.
NTMAX	Maximum number of time steps allowed in this run. (99999)
TIMAX	Maximum time allowed in this run, s. (3.6E+6)
TRFST	Time allowed to write restart tape, s. This variable is used in conjunction with the ANL TLEFT routine.
DT(1)	Time step size until time DTSET is reached.
DT(2)	Time step size after time DTSET is reached.
DTSET	Time at which time step size changes from DT(1) to DT(2). (10000.0)
IT(1)	Number of iterations per time step until time step ITSET is reached.
IT(2)	Number of iterations per time step after time step ITSET is reached.
ITSET	Time step number at which number of iterations per time step changes from IT(1) to IT(2). (10000)
ITMAXE	Number of iterations in SOR solution technique for energy equation. (1)
ITMAXT	Number of iterations in SOR solution technique for the void fraction. (1)
ITMASX	Number of iterations in SOR solution technique for the outer mass loop. (1)
ITVOID	Number of iterations in SOR solution technique for the outer void fraction loop. (1)
CIFF	Interfacial friction constant multiplier. (1.0)
RELAXE	Relaxation parameter in SOR solution technique for the energy. If RELAXE=0.0, the line-by-line solution technique is used. (0.0)
RELAXT	Relaxation parameter in SOR solution technique for the void fraction. If RELAXT=0.0, the line-by-line solution technique is used. (0.0)
PRESO	The inital pressure at point '0'. (1.01353E+5)
XPRESO	The X-coordinate of point '0', m. (0.0)
YPRESO	The Y-coordinate of point '0', m. (0.0)
ZPRESO	The Z-coordinate of point '0', m. (0.0)
PAD	Pressure value added to pressure array when computing properties. (0.0) Note. By setting PAD=0.0, the absolute value of pressure is used throughout. One can use relative pressures for solution of the momentum equation by setting the initial pressure near zero and PAD near the pressure required for the problem.
TEMPO	Initial temperature of internal cells, C.
VGASOF	Cutoff value of gas void fraction (THG) for bypassing the gas momentum equation. (1.0E-10)

GRAVX Gravity vector component in X-direction, m/s**2. (0.0)
GRAVY Gravity vector component in Y-direction, m/s**2. (0.0)
GRAVZ Gravity vector component in Z-direction, m/s**2. (-9.8)
TURBVL Turbulent viscosity for liquid, Pa*s. (0.0)
TURBVG Turbulent viscosity for gas, Pa*s. (0.0)

Turbulent conductivities can be input either directly by specifying TURBCL and TURBCG, or by specifying nonzero values for CHARRE, CHARTL, and CHARTG.

TURBCL Turbulent conductivity for liquid, W/(m*C). (0.0)
TURBCG Turbulent conductivity for gas, W/(m*C). (0.0)
CHARRE Characteristic Reynolds number. (0.0)
CHARTL Characteristic temperature for liquid, C. (0.0)
CHARTG Characteristic temperature for gas, C. (0.0)

CWIREX Coefficient of wire force in X-direction. (0.5)
CWIREY Coefficient of wire force in Y-direction. (0.5)
CWIREZ Coefficient of wire force in Z-direction. (0.5)

The following variables define the thermal conductivity specific heat, and density of materials other than the coolant. These variables are indexed by values of MATWAL and MATERL.

NMATER Total number of materials.
COK(NM) Coefficients for thermal conductivity of material NM.
C1K(NM) CONDUCTIVITY=COK(NM)+TC*(C1K(NM)+TC*C2K(NM))
C2K(NM) J/(s*m*C)
COCP(NM) Coefficients for specific heat of material NM.
C1CP(NM) SPECIFIC HEAT=COCP(NM)+TC*(C1CP(NM)+TC*C2CP(NM))
C2CP(NM) J/(kg*C)
CORO(NM) Coefficients for density of material NM.
C1RO(NM) DENSITY=CORO(NM)+TC*(C1RO(NM)+TC*C2RO(NM))
C2RO(NM) kg/m**3

The following variables define heat transfer coefficient corelations. These variables are indexed by values of IHTWAL and IHTSTR.

NHEATC Number of heat transfer coefficient corelations. (1)
HEATC1(NH) Constants used in heat transfer coefficient corelations.
HEATC2(NH) NU=HEATC1(NH)+HEATC2(NH)*RE**HEATC3(NH)*
HEATC3(NH) PR**(HEATC4(NH))
HEATC4(NH) where NU is the Nusselt number,
RE is the Reynolds number, and
PR is the Prandtl number.
(5.0,0.25,0.8,0.8)

Duct wall modelling uses the following variables.

WALLDX(N) Duct wall thickness, m. (1.0)
WALLQS(N) Duct wall volumetric heat source, W/m**3. (0.0)
HYDWAL(N) Hydraulic diameter or characteristic length.
MATWAL(N) Material number. See input for NMATER.
IHTWAL(N) Heat transfer coefficient corelation number.
See input for NHEATC.

HYDIN Hydraulic diameter of cells adjacent to walls when IGEOM is greater than zero otherwise hydraulic diameter of cells, m.

HYDOUT Hydraulic diameter of cells not adjacent to walls when IGEOM is greater than zero otherwise hydraulic diameter of cells, m.

OMEGAC ???. (1.0)

OMEGAE Relaxation factor for energy and energy correction. (0.5)

OMEGAP Relaxation factor for pressure. (0.8)

OMEGAR Relaxation factor for density. (0.0)

OMEGAT Relaxation factor for void fraction and void fraction correction. (0.5)

OMEGAV Relaxation factor for velocity and velocity correction. (0.7)

OMEGAO Relaxation factor for d(RO)/d(P) and d(RO)/d(H) terms. (0.2)

REL Interfacial heat transfer coefficient. (0.0)

RKVL Interfacial friction coefficient.

The following section of variables are used to specify the heat distribution.

IQ 0--Uniform axial heat flux distribution. (*)
1--Axial cosine heat flux distribution.
2--Axial MU*SIN(MU) heat flux distribution skewed toward the top of the core.
3--Axial MU*SIN(MU) heat flux distribution skewed toward the bottom of the core.

FNZ Axial nuclear hot channel factor used when IQ=1,2, or 3. (1.0)

KLHS Lowest heated K-plane. (1)

KHHS Highest heated K-plane. (KMAX)

QIJ(IND) Normalized radial heat flux distribution. (1.0)

QK(K) Normalized axial heat flux distribution. (1.0)

QTOTAL Total power, W.

Array output is done in subroutine OUTPUT which is called once after initialization and according to the array TPRNT.

TPRNT(1) >0.0--TPRNT can contain up to 50 values of time at which OUTPUT is to be called.
=0.0--OUTPUT is called after initialization and before termination (*).
<0.0--TPRNT(1) is the print frequency in seconds. TPRNT(2) is the initial print time.

The arrays which are printed out at the calls to OUTPUT are coded into the values of ISTPR and NTHPR.

ISTPR Up to 50 coded values which specify the arrays to be printed in the first call to OUTPUT.

NTHPR Up to 50 coded values which specify the arrays to be printed after the first call to OUTPUT.

Each value of ISTPR and NTHPR is a signed five digit integer of the form 'SVVPLL' which is coded according to the following rules:

S
- + Only the plane or surface specified by 'VVPLL' is printed. Plus is assumed and need not be specified.
- - All planes or surfaces (LL) between 'VVPLL' and the next 'VVPLL' specified in ISTPR or NTHPR are printed.

VV
Values between 01 and 50 are for interior arrays.
Values between 51 and 99 are for surface arrays.

01--UL: U-component of liquid velocity.
02--VL: V-component of liquid velocity.
03--WL: W-component of liquid velocity.
04--HL: liquid enthalpy.
05--TL: liquid temperature.
06--VCELL: Cell fluid volume.
07--RLT: Liquid density.
08--PT: Pressure.
09--DL: Residual mass..
10--AREAX: X-direction flow area.
11--AREAY: Y-direction flow area.
12--AREAZ: Z-direction flow area.
13--QSOUR: Volumetric heat source.
14--UG: U-component of vapor velocity.
15--VG: V-component of vapor velocity.
16--WG: W-conponent of vapor velocity.
17--HG: vapor enthalpy.
18--TG: vapor temperature.
19--RGT: Vapor density.
20--GAMMA=THLT*EVAP: Boiling source term.
21--THL: Liquid void fraction.
22--THG: Vapor void fraction.
23--THLT: Liquid void fraction.
24--THGT: Vapor void fraction.
51--VELLBN: Surface liquid velocity
52--VELGBN: Surface gas velocity.
53--QLBN: Surface liquid heat flux.
54--QGBN: Surface gas heat flux.
55--MB: Adjacent internal cell number.
56--HLB: Surface liquid enthalpy.
57--HGB: Surface gas enthalpy.
58--TLB: Surface liquid temperature.
59--TGB: Surface gas temperature.
60--AREA: Surface element area.
61--RLB: Surface liquid density.
62--RGB: Surface gas density.
63--PB: Surface pressure.
64--IJK: Location of adjacent internal cell.
65--The liquid heat transfer coefficient from coolant to wall as used in the transient duct wall model (KTEMP(N)=500) is computed and printed.
66--The gas heat transfer coefficient from coolant to wall as used in the transient duct wall model

(KTEMP(M)=500) is computed and printed.

P — 0--A surface array is printed.
1--An I plane of an internal array is printed.
2--A J plane of an internal array is printed.
3--A K plane of an internal array is printed.

LL — Specific plane or surface to be printed. If S is +, only one plane or surface is indicated. If S is -, the 'IL' values in the current and next values of ISTPR or NTHPR indicate the range of planes or surfaces to be printed.

```
* * * * * * * * * * * * * * *
*    NAMELIST /FLAG/        *
* * * * * * * * * * * * * * *
```

ITMAXP — Number of iterations in SOR solution technique for pressure equation. (1)

IWALL — 1--Simplified model of G. B. Wallis used to compute wall resistance.
2--Bivard and Torrey (Dispersed flow) model used to compute wall resistance.
3--Bivard and Torrey (Annular flow) model used to compute wall resistance.
4--COMMIX-1A model for hexagonal fuel assembly used to compute wall resistance. (*)

IFPCEQ — 0--Bypass pressure correction calculation.
1--Use SIMPLE procedure for pressure correction.
2--Use SIMPLER procedure for pressure correction.
3--Use IPSA procedure for pressure correction.

IFENER — 0--Bypass energy calculation.
1--Perform energy calculation.

NSWEEP — Number of iterations for line-by-line procedure in SOLVE subroutines. (1)

ITENMX — Number of iterations for solution of energy equation. (1)

ITMOMX — Number of iterations for solution of momentum and pressure equations. (1)

IFLAG6 — Debug flag whose value causes on of four levels of debugging information for be printed. (0)

IREBIT — Mass rebalancing is performed inside the pressure correction SOR loop (ITMAXP) when:
MOD(Iteration number,IREBIT)=0.

KFLAG5 — 0--Solve the complete momentum equation to obtain the velocity.
1--Use the algebraic relation between pressure and velocity to obtain velocity.

ITMXPC — Number of iterations in line-by-line solution procedure for pressure correction equation. (1)

IFSOR — 0--Solve pressure equation by using the line-by-line solution technique.
-1--Solve pressure equation by using the SOR solution technique sweeping in the Y- and Z-directions.
-2--Solve pressure equation by using the SOR solution

technique sweeping in the Z- and X-directions.
-3--Solve pressure equation by using the SOB solution technique sweeping in the X- and Y-directions.

NFLAG1 0--Two fluid model used for two-phase model.
2--Homogeneous model used for two-phase model.

NFLAG2 0--No rebalancing in mass conservation calculation.
1--Rebalancing performed in mass conservation calculation.

IFFOPT Interfacial friction using model by:
1--Autruffe et al.
2--Harlow and Amsden.
3--Rexroth and Starkovich.
4--Rivard and Torrey.
5--Constant input from RKVL.
6--G. B. Wallis.
7--RKVI*THIT*THGT

NBOIL Evaporation due to boiling computed using:
1--Nignatulin model with evaporation only.
2--Nignatulin model with Autruffe equation for A.
3--Nigmatulin model with condensation.
4--Nigmatulin model with condensation plus Autruffe equation for A.

VAR9 Relaxation factor for pressure reaction in PCEQN1. (1.0)

VAR10 Relaxation factor for pressure correction in TIMSTP. (1.0)

COEF1 Boiling correlation coefficient.

BUBLEN Number of gas bubbles per cubic meter.

RGAS Gas constant, J/(kg-deg K). (361.0)
Use 361.0 for Sodium and 462.0 for water.

IDRODT 0--Variation of density with respect to pressure is neglected.
1--Variation of density with respect to pressure is accounted for in the transient term of the continuity equation.

IDDDP 0--Use maximum DD/DP for mass-momentum iteration.
1--Use cellwise DD/DP for mass-momentum iteration.

IDRAG 0--Viscous force only.
1--Viscous and nominal drag forces for hexagonal fuel assembly calculations included.

IFROD 0--No fuel rods are included. (*)
1--Fuel rods are included but no default initialization is done. NAMELIST /INPUTQ/ is required in input.
2--Fuel rods are included and a default initialization is done. This initialization sets pressure, temperature, density, enthalpy, and the Z-component of velocity from a solution of the coupled mass, moment and energy equations assuming no transverse velocities.

ISTATE 0--Initial-state: Boundary conditions and initial conditions are specified from input. Other values are zero.
1--Unsteady-state: Any state between initial-state and steady-state.
2--Steady-state: Converged-state or solution based on both specified boundary conditions and inital-state.

3--Transient-state: Any state after steady-state.

ISTRUC 0--No thermal structure present. NAMELIST /STRUCT/ not included in input file.

1--Thermal structures are present. NAMELIST /STRUCT/ must be included in input data.

The following three variables spacify the boundary condition types for all surfaces.

KFLOW(N) Type of velocity boundary.

-5--Continuative mass flow outlet.

-3--Free slip wall.

-2--Continuative velocity outlet.

-1--Continuative momentum outlet.

1--Uniform constant velocity boundary with normal velocity set from VELOCL(N) and/or VELOCG(N) and tangential velocity set to zero. (*)

100+NF--Uniform transient velocity boundary with normal velocity set from the NFth transient function.

KTEMP(N) Type of temperature/heat flux boundary.

1--Uniform constant temperature boundary with temperature set from TEMP(N). (*)

100+NF--Uniform transient temperature boundary with temperature set from the NFth transient function.

200+N --Uniform constant heat flux boundary with normal heat flux set from TEMP(N).

300+NF--Uniform transient heat flux boundary with normal heat flux set from the NFth transient function.

400 --Adiabatic heat flux boundary, i.e., heat flux equal to zero.

500 --Transient duct wall boundary. ???

KPRES(N) Type of pressure boundary condition.

0--???

1--Constant backbround pressure, Pa. (*)

100+NF--Transient background pressure with pressure set from the NFth transient function.

IFLIQ 0--No liquid phase present. Dimensions of liquid phase variables can be set to 1.

1--Liquid phase may be present. (*)

IFGAS 0--No vapor phase present. Dimensions of vapor phase variables can be set to 1. (*)

1--Vapor phase may be present.

IFPLOT -1--No plottape is written. (*)

0--Only the first and last time steps are written to the plot file on tape 11.

N--Every Nth time step is written to the plottape on tape 11.

IFHEAD 0--No geometry header is written to plottape. This option is used when adding plotting data to a previously existing plottape.

1--A geometry header is written to the plottape. (*)

```
                    * NAMELIST INPUTQ *
                    ******************

     SEVERAL OF THE FOLLOWING VARIABLES MUST BE INPUT INTO A ONE
     DIMENSIONAL ARRAY TO OBTAIN THE INDEX, IND, OF THE ONE DIMENSIONAL
     ARRAY FROM THE CELL NUMBER (I,J) THE FOLLOWING RELATIONSHIP IS USED:
                          IND = I+IMAX*(J-1).

     WHEN IGEOM > 0 ALL CELL FLOW AREAS, CELL WETTED PERIMETERS AND
     FRACTION OF PIN IN CELLS ARE INITIALLY SET TO VALUES COMPUTED FROM A
     STANDARD HEXAGONAL FUEL BUNDLE GEOMETRY.  IF THE USER IS CONSIDERING A
     CASE WHICH DEVIATES FROM THIS DEFAULT ANY OF ALL OF THESE PARAMETERS
     CAN BE RESET BY USING THE FOLLOWING THREE VARIABLES:
FLOWA(IJ)        :  FLOW AREA OF CELLS OF TYPE IJ WHERE IJ = IJTYPE(IND),
                    METER* (-1.0)
IJTYPE(IND)      :  CELL TYPE.  CELL TYPES ARE POSITIVE INTEGERS LESS THAN 51
                    ARE USED AS INDICES OF THE FOLLOWING THREE VARIABLES.  IF
                    NON NEGATIVE VALUE IS GIVEN TO ANY OF THE FOLLOWING THREE
                    VARIABLES THEN THE CORRESPONDING PARAMETER WILL BE SET TO
                    VALUE IN ALL CELLS OF THAT TYPE.
WETLN(IJ)        :  WETTED PERIMETER OF CELS OF TYPE IJ WHERE IJ =
                    IJTYPE(IND), (-1.0)
     AN EXAMPLE MIGHT HELP TO CLARIFY THE INPUT FOR THE THREE PREVIOUS
     VARIABLES.  CONSIDER A CASE WITH IMAX = JMAX = 10.
IJTYPE = 15*1,10*2, . :  CELLS (1,1) THROUGH (5,2) ARE GIVEN TYPE 1 AND
                         CELLS (6,2) THROUGH (5,3) ARE GIVEN TYPE 2.
FLOWA(2)=0.028, . . . :  CELLS OF TYPE 2 ARE ASSIGNED FLOW AREAS OF 0.028
                         WHILE CELLS OF TYPE 1 RETAIN THEIR DEFAULT VALUES.
                         CELLS OF TYPE 1 AND 2 ALSO RETAIN THEIR DEFAULT
                         WETTED PERIMETER.

HYDIN    :  INSIDE  HYDRAULIC DIAMETER OVERRIDE (METER)
HYDOUT   :  OUTSIDE HYDRAULIC DIAMETER OVERRIDE (METER)

     THE FOLLOWING THREE VARIABLES ARE UNNECESSARY WHEN IGEOM > 0.

CLADOD           :  CLAD OUTSIDE DIAMETER, METER.
PITCHX           :  PITCH IN X DIRECTION, METER.
PITCHY           :  PITCH IN Y DIRECTION, METER.

                    ***************************
                    *    NAMELIST  STRUCT     *
                    ***************************

NSTRUC      : NUMBER OF THERMAL STRUCTURES (0)
NTSEL(N)    : NUMBER OF ELEMENTS OF THERMAL STRUCTURE N (0)
NTSMAT(N)   : NUMBER OF MATERIAL REGION OF THERMAL STRUCTURE N (0)
ROUTER(N)   : OUTTER RADIUS OF THERMAL STRUCTURE N (0.0 METER)
RINNER      : INNER  RADIUS OF THERMAL STRUCTURE N (0.0 METER)
RODFR(N)    : ROD FRACTION OF T.S.#N  (E.G. .25 INDICATED QUARTER PIN)
```

```
IHTSTR(N)   : NUMBER OF HEAT TRANSFER COEFFICIENT CORRAIATION FOR
              THERMAL STRUCTURE N. (SEE HEAT TRANSFER COEFFICIENT
              CORRELATIONS IN NAMELIST &DATA).
HYDRAD(N)   : HYDRAULIC DIAMETER OR CHARACTERISTIC LENGTH USED IN
              HEAT TRANSFER COEFFICIENT CORRELATION (METER)
IXYZ(N)     : FLAG FOR AXIAL ALLIGNMENT OF THERMAL STRUCTURE N I.E.
              1 :  X-DIRECTION
              2 :  Y-DIRECTION
              3 :  Z-DIRECTION
NTSADO(N)   : NUMBER AF ADJACENT COOLANT CELLS INTERACTING WITH THE OUTER
              SURFACE OF AN ELEMENT OF THERMAL STRUCTURE NUMBER N  (0)
NTSADI(N)   : NUMBER OF ADJACENT COOLANT CELLS INTERACTING WITH THE INNER
              SURFACE OF AN ELEMENT OF THERMAL STRUCTURE NUMBER N  (0)

... MATERIAL REGIONS ARE COUNTED SEQUENTIALLY BEGINNING FROM THE FIRST
    THERMAL STRUCTURE HAVING NTSMAT(1) MATERIALS. FOR EXAMPLE :
    NSTRUC    = 3          ... 3 THERMAL STRUCTURES
    NTSMAT(1)=4,3,2,       ... T.S. #1 HAS 4 MATERIAL REGIONS,
                                 T.S. #2 HAS 3 MATERIAL REGIONS,
                                 T.S. #3 HAS 2 MATERIAL REGIONS
    THEN MATERIAL REGION (M.R.) #5 IS THE FIRST REGION OF T.S. #2 AND
    M.R. #9 REFERS TO THE LAST M.R. OF T.S. #3
... NOTE :  MATERIAL REGIONS ARE COUNTED FROM THE OUTSIDE IN

MATERL(MR) : MATERIAL TYPE OF M.R. #MR
NMPAR(MR)  : NUMBER OF PARTITIONS OF M.R. #MR
DRPAR(MR)  : PARTITION SIZE OF M.R. #MR (METER)
QSPAR(MR)  : VOLUMETRIC HEAT SOURCE FOR M.R. #MR  (J/(SEC-M**3))

... GAPS BETWEEN MATERIAL REGIONS ARE COUNTED SIMILIAR TO MATERIAL REGIONS
    HOWEVER, FOR A THERMAL STUCTURE HAVING NMR NUMBER OF MATERIAL REGIONS
    THERE ARE NMR-1 NUMBER OF GAPS
    FOLLOWING THE ABOVE EXAMPLE GAP #3 REFERS TO THE GAP BETWEEN M.R#3 AND
    M.R.#4 OF T.S.#1   AND  GAP#5 REFERS TO THE GAP BETWEEN M.R.#6 AND
    M.R.#7 IN T.S.#2

NGAPTY      : TOTAL NUMBER OF TYPES OF GAP
SGAP(N)     : SIZE OF GAP TYPE#N
HGAP(N)     : HEAT TRANSFER COEFFICIENT ACROSS GAP TYPE#N (W/(M**2-C))
IGAP(NG)    : GAP TYPE FOR GAP NUMBER NG


*****************************************
* THERMAL STRUCTURE SPECIFICATION CARDS *
*****************************************

... THESE CARDS SPECIFY THE COOLANT CELLS THAT INTERACT WITH THE T.S. ELEMENTS
   FIRST SET OF CARDS ARE FOR OUTER SURFACE AND NEXT SET OF CARDS ARE
  FOR INNER SURFACE OF THERMAL STRUCTURE ELEMENT.

      READ(5,200) N,IB,IE,JB,JE,KB,KE
 200  FORMAT(7I4)
```

```
WHERE :     N  = T.S. NUMBER
            IB = BEGINNING I
            IE = ENDING I
            JB = BEGINNING J
            JE = ENDING J
            KB = BEGINNING K
            KE = ENDING K
C            ***************************************
             * INTERNAL CELL INITIALIZATION CARDS *
             ***************************************
```

THE PURPOSE OF THIS SET OF INPUT CARDS IS TO INITIALIZE THE PHYSICAL PROPERTIES LISTED BELOW INSIDE THE POLYHEDRON. THE END CARD IS REQUIRED EVEN IF NO CARDS IN THIS GROUP ARE PRESENT. EACH CARD OF THIS SECTION CONTAINS THE FOLLOWING VARIABLES IN THE FORMAT (A4,F10.3,6I4):

```
    NAME          RVAL   IB    IE    JB    JE    KB    KE
NAME      AL   :  VOLUME POROSITY ;  THE DIMENSIONLESS RATIO OF FLUID
                  VOLUME IN A CELL TO TOTAL CELL VOLUME .  (1.0)
          ALX  :  SURFACE POROSITY ;  THE DIMENSIONLESS RATIO OF FREE FLOW
                  AREA TO THE TOTAL AREA OF THE SURFACE BETWEEN CELL
                  (I,J,K) AND CELL (I+1,J,K), (1.0).
          ALY  :  SURFACE POROSITY OF THE SURFACE BETWEEN CELL (I,J,K) AND
                  CELL (I,J+1,K), (1.0).
          ALZ  :  SURFACE POROSITY OF THE SURFACE BETWEEN CELL (I,J,K) AND
                  CELL (I,J,K+1), (1.0).
          P    :  PRESSURE, PASCAL. (101.35E+3)
          TG   :  TEMPERATURE, CELSIUS. (0.0)
          THG  :  GAS VOLUME FRACTION.
          THL  :  LIQUID VOLUME FRACTION.
          TL   :  TEMPERATURE, CELSIUS. (0.0)
          UG   :  X-DIRECTION VELOCITY COMPONENT, METER/SEC. (0.0)
          UL   :  X-DIRECTION VELOCITY COMPONENT, METER/SEC. (0.0)
          VG   :  Y-DIRECTION VELOCITY COMPONENT, METER/SEC. (0.0)
          VL   :  Y-DIRECTION VELOCITY COMPONENT, METER/SEC. (0.0)
          WG   :  Z-DIRECTION VELOCITY COMPONENT, METER/SEC. (0.0)
          WL   :  Z-DIRECTION VELOCITY COMPONENT, METER/SEC. (0.0)
          QSOU :  VOLUMETRIC HEAT SOURCE PER COMPUTATIONAL CELL
                  VOLUME  DX*DY*DZ  (W/M**3)  (0.0)

RVAL           :  THE VALUE TO BE ASSIGNED TO THE VARIABLE NAME.
IB,IE          :  BEGINNING AND ENDING I-INDEX LIMITS.
JB,JE          :  BEGINNING AND ENDING J-INDEX LIMITS.
KB,KE          :  BEGINNING AND ENDING K-INDEX LIMITS.
                     *********************************
                     * BOUNDARY INITIALIZATION CARDS *
                     *********************************
```

THE PURPOSE OF THIS SET OF INPUT CARDS IS TO INITIALIZE BOUNDARY VALUES OF ANY OF THE ARRAYS LISTED BELOW. UNIFORM TEMPERATURE AND VELOCITY BOUNDARY CONDITIONS CAN BE MORE EASILY SPECIFIED USING THE VARIALBES 'TEMP' , 'VELOCL' AND 'VELOCG' IN NAMELIST &DATA. THE END CARD IS REQUIRED EVEN IF NO OTHER CARD IN THIS GROUP IS PRESENT. EACH CARD OF THIS SECTION CONTAINS THE FOLLOWING VARIABLES IN THE FORMAT (A4,F10.3,7I4)

```
    NAME          RVAL   IB   IE   JB   JE   KB   KE   N
```

```
NAME :      PB   :  PRESSURE, PASCAL.
            RGB  :  DENSITY, KG/M**3.
            RLB  :  DENSITY, KG/M**3.
            THGB :  GAS VOLUME FRACTION.
            THIB :  LIQUID VOLUME FRACTION.
            TGB  :  GAS TEMPERATURE, CELSIUS.
            TLB  :  LIQUID TEMPERATURE, CELSIUS.
            VEGB :  MAGNITUDE OF THE GAS VELOCITY NORMAL TO THE SURFACE,
                    METER/SEC.
            VELB :  MAGNITUDE OF THE LIQUID VELOCITY NORMAL TO THE SURFACE,
                    METER/SEC.

RVAL             :  THE VALUE TO BE ASSIGNED TO THE VARIABLE NAMED.
IB,IE            :  BEGINNING AND ENDING I-INDEX LIMITS.
JB,JE            :  BEGINNING AND ENDING J-INDEX LIMITS.
KB,KE            :  BEGINNING AND ENDING K-INDEX LIMITS.
N                :  THE SURFACE NUMBER OF THE BOUNDARY BEING SET.

          ***********************************************
          ******   SOME  ADDITIONAL  INFORMATION   ******
          ***********************************************
```

THE FOLLOWING IS THE DESCRIPTION OF SOME OF THE IMPORTANT VARIABLES. THE VARIABLES THAT ARE PREVIOUSLY DESCRIBED ARE NOT REFERRED HERE.

```
                    ******   A. CELL INFORMATION   ******

     I;J;K      : CELL POSITION IN X, Y, AND Z DIRECTION RESPECTIVELY.
     IJK(M)     : (I,J,K) LOCATION OF CELL M OF THE FORM IIJJKK.
     M          : DUMMY COUNTER TO IDENTIFY INTERNAL CELLS.
     NM         : TOTAL NUMBER OF IRREGULAR CELLS.
     NM1        : TOTAL NUMBER OF CELLS.
     X;Y;Z      : COORDINATES.
     MB(L)      : INTERNAL CELL NUMBER ADJACENT TO SURFACE AREA L.
     MIM(M)     : CELL NUMBER ADJACENT TO CELL M IN -X DIRECTION (I-1 CELL).
     MIP(M)     : CELL NUMBER ADJACENT TO CELL M IN +X DIRECTION (I+1 CELL).
     MJP(M)     : CELL NUMBER ADJACENT TO CELL M IN +Y DIRECTION (J+1 CELL).
     MJM(M)     : CELL NUMBER ADJACENT TO CELL M IN -Y DIRECTION (J-1 CELL).
     MKM(M)     : CELL NUMBER ADJACENT TO CELL M IN -Z DIRECTION (K-1 CELL).
     MKP(M)     : CELL NUMBER ADJACENT TO CELL M IN +Z DIRECTION (K+1 CELL).
     MS(I,J,K)  : CELL NUMBER AT (I,J,K) LOCATION

       NOTE : NEGATIVE VALUE OF THE ABOVE 6 ARRAYS INDICATE THAT ADJACENT
              IS A SURFACE. FOR EXAMPLE : MIP(20) = -43 MEANS THAT NEXT TO
              CELL NUMBER 20 IN +X DIRECTION IS A SURFACE. MIP(M) = 0
              INDICATES THAT NO CELL AND NO REGULAR SURFACE IS ADJACENT
              TO CELL IN +X DIRECTION.

             ******   B.  OVERALL SURFACE INFORMATION   ******

     N          : DUMMY COUNTER USED FOR SURFACES.
```

```
NSURF      : TOTAL NUMBER OF SURFACES.
XNORML(N)  : COORDINATES OF UNIT SURFACE NORMAL VECTOR POINTING INTO
YNORML(N)  : DOMAIN OF INTEREST FROM SURFACE N.
ZNORML(N)  : SEE ABOVE.

NOTE:  EACH SURFACE IS RESOLVED BY THE PARTITIONING DESCRIBED ABOVE
       AND IS SLICED UP INTO SMALL AREAS WHICH COVER EACH SURFACE.  IF
       THE PARTITIONED AREA IS NOT NORMAL TO ANY AXIS,  IT IS TERMED
       IRREGULAR AND IS COUNTED SEPARATELY ALONG WITH ITS ASSOCIATED
       INTERNAL CELL.

I       :  DUMMY COUNTER USED TO IDENTIFY PARTITIONED SURFACE AREA.
LCI(N)  :  NUMBER OF LAST IRREGULAR SURFACE AREA FROM SURFACE N.
LCX(N)  :  NUMBER OF LAST SURFACE AREA NORMAL TO X AXIS FROM SURFACE N.
LCY(N)  :  NUMBER OF LAST SURFACE AREA NORMAL TO Y AXIS FROM SURFACE N.
LCZ(N)  :  NUMBER OF LAST SURFACE AREA NORMAL TO Z AXIS FROM SURFACE N.
NI      :  TOTAL NUMBER OF IRREGULAR SURFACE AREAS.
NI1     :  TOTAL NUMBER OF SURFACE AREAS.

        ******   C.  PARTITIONED SURFACE INFORMATION   ******

ITH PARTITIONED SURFACE ELEMENT  :  SURFACE NUMBER  1
    (1.LE.L.LE.LCI(1))          IS AN IRREGULAR SURFACE ELEMENT
    (LCI(1).LE.L.LE.LCX(1))     IS A SURFACE AREA NORMAL TO X-AXIS.
    (LCX(1)+1.LE.L.LE.LCY(1))   IS A SURFACE AREA NORMAL TO Y-AXIS.
    (LCY(1)+1.LE.L.LE.LCZ(1))   IS A SURFACE AREA NORMAL TO Z-AXIS.

LTH PARTITIONED SURFACE ELEMENT  :  SURFACE NUMBER  N
  (LCI(N-1)+1.LE.I.LE.LCI(N))   IS AN IRREGULAR SURFACE AREA
  (LCZ(N-1)+1.LE.L.LE.LCX(N))   IS A SURFACE AREA NORMAL TO X-AXIS
  (LCX(N)+1.LE.L.LE.LCY(N))     IS A SURFACE AREA NORMAL TO Y AXIS
  (LCY(N)+1.LE.L.LE.LCZ(N))     IS A SURFACE AREA NORMAL TO Z-AXIS

   AREA(L)            AREA OF LTH PARTITIONED AREA (A**2)
   ISURF(L)           SURFACE NUMBER OF LTH PARTITIONED AREA

                 ******   D.  POROSITIES   ******

AL(M)       :  GEOMETRIC VOLUME FRACTION OF CELL M ;  VOLUME OCCUPIED
               FLUID /CELL VOLUME
ALX(M)      :  SURFACE PERMEABILITY IN X-DIRECTION; GEOMETRIC AREA
               FRACTION OF SURFACE BETWEEN CELL M AND CELL MIP(M)
ALY(M)      :  SURFACE PERMEABILITY IN Y-DIRECTION; GEOMETRIC AREA
               FRACTION OF SURFACE BETWEEN CELL M AND CELL MJP(M).
ALZ(M)      :  SURFACE PERMEABILITY IN Z-DIRECTION; GEOMETRIC AREA
               FRACTION OF SURFACE BETWEEN CELL M AND CELL MKP(M).

EXAMPLE: CROSS SECTIONAL FLOW AREA OF SURFACE BETWEEN CELL M AND
CELL MIP(M) IS  DY(J)*DZ(K)*ALX(M)

                 ******   E.  PHYSICAL VARIABLES   ******
```

SUBSCRIPTS

B	:	BOUNDARY.
G	:	GAS.
L	:	LIQUID.
T	:	UPDATED VALUE.
0	:	CELL I,J,K
1	:	CELL I-1,J,K
2	:	CELL I+1,J,K
3	:	CELL I,J-1,K
4	:	CELL I,J+1,K
5	:	CELL I,J,K-1
6	:	CELL I,J,K+1
OLD	:	VALUES AT PREVIOUS TIMSTEP

CELL CENTERED VARIABLES

HG;HGT	:	GAS ENTHALPY. (JOULES/KG)
HL;HLT	:	LIQUID ENTHALPY. (JOULES/KG)
P;PT	:	PRESSURE, UPDATED PRESSURE. (PASCALS)
RG;RGT	:	GAS DENSITY. (KG/M**3)
RL;RLT	:	LIQUID DENSITY. (KG/M**3)
THL;THG	:	VOID FRACTION. (DIMENSIONLESS)
THLT;THGT	:	UPDATED VOID FRACTION. (DIMENSIONLESS)
TL;TG	:	LIQUID TEMPERATURE; GAS TEMPERATURE. (DEGREE CENTIGRADE)
PC	:	PRESSURE CORRECTION

VARIABLES DEFINED AT THE SURFACE OF A CELL:

UG;VG;WG	:	GAS VELOCITIES IN X,Y, AND Z DIRECTION. (M/SEC)
UL;VL;WL	:	LIQUID VELOCITIES IN X,Y, AND Z DIRECTIONS. (M/SEC)

BOUNDARY SURFACE VARIABLES:

HLB;HGB	:	ENTHALPY. (JOULES/KG)
QLBN;QGBN	:	NORMAL HEAT FLUX. (JOULES/M**2)
RLB;RGB	:	DENSITY. (KG/M**3)
PB	:	PRESSURE. (PASCALS)
THLB;THGB	:	VOID FRCTION. (DIMENSINLESS)
TLB;TGB	:	TEMPERATURE. (DEGREE CENTIGRADE)
VELLBN	:	SURFACE NORMAL VELOCITY. (M/SEC)
VELGBN	:	SURFACE NORMAL VELOCITY. (M/SEC)

****** F. SOME ADDITIONAL VARIABLES ******

```
ACOF0    :
ACOF1    :  COEFFICIENTS OF A DISCRETIZED EQUATION OF THE FORM
ACOF2    :
ACOF3    :     A0*PHI(M) = A1*PHI(M1) + A2*PHI(M2) + A3*PHI(M3)
ACOF4    :               + A4*PHI(M4) + A5*PHI(M5) + A6*PHI(M6) + B0
ACOF5    :
ACOF6    :
BCOF0    :
```

```
UHATL    :
VHATL    :  PSEUDO VELOCITY IN THE ALGEBRAIC FORM OF THE MOMENTUM
WHATL    :  EQUATION.  FOR EXAMPLE :
UHATG    :
VHATG    :    UL(M) = UHATL(M) + DUOL(M)*(PT(M) - PT(M2))
WHATG    :

DUOL     :
DVOL     :  COEFFICIENT IN THE ABOVE ALGEBRAIC FORM OF THE MOMENTUM
DWOL     :  EQUATION
DUOG     :
DVOG     :
DWOG     :

UWIRE    :
VWIRE    :  THE PROJECTED WIRE WRAP AREAS
WWIRE    :

HSTREO   :  HEAT TRANSFER COEFFICIENT FOR COMPUTING HEAT TRANSFER
HSTREI   :  FROM THE SURFACES OF A THERMAL STRUCTURE

DULMAX   :
DVLMAX   :  MAXIMUM CHANGE IN THE MAGNITUDE OF A VARIABLE IN THE ENTIRE
DWLMAX   :  FIELD DIVIDED BY THE MAXIMUM MAGNITUDE OF THE VARIABLE IN
DUGMAX   :  THE ENTIRE FIELD
DVGMAX   :
DWGMAX   :
DHCR     :

FCX1     :
FCX2     :
FCX3     :  COEFFICIENTS USED IN THE WIRE WRAP RESISTANCE MODEL
FCX4     :
FCX5     :
FCY1     :
FCY2     :
FCY3     :
FCY4     :
FCY5     :

AREAX    :
AREAY    :  CROSS SECTIONAL FLOW AREA IN X  Y  Z  DIRECTION
AREAZ    :
VCELL    :  VOLUME OF CELL OCCUPIED BY THE FLUID

NPHASE   :  =  1  SINGLE PHASE ;  =  2  TWO PHASE
DTIME    :  TIME STEP SIZE
DCONV    :  CONVERGENCE PARAMETER
            =   EPS1*(EPS2 + MAX(U/DX + V/DY + W/DZ))
EVAP     :  RATE OF EVAPORATION
QUAL     :  MASS FRACTION OF VAPOR PHASE
```

ACKNOWLEDGMENTS

We are indebted to Prof. S. L. Soo and Prof. B. T. Chao, University of Illinois, Urbana, Prof. S. V. Patankar, University of Minnesota and our colleagues, Drs. W. Baumann, Y. S. Cha, B. C-J. Chen, S. P. Vanka, and C. I. Yang for stimulating discussions and their constructive comments; to Drs. R. T. Curtis, C. N. Kelber, and P. M. Wood of the United States Nuclear Regulatory Commission for their support, without which this work would not have been possible.

REFERENCES

1. F. H. Harlow and A. A. Amsden, *Flow of Interpenetrating Material Phases*, J. Comp. Phys. *18*, p. 440 (1975).
2. W. T. Sha, H. M. Domanus, R. C. Schmitt, J. J. Oras, and E. I. H. Lin, *COMMIX-1: A Three Dimensional Transient Single-Phase Component Computer Program for Thermal Hydraulic Analysis*, MIREG-CR-0415; ANL-77-96 (Sept 1978).
3. S. V. Patankar, *Numerical Heat Transfer and Fluid Flow*, Numerical Heat Transfer, Vol. 2, McGraw-Hill, New York (1979).
4. D. B. Spalding, *A Novel Finite-difference Formulation for Differential Expressions Involving Both First and Second Derivatives*, Int. J. Num. Methods in Eng., Vol. 4, p. 551 (1972).
5. D. B. Spalding, *The Calculation of Free-convection Phenomena in Ga-liquid Mixture*, Imperial College, Heat Transfer Section Report, HTS/76/11 (1976).
6. W. T. Sha and B. E. Launder, *A General Model for Turbulent Momentum and Heat Transport in Liquid Metals*, Argonne National Laboratory Report, ANL-77-78 (Mar 1979).
7. W. T. Sha et al., *Conservation Equations for Finite-Control Volume Containing Finite, Dispersed, Fixed Heat Generating (or Absorbing) Solids*, Argonne National Laboratory Components Technology Division Report (to be published).
8. M. I. Autruffe, G. J. Wilson, B. Stewart, and M. S. Kazimi, *A proposed Momentum Exchange Coefficient for Two-Phase Modeling of Sodium Boiling*, personal communication.
9. F. H. Harlow and A. A. Amsden, *Numerical Calculation of Multiphase Fluid Flow*, J. Comp. Phys. *17*, 19 (1975).
10. P. E. Rexroth and V. Starkovich, *Two-Phase Momentum Exchange Experiment and Analysis*, Trans. Am. Nucl. Soc. *28*, 445 (1977).
11. W. C. Rivard and M. D. Torrey, *Numerical Calculation of Flashing from Long Pipes Using a Two-Fluid Model*, Los Alamos Scientific Laboratory Report LA-6104-MS (Nov 1975).

12. M. R. Granziera and M. S. Kazimi, *A Two-Dimensional, Two-fluid Model for Sodium Boiling in LMFBR Fuel Assemblies*, Energy Laboratory Report No. MIT-EL-80-011, MIT (May 1980).

13. F. W. Dittus and L. M. K. Boelter, *Heat Transfer in Automobile Radiators of the Tubular Type*, Publications in Engineering, University of Calif., Berkeley 2, pp. 443-461 (1930).

14. E. N. Sieder and G. E. Tate, *Heat Transfer and Pressure Drop of Liquids in Tubes*, Industrial Engineering Chemistry, Vol. 28, No. 12, pp. 1429-1435 (1936).

15. W. H. McAdams, Heat Transfer, New York, McGraw-Hill Book Company, Inc., 1967.

16. L. Biasi, et al., *Studies on Burnout*, Part 3, Energia Nucleare *14*(9), pp. 530-536 (1967).

17. N. Zuber, et al., *The Hydrodynamic Crisis in Pool Boiling of Saturated and Subcooled Liquids*, International Developments in Heat Transfer, Part 2, No. 27, 1961 Int. Heat Transfer Conf., Boulder, Colorado, pp. 230-236.

18. F. H. Lienhard and V. K. Dhir, *Hydrodynamic Prediction of Peak Pool-Boiling Heat Fluxes from Finite Bodies*, Journal of Heat Transf., Vol. 95, No. 2, pp. 152-158 (1973).

19. T. A. Bjornard, *Blowdown Heat Transfer in a Pressurized Water Reactor*, PHD-Thesis, Massachusetts Institute of Technology, (Aug 1977).

20. D. C. Groeneveld and S. G. J. Delorme, *Prediction of Thermal Non-Equilibrium in Post Dryout Regime*, AECL-5260 (1976).

21. R. L. Dougall and W. M. Rohsenow, *Film Boiling on the Inside of Vertical Tubes with Upward Flow of the Fluid at Low Qualities*, MIT-TR-9079-26 (1963).

22. F. C. Chato, *Laminar Condensation Inside Horizontal and Inclined Tubes*, A.S.H.R.A.E. Journal *4*, 52-60 (1962).

23. J. G. Collier, *Convective Boiling and Condensation*, McGraw-Hill, (1972).

24. E. F. Carpenter and A. P. Colburn, *The Effect of Vapor Velocity on Laminar and Turbulent Film Condensation*, Trans. ASME *78*, 1637-1643 (1956).

25. S. V. Patankar, *A Numerical Method for Conduction in Composite Materials, Flow in Irregular Geometries and Conjugate Heat Transfer*, Proceedings of the Sixth Int. Heat Transfer Conference, Toronto, Vol. 3, p. 297 (1978).

26. G. H. Golden and J. V. Tokar, *Thermophysical Properties of Sodium*, ANL-7323 (Aug 1967).

Distribution for NUREG/CR-1807 (ANL-81-10)

Internal:

E. S. Beckjord
C. E. Till
R. S. Zeno
J. G. Bartzis
A. R. Brunsvold
H. M. Domanus
D. M. France
P. L. Garner
J. J. Lorenz
C. C. Miao
J. L. Krazinski
W. T. Sha (5)
V. L. Shah (5)
Y. W. Shin
M. Weber
S. P. Vanka
B. C-J. Chen
D. H. Cho
M. Ishii
D. R. Ferguson
D. P. Weber
W. L. Baumann
R. C. Schmitt
L. W. Deitrich
R. M. Singer
G. K. Leaf
P. B. Abramson
H. H. Hummel
J. E. Sanecki
ANL Contract File
ANL Libraries (2)
TIS Files (3)

External:

USNRC, Washington, for distribution per R7 (380)
DOE-TIC (2)
Manager, Chicago Operations and Regional Office, DOE
Chief, Office of Patent Counsel, DOE-CORO
President, Argonne Universities Association, Argonne, Ill.
Components Technology Division Review Committee:
- F. W. Buckman, Consumers Power Co., Jackson, Mich. 49201
- R. A. Greenkorn, Purdue U., West Lafayette, Ind. 47907
- W. M. Jacobi, Westinghouse Electric Corp., Pittsburgh, Pa. 15230
- M. A. Schultz, North Palm Beach, Fla. 33408
- J. Weisman, U. Cincinnati, Cincinnati, O. 45221

P. M. Wood, USNRC, Silver Spring, Md. 20910
S. L. Soo, U. Illinois, Urbana, Ill. 61801
B. T. Chao, U. Illinois, Urbana, Ill. 61801
J. C. Slattery, Northwestern U., Evanston, Ill. 60201
N. E. Todreas, Massachusetts Inst. Technology, Cambridge, Mass. 03129
A. A. Bishop, U. Pittsburgh, Pittsburgh, Pa. 15261
M. S. Kazimi, Massachusetts Inst. Technology, Cambridge, Mass. 03129